



This is a repository copy of *Fire spalling behavior of high-strength concrete : a critical review*.

White Rose Research Online URL for this paper:
<https://eprints.whiterose.ac.uk/187407/>

Version: Accepted Version

Article:

Amran, M., Huang, S.-S., Onaizi, A.M. et al. (2 more authors) (2022) Fire spalling behavior of high-strength concrete : a critical review. *Construction and Building Materials*, 341. 127902. ISSN 0950-0618

<https://doi.org/10.1016/j.conbuildmat.2022.127902>

© 2022 Elsevier Ltd. This is an author produced version of a paper subsequently published in *Construction and Building Materials*. Uploaded in accordance with the publisher's self-archiving policy. Article available under the terms of the CC-BY-NC-ND licence (<https://creativecommons.org/licenses/by-nc-nd/4.0/>).

Reuse

This article is distributed under the terms of the Creative Commons Attribution-NonCommercial-NoDerivs (CC BY-NC-ND) licence. This licence only allows you to download this work and share it with others as long as you credit the authors, but you can't change the article in any way or use it commercially. More information and the full terms of the licence here: <https://creativecommons.org/licenses/>

Takedown

If you consider content in White Rose Research Online to be in breach of UK law, please notify us by emailing eprints@whiterose.ac.uk including the URL of the record and the reason for the withdrawal request.



eprints@whiterose.ac.uk
<https://eprints.whiterose.ac.uk/>

Fire spalling behavior of high-strength concrete: A critical review

Mugahed Amran^{1,2,*}, Shan-Shan Huang³, Ali M. Onaizi⁴, G. Murali⁵, Hakim S. Abdelgader⁶

¹ Department of Civil Engineering, College of Engineering, Prince Sattam Bin Abdulaziz University, 11942 Alkharj, Saudi Arabia

² Department of Civil Engineering, Faculty of Engineering and IT, Amran University, 9677 Amran, Yemen

³ Department of Civil and Structural Engineering, University of Sheffield, Mappin Street, Sheffield, S1 3JD, UK.

⁴ School of Civil Engineering, Faculty of Engineering, Universiti Teknologi Malaysia, Skudai 81310, Johor, Malaysia

⁵ School of Civil Engineering, SASTRA Deemed University, Thanjavur, India

⁶ Department of Civil Engineering, Faculty of Engineering, University of Tripoli, Tripoli, Libya

Corresponding author: m.amran@psau.edu.sa and mugahed_amran@hotmail.com

Abstract: Building and infrastructure damages, such as tunnels, have become a more important issue because of the continuous expansion of rural and urban constructions. It is well-known that when high-strength concretes (HSCs) are exposed to high temperatures; it is more likely to experience explosive fire-induced spalling than conventional strength concrete. Spalling might result in catastrophic loss of life and damage to nearby critical infrastructure. The exposure of reinforcement bars to elevated temperature, decreased permeability, higher density, moisture transfer, and brittleness of the HSC contribute to spalling. The concrete on a structural member's surface may be violently ripped apart by a high and fast rising temperature during a fire. Despite being a non-combustible material, the physics-chemo-mechanical properties of concrete deteriorate when subject to high temperatures. The magnitude and duration of a fire in a concrete structure define the severity of the fire. The resistance to fire spalling of HSCs under different fire conditions, extremes, and tendencies must be explored urgently. Cementitious materials exhibited a positive impact as an alternative to cement in HSC because they are known as environmentally friendly concrete materials with superior fire-resistant properties. In addition, the inclusion of fibers as an additive reinforcement is adopted to prevent and mitigate fire spalling in HSCs. Therefore, the establishment of appropriate fire-safety measures is a fundamental requirement in building design to ensure the safety of its inhabitants. While the process of fire spalling for HSC during a fire has not yet been completely understood. For this reason, a critical literature study on recent developments in HSC fire-resistance performance should be conducted to determine the present fire spalling behavior of HSC in the event of high temperatures and/or a fire. This article systematically reviews the mechanisms, influential factors, and types of fire spalling. This literature also reviews the behavior, fire spalling modelling, and strategies to prevent spalling in HSC applications. Given the advantages of the research subject, several hotspot research topics for scientific investigations are also suggested to facilitate the widespread use of HSCs in advanced construction applications.

Keywords: Fire, spalling, fibers, factors, mechanisms, prevention, models, high-strength concrete.

Table of Contents

1	Introduction	3
2	Mechanisms of heat-induced spalling	7
2.1	Spalling mechanisms	7
2.2	Factors influencing spalling	16
2.2.1	External factors	17
2.2.2	Some of the factual factors	17
2.3	Spalling types	19
2.3.1	Aggregate spalling	20
2.3.2	Violent spalling	23
2.3.3	Progressive gradual spalling	25
2.3.4	Corner spalling	26
2.3.5	Explosive spalling	27
2.3.6	Post-cooling spalling	29
3	Fire-induced spalling behavior of HSC conform to ISO 834 standard fire test	31
4	Roles and assessment techniques of HSC spalling	38
4.1	Spalling tendency	38
4.2	Residual strength tests	39
4.3	Sorptivity test	41
4.4	X-ray diffraction	44
5	Strategies to prevent spalling in HSC	46
6	Modelling of heat-induced spalling	49
7	Conclusion	52
8	Acknowledgments	54

Abbreviations

AAC	Alkali-activated concrete	NSC	Normal strength concrete
AA-HSC	Alkali-activated high-strength concrete	OPC	Ordinary Portland cement
AAM	Alkali-activated materials	PVA	Polyvinyl Alcohol
AEA	Air entraining agent	SCM	Supplemental cementitious material
Ca(OH) ₂	Calcium hydroxide	SF	Silica fume
Ca:Si	Calcium:Silicome	w/s	Water/Solid
CTE	Coefficient of thermal expansion	w/c	Water/cement
EDS	Energy dispersive spectroscopy	X-ray CT	X-Ray computed tomography
FEM	Finite element modelling	XRD	X-ray diffraction
FRC	Fiber reinforced concrete	SF	Silica fume
FTIR	Fourier transform infrared spectroscopy	MK	Metakaolin
GGBS	Ground granulated blast furnace slag	RM	Red mud
GPC	Geopolymer concrete	RHA	Rice husk ash
HSC	High-strength concrete	FA	Fly ash
HSC-PPAG	HSC with PPF and aggregate	NC	Normal concrete
ITZ	Interfacial transition zone	ECC	Engineered cementing composite
KASH	Potassium aluminosilicate hydrate	PPF	Polypropylene fiber
MIP	Mercury intrusion porosimetry	SCC	Self-compacting concrete

1 Introduction

In high-strength concrete (HSC), water is located, adsorbed, or chemically bound in extremely fine pores as capillaries [1]. Subject to fire or other extreme thermal conditions, a significant amount of water reserved inside the concrete matrix is released and evaporated. Furthermore, elevated temperature conditions lead to the decomposition of hydration products of cementitious composites [2]. A combination of pore pressures, driven by temperature gradients, and shrinkage caused by water release, creates internal stresses in concrete [3]. When internal stresses exceed the maximum permitted tensile stresses of the concrete components, thermal cracks and spalling begin to occur in the material. The deformation behavior under the uniaxial stress of concrete composite based on the concrete composite type is exhibited clearly. Fig. 1 shows the deformation behavior of plain concrete (Fig. 1a), fiber-reinforced concrete (FRC) (Fig. 1b), and strain hardening cementitious concrete (SHCC) (Fig. 1c) [4]. HSC has a tensile strain capability of between 1% and 5%, which is 100–500 times that of plain concrete [5]. However, HSC is developed with high capacity of tensile strain at moderate amount of fiber, to have the capability to transform the failure from brittle to ductile.

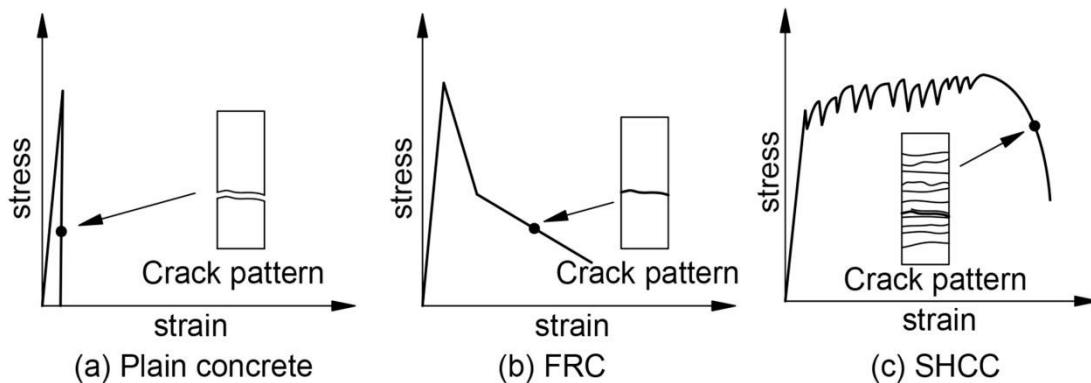


Fig. 1: Deformation behavior of SHCC, FRC, and plain concrete under uniaxial tension (Adapted from [4])

Spalling has been reported on the structure's concrete surface. The procedure continues on the premise that the standards have been met (progressive spalling); the concrete structure could also instantaneously disintegrate with a massive energy release [2,6]. In general, fire may significantly impact structural behavior because of the degradation of material characteristics at elevated temperatures and the provision of indirect effects generated by restricted thermal expansion [7]. In fact, concrete structures often exhibit adequate fire resistance and satisfactory behavior in elevated temperature situations due to their low thermal expansion. Also, the temperature drops gradually from the externally exposed surface to the inner core, thereby shielding the majority of the section and reinforcing bars [8]. The interplay of many distinct materials and structural factors makes the generation of comprehensive knowledge on the spalling phenomena and predicting the mechanism and intensity of its occurrence during the design process particularly difficult [9]. Concrete spalling due to fire

is not new. Spalling risks have always been associated with the rapid heating of concrete. The introduction of superplasticizing additives in the 1970s enabled the production of dense concretes by mixing micro-silica fume (SF) between the cement grains [10]. Hertz [11] was the first to observe that these materials were prone to explosive spalling to the degree that was not observed previously. For instance, spalling occurred at a very low heating rate of only 1 °C/min. Since then, many authors, including Zhang et al. [12], Yoon [13], and Sanjayan et al. [6], recognized the extremely high risk of heated-induced spalling in dense concrete. Recently, new evidence, such as that reported by Liu [14], has confirmed this further. One of the most well-known examples of concrete spalling in real fires is the fire that broke out in the tunnel that connects Britain and France (named Great Belt Fixed Link) [15] and the one that erupted in the Danish tunnel beneath the Great Belt [16], which caused severe damage due to spalling of dense concretes.

However, given that higher strength and more durable (and denser) concrete mixes have been developed with distinguished properties (Fig. 2) and used in modern construction (the probability of extremely severe concrete spalling in the elevated temperature has become higher, thereby prompting an increased interest in unravelling this phenomenon. Industrial by-products are unaffected by fire and other thermal stresses, such as ground granulated blast furnace slag (GGBS) [17–19], silica fly ash (FA) [20], rice husk ash (RHA) [21–23], red mud (RM) [24], silica fume (SF) [25], and metakaolin (MK) [26], which are used as the main precursors to make a sustainable HSC, because they exhibit outstanding resilience to stresses (fire and thermal), as proved by greater strength retention, reduced cracking seriousness, and the non-appearance of spalling at extreme temperatures as compared with standard Ordinary Portland cement (OPC) binders [27].

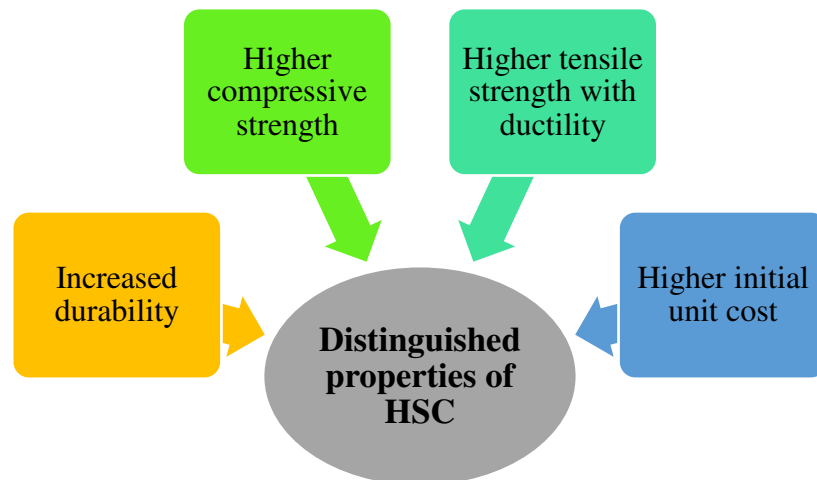


Fig. 2: Distinguished properties of HSC

However, certain HSC systems display low thermal performance in terms of fire resistance [28,29]. The thermal behavior of HSC is largely dependent on the binder's chemistry and microstructure, and thus cannot be generalized across different binder systems [30]. When compared with OPC, low-calcium HSC demonstrated better thermal stability because of a water content in the gel is lowered that could be ascribed to the nature of water within the concrete matrix. In hydrated OPC, the bound water is a key element of the calcium silicate hydrate gel and the portlandite microstructure [31]. While in low-calcium HSC, an unbound water pore network (i.e., pore solution) was produced by calcium activation with sodium hydroxide or sodium silicate in the sodium-aluminosilicate hydrate gel [32]. Though, ambient curing strength of low-calcium HSC systems is smaller than that of high-calcium HSC systems [33]. GGBFS is added to the system, which raises the calcium content of the system and promotes the generation of alkali and aluminum-substituted calcium silicate hydrate gel blends when the alkali is activated [34]. It has been established that improving the performance of MK-based HSC below 800 °C may be accomplished [35]. Fig. 3 shows the comparison between HSC and the other types of concrete in terms of the trend of compressive strength and w/c ratio.

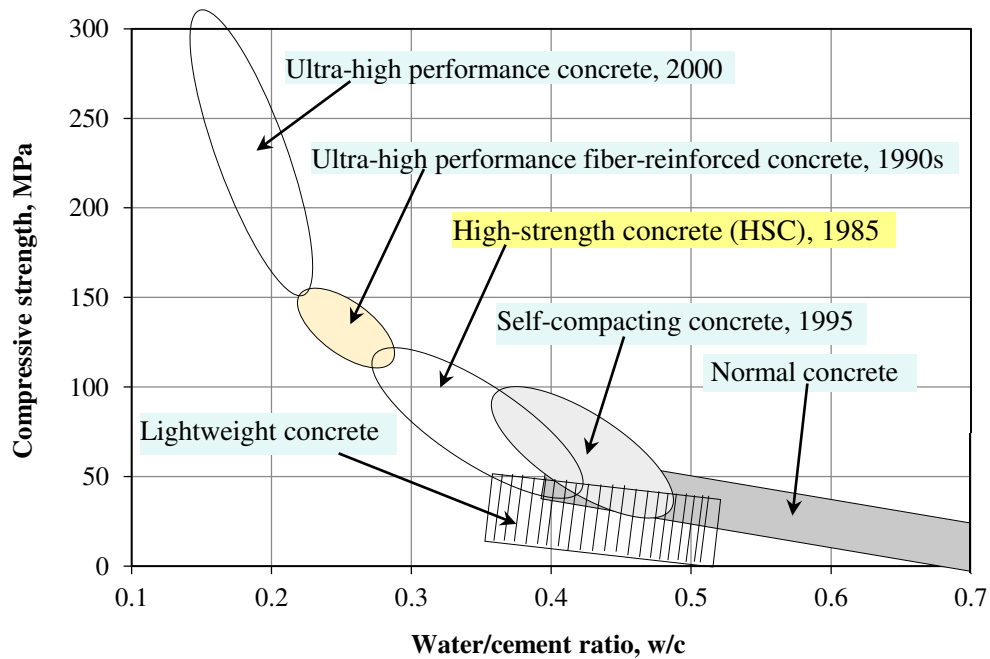


Fig. 3: Comparison between the HSC and the other types of concrete (Data adapted from [36–52])

The capacity of HSC's binder to build a network of connected pores is also credited with the HSC's greater performance at high temperatures, that allows trapped steam to permeate to the binder's surface. Steam transfer to the surface is considerably reduced in cracking and spalling by reducing water vapor pressure buildup in closed pores [53,54]. Reduced sintering thermal and conductivity at high temperatures have also

been cited as factors for HSC's superior fire-resistance than OPC binders, which lose strength rapidly at temperatures above 450 °C [55]. By maintaining the amorphous gel structure at high temperatures while using proper HSC formulation and curing, exceptional thermal stability may be accomplished [55]. When heated over 800 °C, poorly cured HSC with high water content or unreacted alkali and silicates exhibits poor thermal stability, resulting in the formation of various crystal phases. [31,56]. At temperatures that exceed 800 °C, the strength of FA-based HSC systems declined in sharp contrast to that observed with preservation rate in strength with rising temperature (up to 800 °C) [29]. In addition, when strength is improved at ambient temperature and post-heat shrinkage, the curing pressure is high, but strength retention is reduced at increasing temperatures due to poor porosity [29].

Thermally induced shrinking of alkali-activated FA binders occurs at higher temperatures. This shrinkage causes a significant damage and expansion of aggregates, thereby resulting in loss of strength, which is proportional to the size of the aggregate [57,58]. However, this shrinkage can be minimized by using inorganic fillers derived from alumina in the binder. The Si/Al ratio increases the thermal shrinkage of alkali-activated MK binders, and that the shrinkage is greater at low Si/Al ratios when the alkalication is sodium as opposed to potassium [27]. Though, when the ratio of Si/Al is increased, discrepancies in charge-balancing alkalications within the binder cause modest changes in the behavior of thermal shrinkage [59,60]. Additionally, the thermal shrinkage of alkali-activated materials (AAM) has increased when the water/solid ratio and salt concentration rise. Potassium aluminosilicate hydrate (KASH) systems have higher strength than AAM-based systems after being heated up to 1000 °C. The reason is that the HSC systems have more cracking at higher temperatures, more porosity and more crystalline phases than AAM-based systems [29,61].

Under simulated fire circumstances, the performance of fiber-reinforced alkali-activated MK [62] and alkali-activated FA [63–65] samples (microstructurally diverse, ranging from porous to solid) was investigated. The findings revealed that despite the decreased heat conductivity of porous samples, solid HSC samples had better fire resistance rating. Phases that are not involved in the creation of alkali aluminosilicate gels also affect the performance at elevated temperatures [59]. Increased temperature has been shown to cause the shattering of iron-rich phases with a larger thermal expansion than the N-A-S-(H) gel. However, in alkali-activated concrete composites, the thermal performance of crystalline silica phases had a negligible impact [66]. Scientifically, the use of cementitious materials as an alternative to cement in HSC (Table 1) exhibited a positive impact because they are known as environmentally friendly concrete materials with superior fire-resistant properties. In addition, the inclusion of fibers as an additive reinforcement is adopted to prevent and mitigate fire spalling in HSCs.

Therefore, the establishment of appropriate fire-safety measures is a fundamental requirement in building design to ensure the safety of its inhabitants. The fire spalling mechanism for HSC during a fire is yet to be fully discovered. HSC's ability to withstand high temperatures and a fire should be examined in a critical literature study to discover the present behavior and performance of HSC in a fire. This article reviews the mechanisms, influential factors, and types of fire spalling systematically. This literature also delivers thorough reviews on the behavior, fire spalling modelling, and strategies to prevent spalling in HSC applications. Given the advantages of the research subject, several hotspot research topics for scientific investigations are also suggested to facilitate the widespread use of HSCs in advanced construction applications.

Table 1: Properties and compositions of NC, HSC, and UHPC (data adapted from [36,38,40–48,67–69])

Property/materials	NC	HSC	UHPC
Properties			
Compressive strength, MPa	20 -42	> 42 - 100	> 100
Tensile strength, MPa	2 - 5	> 5 - 10	> 10 - 45
Flexural strength, MPa	≈1.5 – 5	≈ 5 – 22	≈ 22 – 53
Permeability coefficient	≈ 10 ⁻¹⁰	≈ 10 ⁻¹¹	≈ 10 ^{-(12 to14)}
Freeze-thaw protection	Air entrainment	Air entrainment	Air entrainment
Toughness	Medium	high	Very high
Durability	Medium	high	Very high
Raw materials (approx., ≈)			
Chemical admixtures	Water reducing agent	Water reducing agent/High range water reducer	High range water reducer
Cementitious materials	FA, RHA, MK, RM, GGBS	FA, RHA, MK, RM, GGBS, Silica fume	FA, RHA, Silica fume
Silica fume	Designated	≈ 40	≈ 50–300
Super-plasticizer (SP)	Designated	10	≈ 10–70
Reinforcement/Fibers	Designated	< 40	40–250
Water	> 200	≈ 100–150	110–260
Cement	< 400	400	600–1000
Fine aggregate (sand)	≈ 700	600	≈ 1000–1200
Coarse aggregate	≈ 1000	≈ 900	Designated
Maximum aggregate size	19.0–25.5	9.5–12.5	≈ 0.15–0.6
Water/binder (w/b)	Designated	<0.28	<0.27
Water/cement (w/c)	0.41–0.70	0.25–0.40	0.15–0.28

Annotations: Normal concrete (NC), High-strength concrete (HSC), and Ultra-high performance concrete (UHPC)

2 Mechanisms of heat-induced spalling

2.1 Spalling mechanisms

In general, the primary parameters that affect spalling are the rate of heating, the permeability of system, applied load and initial pore saturation level [70–72]. Despite its higher tensile strength, HSC is more likely to

explode than conventional strength concrete [73]. This happens because of the material's reduced ductility and the greater pore pressures that form during heating as a consequence of the material's reduced permeability [74]. In addition, some other factors play a role, for example, the cross sectional shape and size, concrete age, heating profile, type, fibers (Table 2 [75]) and size of aggregates, the reinforcement bars and the existence of cracking [71,76,77]. Each type of concrete spalling results from a distinct set of chemical or physical factors (Fig. 4) as follows:

- At high temperatures, pore pressure rises as water inflates and evaporates [78];
- Compression of the heated surface due to a temperature differential across the member's section [79];
- Internal cracking as a result of thermal extension differences between cement paste and aggregate [80];
- Cracking attributable to thermal distortion differences between reinforcement bars and concrete [81];
- Due to temperature gradients, pore pressure, and internal cracking [8,82,83].
- Due to a loss of strength owing to the chemical deterioration during the heating phase [2] and internal cracking of the concrete paste [84,85].
- Due to cracking patterns caused by the different thermal distortions of concrete mass and the main reinforcements at the corner of the concrete section [86] and due to the amalgamation of the thermal gradients and pore pressure in the members' cross-section [12,82,87,88].
- Due to internal cracking induced by differing thermal expansions of aggregate and strength loss caused by chemical transitions [89–91].

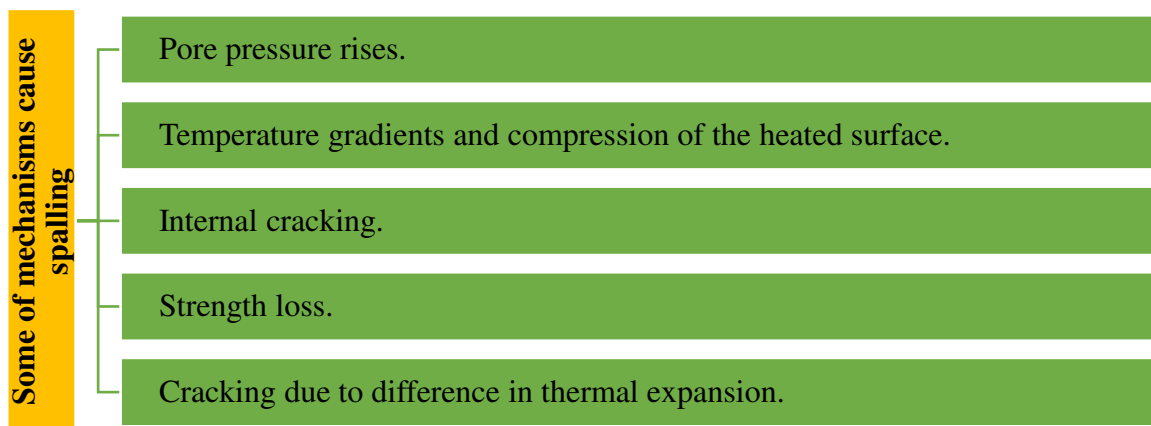


Fig. 4: Some of mechanisms cause spalling

Table 2: Different typical fibers used to diminish the risk of spalling

Fiber	Volume of fiber, kg/m ³	Degree of temp. °C	Action mode and effectiveness	Refs.
PPF	1 - 3	475–550	- As a rule of thumb, 1 - 3 kg/m ³ fibers (6 mm length, 10 -100 μm dia.) appear to be the most efficient in terms of spalling prevention.	[92]
PPF	3	Up to 600	- Melting at T ≈ 170 °C lowers high pore pressure and upsurges permeability.	[75]
steel fibers	196.3		- PPFs is particularly extremely thin fibers, may have a detrimental impact on workability.	[37]
Polyvinyl alcohol (PVA)	195	30 - 300	- The combination of PP and steel fibers, as well as PP fibers and bigger aggregates, had a powerful synergistic activity on permeability.	[93]
			- Melting at 167 °C and thus dissipating vapor pressure due to the permeability of the fibers is increased after melting.	
PPF and nylon fibers	1 – 3	160 -220	- The highest pore pressure observed in the specimens was lower the larger the permeability.	[41]
			- Under both high and low heating conditions, tests revealed that raising the loading level had no effect on the likelihood of concrete spalling.	
Waste rubber fibers	16 - 80	150 - 600	- This can produces dangerous chlorides; thus, it is not preferable to be used in HSC.	[94]
			- The spalling occurred before PVA melted, however inclusion of PVA improved concrete spalling resistance by increasing permeability via enlarging empty zone around PVA fibers	
Steel fiber	45	150 -600	- T ≈ 200 °C is a fairly high melting temperature, and it might be very high for some mixtures.	[95]
			- The integration of the two fibers can enhance spalling prevention by affording networks between pores with a lower content of PPF by incorporating both the relatively low melting temperature of PP fiber.	
Polymer fibers (e. g. PPF)	1 – 3	105 - 400	- This is helpful in the development of a fire, and the higher proportion of fibers that could be used due to the thinner diameter of nylon fiber, which is useful in the later stages of a fire.	[96]
			- Increase permeability, void ration and micro-cracks at elevated temperatures.	
Polyethylene (PE) fibers	1 – 3	Up 300	- It has been found that up to 10% sand substitution with rubber fiber has no influence on the residual characteristics of waste rubber fibered-HSC when exposed to extreme temperatures of up to 150 °C.	[97]
			- With short spacing between the ties, HSC becomes more ductile and columns become more resistant to spalling. In testing, however, there was no discernible gain in resistance with other structures.	
			- The major contributions of the inclusion of steel fibers into the mix design of HSC are to improve the ductility of HSC column, to increase its load-carrying capacity to a certain degree and to further enhance its resistance to fire to some extent.	
			- A connected network of matrix fractures can be generated by using a temperature difference between the added PPFs and matrix to increase permeability and reduce the likelihood of explosive spalling.	
			- The network of fractures is attributable to higher permeability and, as a result, lowering the vulnerability of HSC to explosive spalling.	
			- Low melting point (T ≈ 90 °C) but molten PPFs with high viscosity can reduce the increment of permeability; therefore, it makes a less beneficial.	

Two factors primarily cause concrete damage in a fire: i) thermal expansion is directly related to the heat action [Fig. 5a], and ii) vapor pressure is related to liquid phase mass transfer [Fig. 5b] [98]. In case of structures exposed to shear forces, as the percentage of shear reinforcing bars increases, the concentration of beam shear cracks decreases; resulting flexure takes over control of the fracture pattern, rather than shear as the primary driving force [99]. Fiber-reinforced concrete buildings have a similar trend, with fibers enhancing shear resistance to resistance more resistance to flexure [100,101].

As a consequence, increasing the fibers' percentage in geopolymer concrete (GPC) beams increased flexural performance and flexural cracks. Additionally, the inclusion of prefabricated floor slab has a comparable but more inefficient impact on minimizing shear cracks because of the PFs' lower stiffness and fewer fibers that bridge the cracks [102]. Owing to the bridging action of fibers, GPC beams covers may be mitigated or even prevented from spalling due to reflected tensile stress waves [103]. Smaller aggregates (10 mm) were used in another study, and this worsened spalling and led to major fractures appearing in the GPC; although the usage of larger aggregates resulted in better results as temperatures increased [58]. Concrete, on the other hand, degrades when exposed to high temperatures. Additionally, three distinct forms of fire-induced concrete degradation exist: i) thermo-hygral damage (Fig. 5a) [71], the restriction of moisture causes pore pressure (Fig. 5b) to develop up in concrete at temperatures between 220 and 320 °C; ii) thermochemical damage, caused by the decomposition of CaO above 700 °C; and iii) thermomechanical damage resulting from high temperatures, which may be induced by external stresses and temperature gradients 430-660 °C [71]. Particularly, the addition of polypropylene fibre (PPF) to concrete mitigates damage [70,104].

An example of concrete wall thermo-hygral spalling is shown in Fig. 6a, which was heated from one side alone [78]. Fire exposure causes a temperature differential in the vicinity of the fire-exposed side of concrete. As the temperature rises, chemically bound water and the water in the hydration gel are liberated into concrete micropores and becomes free water, thereby causing pore pressure to build gradually as a result of temperature increase and improve the vapor water in pores (Fig. 6b)[71]. Because of the disparity in temperatures and the degree of pore saturation, a pressure gradient causing internal stress of concrete system is created inside the pores. The pressure gradient drives moisture in two opposed ways, one toward the hot face and the other into the deeper, colder zone. As a result, three zones; saturated(the so-called moisture clog), wet and dry are formed [105]. Thus, when the stress caused by water pressure inside pores exceeds the ultimate flexural strength of concrete, bursting failure occurs (Fig. 6b).

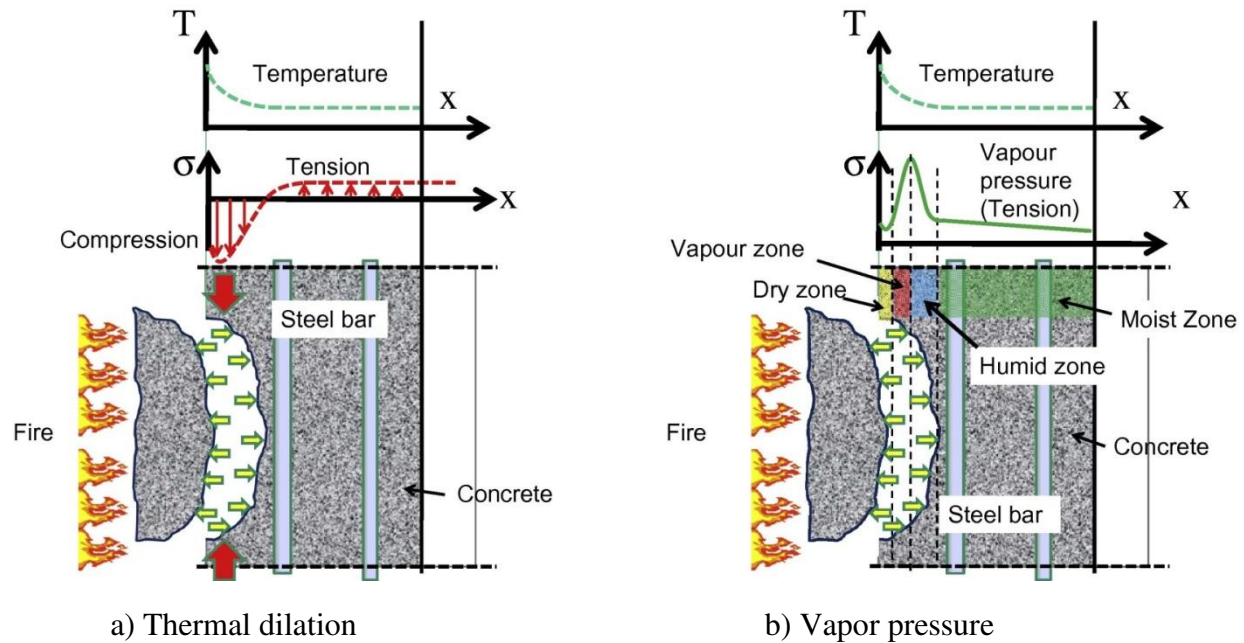


Fig. 5: Mechanism of spalling (Adapted from [98])

There is the greatest pressure in front of the saturated zone, which is the damp area [98]. The water in the wet zone is a combination of water vapor and liquid water, with the pore pressure equal to dry air partial pressure and sum of saturated vapor pressure [106]. Given that the air pressure is usually negligible, this peak pressure may be approximated by the saturated vapor pressure, which agrees with experimental observations [2]. In addition, concrete spalling has been the subject of several experimental and analytical investigations to provide active or passive protection [107]. Experiments on the addition of PPFs to RPC or the application of fire insulation on the surface of RPC beams were reported [36,107–111]. Despite this, there were few investigations on the simulation analysis of RPC beam performance under fire. It is developed a three-dimensional FEM using ABAQUS software to monitor the fire performance of hybrid-fibre-reinforced RPC beams covered with fire insulation [110,112]. However, the analysis did not take into account RPC's explosive spalling. The most destructive impact on RPC structural elements is fire induced spalling, which is caused by a incorporation of hydrothermal, mechanical, and thermal deteriorating processes [36,110].

The considerable spalling that resulted in the RPC beams was also shown to be the cause of accelerated failure under fire [111]. These findings emphasize the need of taking spalling into consideration when estimating RPC member fire behavior. Moreover, based on RPC's biaxial strength theory, a better spalling criterion was suggested to determine if spalling happens in RPC members [107]. The impact of updated and prior spalling criteria (based on the uniaxial strength theory) on RPC beam firing performance prediction was also investigated. The enhanced spalling criterion was proven to be more efficient in predicting spalling and fire

efficiency for RPC beams because it takes into account both the stresses induced by pore pressure, thermal gradients, and applied load, as well as the modify in concrete strength induced by spatial stress quantum system [107].

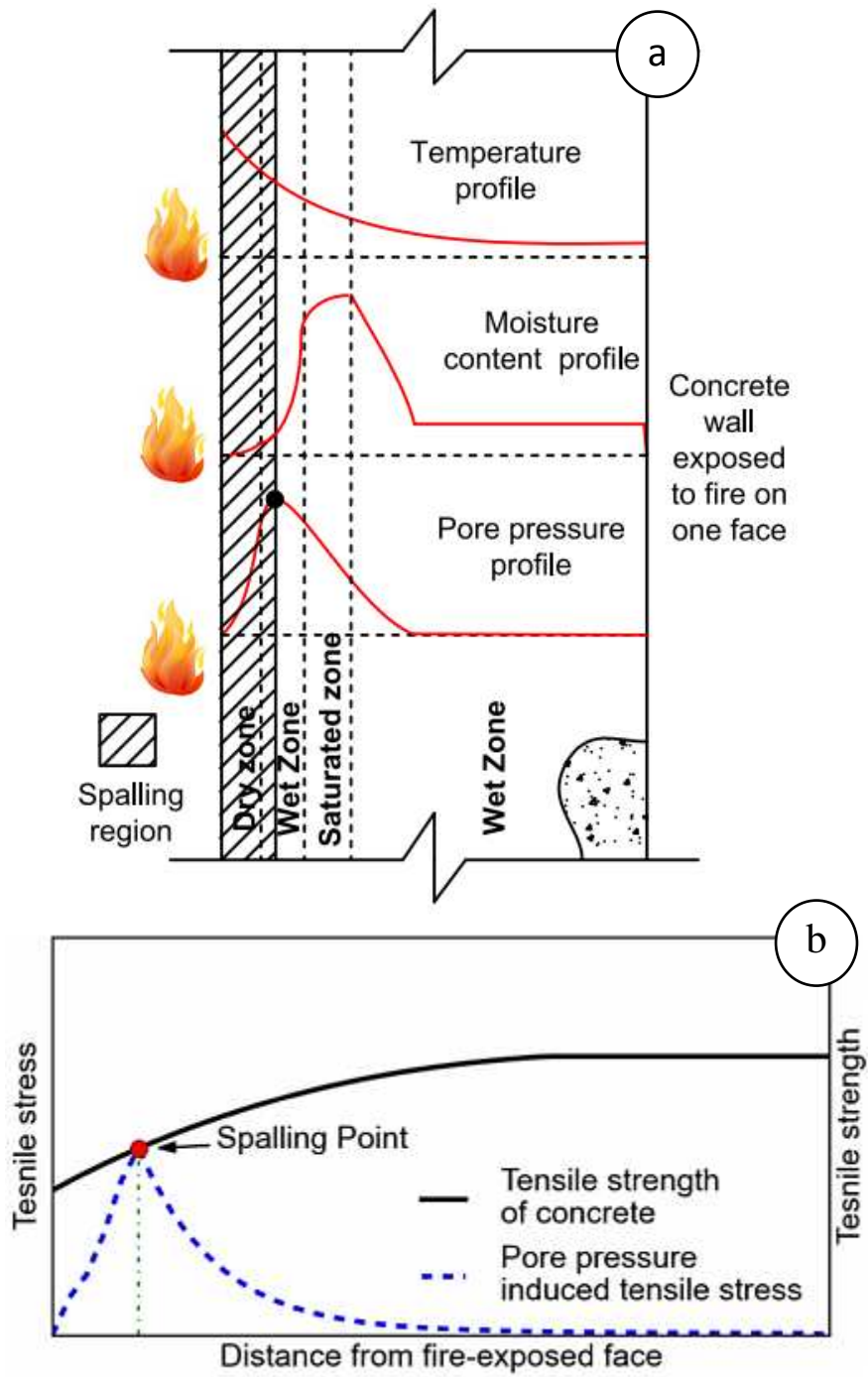


Fig. 6: A depiction of thermo-hydral concrete wall spalling fired on one face, b) a tensile stress profile instigated by pore pressure at the moment of spalling (Adapted from [71])

For example, there are very minute weight losses when PPFs are added to concrete below 150 °C; however, these losses upsurge dramatically in the range from 150 °C to 350 °C. [113], because of the frequency with which PPFs melt at temperatures between 166 °C and 170 °C [36,114]. After fire exposure, the sort and shape of fibers also influence the pore pressure of HSC. For example, when 12 mm PPFs were used, more fire damage resistance was seen than when 6 mm PPFs were used [115]. Additionally, the performance of concrete with using of 12 mm PPFs outperformed that of 6 mm PPFs at a great temperature of 600 °C [116]. Evidence from repeated reheating–cooling cycles at 600 °C on plain and FRP specimens showed that when subjected to high temperatures, plain concrete cracked and partially spalled. Furthermore, the cracks in the plain concrete samples seem to be deep and to have stretched all the way around their surfaces. In comparison with the plain concrete examples, it shows RGPC specimens with less cracking, the fractures look narrower and shorter. One might conclude that GPCs and HSCs are more fire resistant than OPC concrete [117–120].

Moreover, it is well-known that spalling is a catch-all word for different damaging processes in a concrete building after fire [121]. Various processes induce these occurrences, including a) increase in pore pressure as temperature rises [78]; b) separating the heated surface due to the developed compression that resulted from the thermal gradient in the cross-section [79]; c) thermal expansion/deformation discrepancies between aggregate and cement paste might lead to interior cracks [80]; e) concrete and reinforcing bars breaking as a result of thermal expansion and deformation discrepancies [81], and d) heating causes chemical changes that reduce the material's strength [2]. During a fire, concrete that has been spalled causes significant damage to concrete buildings and high financial costs and a danger to human life. [122]. Furthermore, several investigations on concrete spalling failures have been conducted [6,12,13,70–72,74,76,77,83,123].

Concrete spalling in fire refers to the dislodgement of smaller pieces of concrete (30–50 mm) from the concrete surface, associated with explosive forces [124]. Spalling often occurs between 15 and 30 minutes following the start of the fire, which is considered the key period for firefighting and minimizing its effect [6]. Several researchers have proposed several theories to explain the damage caused by the spalling, which are summarized as follows: 1) moisture-induced pressure damage [125]; 2) thermal damage due to heat [88]; 3) cement paste and aggregates are incompatible because of their differing temperatures [126]; and 4) aggregate physicochemical alterations, such as polymorphic inversion of quartz [127].

The binder of alkali-activated high-strength concrete (AA-HSC) is synthesized by alkali activating calcium raw materials, as well as a reaction product, which is then polymerized under high pH hydrothermal conditions at relatively low temperatures (as low as 120 °C) [128]. Conversely, OPC binder primarily depends on silicon dioxide and calcium oxide hydration processes to generate calcium silicate hydrates [57,129].

Compared to OPC, geopolymer has several advantages due to its chemical structural change and superior strength under elevated temperatures [58]. The occurrence of concrete spalling in various concretes with varying sizes of aggregate, irrespective of whether the concrete is AA-HSC or OPC [124]. Additionally, MK-based AA-HSC outperforms OPC in mechanical qualities at room temperature but is prone to cracking and strength loss when exposed to elevated temperatures. Their early strength is much lower than MK-based GPCs and OPC-based concrete [130,131].

The changes in the physical appearance of GPC cylinders are depicted in Fig. 7 [81]. In the GPC cylinders, this form of spalling was not detected. Fig. 7b depicts a longitudinal segment of an GPC-HSC cylinder following exposure to a 1000 °C fire. As demonstrated in this figure, GPC remains essentially solid, in contrast to the considerable deterioration of the OPC concrete depicted in Fig. 7a. After being exposed to the four various temperature ranges, the color of GPC-HSC changed dramatically [81]. The GPC-HSC samples did not show a significant change in color at 400 °C, with all the samples having a relatively similar surface color, having only a little light brown tint. The surface color of the GPC-HSC specimens was quite comparable at 650 °C, although it had altered to a light brown color. Both the high and regular strength concretes had a dark red color at 800 °C, which was a distinct contrast from the original color. The surface was initially rather dark, but this could be scraped away to expose the earthy red color beneath [81]. The red color became particularly noticeable at 1000 °C, with the high strength GPC-HSC standing out more than the conventional strength GPC-HSC. The increased iron oxide concentration of the FA caused the color variations in the GPC-HSC samples.



a) After 400 , 650, 800, and 1000 °C exposure



b) After 1000 °C exposure

Fig. 7: GPC-HSC specimens under fire (Adapted from [81])

The AA-HSC sample's higher resistance to disintegration and spalling could be attributed to their excellent tensile strength than OPC concrete. When comparing the splitting strengths of AA-HSC and OPC, it was discovered that heat-cured FA-based AA-HSC had an excellent tensile strength than OPC concrete [132]. When OPC concrete is exposed to a high-temperature fire, it may be limited in its effective cross-sectional area because of significant cracking and spalling. This decrease in the OPC concrete element's effective cross-sectional area may eventually result in a loss in the element's load capacity [81]. The relative reduction of cracking and spalling in AA-HSC implies that it is more resistant to fire than OPC concrete.

It is also examined the behavior of normal and high-strength concrete performance incorporating supplementary pozzolanic materials in elevated temperatures [133]. The results showed that MK-based AA-HSC had greater strength of up to 200 °C and remained stronger at 400 °C than FA-based AA-HSC, SF concrete, and standard OPC concrete. Additionally, all of the HSCs quickly degraded after reaching 400 °C. Although higher strength is displayed at conditions below 400 °C, the MK-based AA-HSC taken the lowermost ultimate compressive strength above 400 °C, and it is vulnerable to a specific higher temperature variety [81]. In general, the pozzolanic concretes thermal performance varies widely. Once the temperature approaches 400 °C, pozzolanic material-based concretes exhibit substantial early strength gains and thermal stability, tracked by speedy worsening and a lower ultimate strength than conventional concrete. The fast degradation and high-strength loss at elevated temperatures are attributed to the high content of hydration products that decompose the origin components at a temperature range of 400 °C –800 °C [134].

Similarly, there has been researched on high-temperature heat and strain rate effects on FA and SF ternary mixed concrete. After 400 °C, a significant decrease in strength was observed after 10 minutes of heat exposure at 800 °C, a 25% decrease in the compressive strength of 25 mm cubes of the MK-based AA-HSC paste specimens [81,135]. Furthermore, small HSC panels constructed using MK and 10 mm thick granulated slag infill are examined. Exposure of 1100 °C on one side of the panel after 35 minutes, the temperature on the opposite side was recorded at 350 °C [18,118]. As a novel material, few test data on the behavior of FA-based AA-HSC exposed to flames at various temperatures in the literature. The strength of FA-based AAC increased when exposed to relatively moderate temperature heat at 200 °C because it was weakened by temperatures of a higher temperature [57]. As a result, a thorough investigation is still needed to determine the variations in low-calcium FA-based AA-HSC when exposed to flames at higher temperatures [136].

For this goal, extensive experiments and analytical analyses were conducted. Thicker concrete is more probable to spall, as one research has shown, and the risk of spalling rises as the pace at which the concrete is heated and its moisture content increases [137]. Reinforced concrete slabs were studied for fire spalling, which

was more common in the early stages of fire [6]. The significant findings of the experiments on cylinder examples suggest that vapor pressure is the primary cause of fire spalling on HSC, with thermal stress prompted by higher temperature gradients performing as a minor cause [138,139]. It was also established experimentally that cubic HSC specimens had a high risk of fire spalling [140]. The greater the moisture content and strength of concrete, the greater the chance of concrete spalling occurring at high temperatures [140]. Regarding the effect of aggregate shape on the occurrence probability of concrete spalling due to fire, concrete with crumpled aggregates is further susceptible than spherical aggregate when it comes to spalling [141]. Moreover, spalling is even more severe in thicker and more significant concrete panels with high strength [142]. According to a study, different sized heated concrete spheres break apart in unique ways; that is, the size of the concrete element plays a role in the concrete spalling pattern [143]. In addition, aged dry concrete L-shape beams are less vulnerable to spalling risks than new concrete beams [43].

Furthermore, HSC mixed with SF is more prone to spalling than HSC combined with FA and blast furnace slag [144,145]. The problem of building spalling has been recognized for decades, but it has recently been emphasized in Europe owing to the recent intense tunnel fires [122,146]. The fire resistance of freshly created concrete types has been questioned due to extensive damage caused by spalling and the inability of tunnels to function for an extended period after a fire [147]. Observations of concrete spalling during fire tests cover a wide range, in random order: slow (1 °C/min.) or fast (250 °C/min.) heating, spalling at the start of heating or after a time of heating, cracking along or through aggregate grains, from gradual to explosive spalling, either ceasing after a while or progressing, and halting at the level of reinforcement or going far beyond it [148]. In general, researchers also discovered that external loading contributes significantly in the occurrence of spalling.

2.2 Factors influencing spalling

Structure is exposed to high or rapidly increasing temperatures, spalling may occur, in which layers or pieces of concrete are violently or semi-violently separated from its surface [83]. Numerous material properties (e.g., reinforcement cracks, type and size of aggregate, saturation level and permeability), environmental properties (e.g., load level, heating profile and rate) and geometric properties (e.g., size and shape of section). These properties have revealed factors that influence concrete spalling in the event of a fire. [70–72,74,76,77,83,123]. According to the study, concrete spalling may be caused by a variety of factors. All of the variables may be classified into two categories:

2.2.1 External factors

The structural concrete degradation in fire is indeed variable in accordance with the type of heat source (e.g., fuel type, maximum temperature and rate of temperature) and the external loads [1]. Spalling occurs when concrete is contacted to fire at a elevated rate of heating (particularly more than 3 °C per minute), as established by previous studies and tests [76]. However, ambiguity regarding the prevalence of spalling exists in different circumstances [149]. A temperature rise of just 1 or 2 °C each minute, explosive spalling can also be observed [150]. Moreover, the external loading factors exert a significant impact on the concrete's failure mechanisms in case of fire [76]. During a fire, reinforced concrete columns under compression are prone to collapse due to compression zone concrete failure when the concrete strength decreases with increasing temperature. Several previous studies revealed that prestressed concrete is more prone to explode than unprestressed concrete [42,150].

2.2.2 Some of the factual factors

Several microstructural and functional factors affect the degree of concrete spalling; a lower water-to-cement ratio (w/c) raises the likelihood of explosive spalling [76]. The utmost parameters controlling thermally prompted explosive spalling are grade of concrete strength and moisture content. Typical strength concrete will not spall easily, even at high moisture content levels. However, with the higher the moisture content of HSC, the probability of spalling is greater (Fig. 8) when the moisture level exceeds a threshold value [151]. Fig. 8 depicts the maximum elastic strain energy at which spalling begins for a sample with a 90% moisture content [141]. Meanwhile, thermal expansion is responsible for most of the elastic strain energy produced at spalling; only 12.6% of the energy generated during spalling is derived from strain energy generated by vapor pressure.

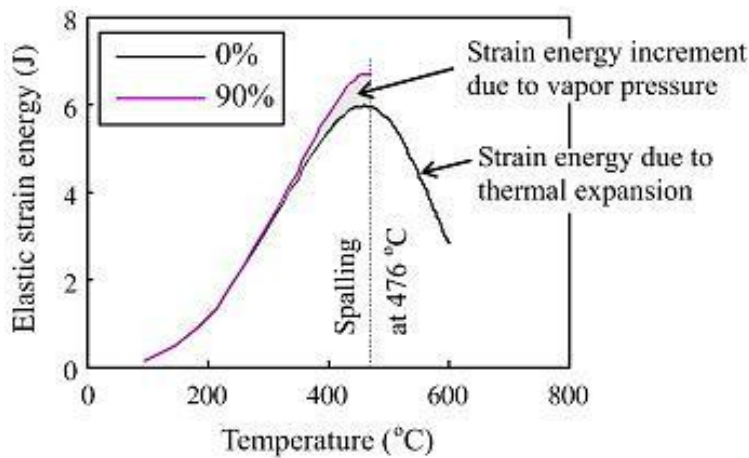


Fig. 8: The temperature-dependent evolution of elastic strain energy in samples with starting moisture levels of 0 and 90% (Adapted from [141])

Thermal expansion-induced strain energy is the most important factor in fire spalling, which agrees with the prior findings [141]. Low calcium:Silicium (Ca:Si) ratio in the initial mix resulted in a low calcium hydroxide (Ca(OH)₂) level, thereby ensuring a more favorable hydrothermal reaction [1]. The Ca(OH)₂ is undesired due to its decomposition into CaO and CO₂ at a temperature of 400 °C. In addition, CaO rehydrates expansively and negatively upon being cooled and exposed to moisture [152]. However, lowering the Ca:Si ratio in practice by using industrial by-products as cement alternatives, such as slag, PFA, or SF, is possible. Table 3 shows the influential parameters of the used materials on heat-induced spalling [75].

Table 3: Influential parameters of the used materials on heat-induced spalling

Parameters of used materials	Degree of spalling risk	Impact on spalling	Refs
Moisture content	Very high	Relying on the concrete's permeability. It's challenging to get critical moisture content, especially for HSC.	[153]
		Because greater vapour pressure must be released, higher moisture content raises the likelihood of explosive spalling.	[154]
Hardened parameter Tensile strength		It is reported that while the precipitated water flow may be small when concrete is subjected to high temperatures, its existence has a substantial influence on fluid transport performance and pore pressure prediction.	[155]
		High tensile strength is thought to reduce the chance of explosive spalling.	
Heating characteristic parameter High heating rate		It is described the fire experiments that revealed the increased danger of explosive spalling of HSC densified by silica fume for the first time.	[9,156]
		Larger heating levels typically contribute to explosive spalling with high strength concrete mixes	
Cement content	High	Even with low w/c ratios, a high cement percentage upsurges the overall quantity of water injected into the concrete.	[154,157]
Compressive strength		Because of the lower permeability and w/c ratio, higher strength grades typically raise the risk of explosive spalling.	[154]
Geometry and cross section		Fixed ends as eccentric load, boundary conditions, or bending upsurges risk	[158]
Thermal expansion		After spalling, the strength capacity of concrete members will be remained.	[155]
		A round cross-section, tolerable concrete cover, rounded corners and spacing, and an altered tie design reduce or eliminates spalling.	[159]
Applied load		Because tiny fissures utilized for vapour release are forced together, it's unclear if a low preload reduces the likelihood of spalling.	[143]
		Spalling is more likely when the preload is less than 5% of the cold strength.	[153]
Exposure on multiple surface		Due to larger thermal pressures and temperature gradients, heat exposure raises the risk of explosive or corner spalling on more than one side.	[160]
Temperature gradient		Due to thermal stresses, it can endorse the risk of explosive spalling ($\delta t > 1.0$ k/mm)	[161]

		Inextricably linked to the heating rate leads to a higher risk with temperature gradients.	
Size of aggregate		Due to a low surface-to-mass ratio, bigger aggregates have a greater danger of explosive spalling.	[83]
Absolute temperature	Medium	With extreme temperatures of greater than 1000 °C, it upsurges the threat of post-cooling spalling. Also, explosive spalling commonly occurs with temperatures up to 350 °C.	[9,81,156]
Internal cracks		The heated surface may increase the risk of spalling.	[157]
Cracks (internal)	Irregular	There are two opposing impacts. Small fissures may allow high pressure to escape and lessen the likelihood of spalling. Parallel cracking near the surface, on the other hand, Young concrete has higher free water, making it more prone to spalling. Due to the limited permeability of HSC, this impact is reduced.	[83]
Age of concrete			[153]
Tensile strength	Low	It has high thermal stresses, gradients and expansion. It can offer a greater resistance: Due to bigger pore pressure, there is no risk of spalling. It has thermal stresses or corner spalling from two sides Due to a higher application, the risk of spalling rises.	[146]
Carbonate aggregates		Even at very high temperatures, it remains stable and has a very low thermal expansion.	[12] [153]

According to several studies, SF cement paste performs poorly at high temperatures (contrasted with its impressive long-term stability at ambient temperatures). This phenomenon is due to its high-dense microstructure and low permeability, which hinder vapor escaping from the concrete matrix and thus encourage pore pressures to build up quickly during the heating process [133,137,162].

However, concrete spalling due to fire can be minimized in low permeability concrete by adding PPFs to the mix or by covering the exposed concrete surface with thermal insulation [133]. Aggregates are also important since some, like flint, will degrade at low temperatures (below 350 °C), while others, like limestone (600 °C), can withstand greater temperatures [159]. The composition and thermal stability of aggregate varies based on the aggregate type, which could be rated from high to lower thermal stability as gabbro > granite > basalt > limestone > flint [1]. Other desirable aggregate characteristics include (1) low thermal expansion rate, which may equate to thermal expansion associated with the cement paste; (2) the surface is rough and angular, strengthening the physical connection between the cement paste and the aggregate and (3) reactive silica, which increases the cement paste's chemical bond [163,164].

2.3 Spalling types

Spalling is classified into five types; post-cooling spalling, explosive spalling, corner spalling, sloughing-off, forceful spalling, surface spalling, pore pressure spalling, thermal stress spalling and aggregate spalling

[123]. Reportedly, numerous material (e.g., type of aggregate), manufacturing (e.g., casting method), geometric (e.g., size and shape of section), and environmental (e.g., rate of heating) parameters were found to impact concrete spalling in fire significantly [83]. Fire palling behavior is still a challenge, particularly when spalling in a fire. Therefore, knowing HSC spalling behaviors when subjected to high temperatures is crucial for assuring the safety of a structural fire design that incorporates HSC. Five spalling types include post-cooling, explosive, corner, sloughing-off and violent. The usual spalling behavior is described in Table 4 and the influencing factors that cause it.

Table 4: Description of typical spalling phenomena with its related mechanisms

Compartment	Type	Violent	Sloughing-off	Corner	Explosive	Post-cooling	Refs. [83]
	Pore pressure is caused by evaporation of moisture.	√	x	x	√	x	[78].
	Compression resulting from a thermal gradient.	√	x	x	√	x	[79]
	The heat expansion of aggregate and cement paste causes internal cracking.	√	√	x	x	√	[80]
	Steel and concrete have differing thermal deformations, which causes cracking.	x	x	√	x	x	[2]
	Strength loss as a result of chemical transitions.	x	√	x	x	√	[81]

2.3.1 Aggregate spalling

The bursting or splitting of aggregates at the concrete surface is usually linked to aggregate spalling. Aggregate spalling occurs when aggregate fails at the surface, causing tiny fragments to shoot off the surface [165]. This spalling does not affect structural performance and solely causes cosmetic harm. Several solutions have been presented to prevent concrete from spalling explosively at high temperatures [36]. The addition of PPFs to high-strength concrete can mitigate explosive spalling [115,166,167]. Moreover, the inclusion of steel fibers [115,166–168] and larger aggregates [93,154,169] substantially affects the concrete's explosive spalling. High-temperature melting of PPFs results in the formation of empty fiber tunnels that link the porous interface transition zone (ITZ) between the matric and aggregate, thereby increasing the concrete permeability. [147,170]. According to some reports, high moisture conditioned aggregates in HSC, such as saturated lightweight aggregate, can result in severe violent spalling due to the addition of water [171].

Researchers have proposed different theories to explain spalling, including aggregate physicochemical changes, such as polymorphic inversion of quartz [159] and thermal incompatibilities between aggregate and cement paste [126]. The PPFs are hypothesized to connect the aggregates' ITZs, forming a percolated network, thus releasing developed pressure from water vapor [172]. Also, that cannot account for the effect of PPFs in

HSC and UHPC, which lack a distinct porous ITZ [173]. According to scanning electron microscope (SEM) observation (Fig. 9), the thermal mismatch between the embedded PPFs and the concrete matrix results in the formation of microcracks that facilitate the formation of an interconnected network for moisture release [96]. According to another study [115], concrete supported with PPFs of 18 μm in diameter had a lower maximum pore pressure than that containing PPFs of 11 - 28 μm in diameter. As their high fiber aspect ratio allows percolation through the concrete matrix, longer PPFs are more effective at decreasing pore pressure [115,174]. Because cement paste has a higher coefficient of thermal expansion (CTE), aggregates have a lower CTE [175,176]; this means that maximal principal stress lengthways with the matrix–aggregate contact happens in the aggregates outspread direction. Therefore, fractures spread largely in the peripheral direction at the matrix–aggregate contact and might spread into the matrix due to this phenomenon [175,177].

Additionally, the optimal fiber length for spalling protection based on the size of aggregate (i.e., coarse aggregate is greater in size, it has a longer ideal length of fiber for spalling prevention) [178,179]. As illustrated in Fig. 9, thermal expansion of PPFs and aggregates caused microcracks to emerge, according to microstructural analysis, indicating that both increased the connectivity of PPF channels and thus facilitated pore pressure release [36,37,179]. Additionally, the size and geometry of PPFs have a substantial influence on the system of pore pressure at elevated temperatures. It is extra operative to decrease pore pressure with micro PPFs (18 m diameter) than macro PPFs (740 m diameter), since pore pressure may be reduced by increasing the fibers number per unit volume [166]. Melting PPFs leaves pathways between the porous ITZs between the matrix and aggregates [36], thereby increasing the concrete permeability at elevated temperatures, as demonstrated in Fig. 10a [180].

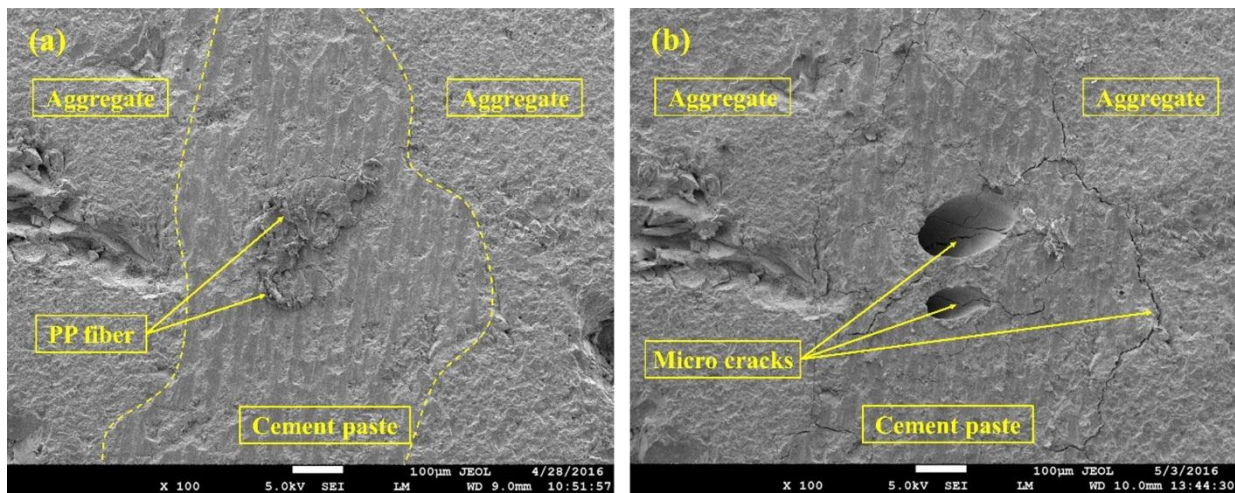


Fig. 9: Microcracks produced as a result of the thermal expansion of PPFs and aggregates after being exposed to high temperatures (Adapted from [36])

The ITZ accounts for a large portion of the overall paste volume in conventional mortars and concretes [181]. However, no substantial porous ITZ between matrix interfaces or aggregates and or between matrix interfaces and fibers were detected in HSC [182]. This phenomenon is due to the very low w/b ratio and the tiny particle size of the SF in the cement paste that caused the pozzolanic reaction, which resulted in a compacted cement paste [181]. The Ca(OH)_2 formed during the first stage of the hydration process and interacted with silica particles to form additional CSH [183]. On the other hand, fine silica particles contributed to a more dense microstructure by filling in gaps and holes within the cement matrix and ITZs. In light of the microstructure analyses stated above, new models are offered in this work to reflect the impact of PPFs and coarse aggregates on HSC permeability at increased temperatures [36]. Micro-cracks can be generated in HSC samples by PPFs and/or coarser aggregates thanks to the thermal extension and divergence between matrix and aggregate/fiber, as stated in the previous section. High-stress locations generate microcracks, which spread to the weakest points of the material, releasing tension [184]. Due to micro-cracks forming at increased temperatures, unfilled PPF tunnels in UHPC-PPF may be linked together (Fig. 10a), bond cracks alongside with aggregate in HSC-AG (Fig. 10c [36]), or both in HSC with PPF and aggregate (HSC-PPAG) (Fig. 10b). HSC permeability has increased due to the formation of this microcracks network and releasing a large portion of stress due to heating. The combination of PPFs and larger aggregates causes matrix cracks (Fig. 10d) [36].

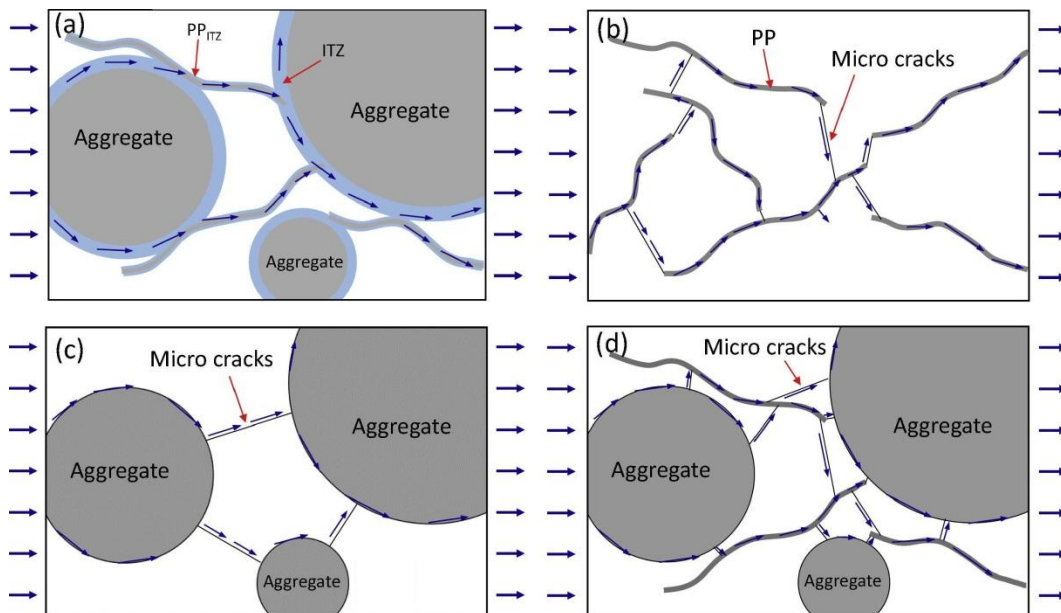


Fig 10: Permeability model (a) larger aggregates with PPFs in normal concrete. [180], (b) HSC with PPFs, (c) larger aggregates in HSC, and (d) larger aggregates with PPFs in HSC at elevated temperature (Adapted from [36])

The specific surface area of matrix cracks, number of micro cracks and volume fraction are projected to be bigger in HSC-PPAG, explaining why permeability increases at increasing temperatures. Research into the characterization of microcrack systems is required to deliver measurable analyses. However, the matrix-aggregate interface and the matrix-fiber interface in HSC did not show any significant porous ITZ. In summary, additional study is needed to determine the efficiency of utilizing aggregates and fibers in HSC to avoid explosive spalling. Table 5 presents the different classifications of HSC spalling and their corresponding prompting agents.

Table 5: Different classifications of HSC spalling and their corresponding prompting agents

Type	Nature	Time of occurrence, minutes	Sound aspects	Controlling factors	Degree of risk	Refs.
Explosive	Violent	7 - 30	Loud explosions/ bangs	Material, mechanical, structural, and temperature	Severe	[72]
Progressive gradual	Nonviolent	At the stage of final strength loss capacity	N/A	Mechanical / structural	Semi-severe	[121,185]
Surface	Violent	7 - 30	Existence of creaking/cracking	Material	Semi-severe	[1]
Post-cooling	Nonviolent	During and after cooling of moisture absorption	N/A	Mechanical / structural	Semi-severe	[91]
Corner	Nonviolent	30 - 90	N/A	Mechanical, structural, and temperature	Semi-severe	[1,86]
Aggregate	Cracking	7 - 30	Small pops	Material	Shallow	[105]

2.3.2 Violent spalling

Small or large concrete fragments may be violently spalled from the cross-section of concrete elements. This releasing energy involves snapping the pieces and little slices off at a certain pace while generating a popping or cracking sound [186]. In this kind of spalling, the internal meso-level cracking, pressure gradients and temperature changes in the pores all play a role [87]. Because of lateral restriction, the massive thickness of concrete, prestressing, rapid heating and reinforcing resulting in surface compression might increase during heating. Thus, porosity, permeability, moisture content and heating rate, and PPFs affect pore pressures [2,88,115,121].

There are two types of fire-induced concrete spalling based on behavior of fire spalling: violent and non-violent spalling [186]. The spalling mechanism can be divided into thermochemical, thermo-hydraulic, and thermo-mechanical spalling [87]. Thermo-hygral spalling, often known as “violent spalling,” is aggressive in

nature, whereas thermo-chemical and thermo-mechanical spalling are typically non-violent [187]. The thermo-hygral spalling is the most severe of the three forms of thermal spalling because thermo-hygral spalling happens quickly and because it happens in the early phases of fire [71]. As a result, predicting and preventing concrete thermo-hygral spalling is critical [186].

When it comes to improving the mechanical properties of concrete, steel fiber is a typical choice of fiber. [188,189]. In terms of fire spalling conditions, steel fibers embedded into concrete positively impact the concrete mechanical behavior at high temperatures, thus boosting toughness and reducing cracking [190,191]. On the first hand, the extent to which steel fibers might prevent violent concrete spalling is currently not fully known [192]. To address this scientific issue, it is reported that the addition of steel fibres of 2.0 vol.% and PP fibres of 0.2 vol.% were added to the RPC matrix. The test results showed that only a small number of RPC pieces fell off from the specimen surface, and the spalling effect on the response of RPC beams to fire was not significant [109]. Further, four RPC beams coated with fire insulation under fire. The observations after the fire test showed that no spalling occurred in these RPC beams [193]. Besides, the results were compared to FE predictions and existing fire test results including the effect of fire insulation parameters (e. g. the thickness, thermal properties, setting mode, height, and damage to local fire insulation) on reinforced RPC beams' fire resistance and exhibited that the failure of reinforced RPC beams with partial loss of fire insulation occurred at the area of lacking fire protection [110,194]. It is also revealed that the steel fibers can increase the elasticity of concrete, thereby reducing the risk of this kind of spalling [83,195–197]. On the other hand, steel fiber diameter and length have not been well studied in aggressive spalling [198]. However, conducting extensive experimental tests is the simplest technique for determining the aggressive spalling of concrete [199].

The violent spalling resistance of steel FRC has been examined in several experiments [39,199,200]. However, experimental tests are usually expensive and time-consuming, and they are only applicable to specific concrete mixes. As a result, alternative methodologies for evaluating the violent spalling resistance of steel FRC are required. To predict the violent spalling of concrete, the finite difference approach and the finite element method (FEM) are considered two alternative techniques [82,141,153,201]. However, these numerical models were only utilized to assess simple concrete situations and did not consider steel fibers [153]. Additionally, these models require the permeability of concrete as a critical parameter, which is exceedingly tough to determine. Historically, some permeability tests on concrete were conducted at isothermal or residual temperatures [202,203]. Meanwhile, the numerical models require permeability in a transient hot state. Consequently, using these models to predict the severe spalling of various steel FRC combinations is presently

unconvincing. In summary, in addition to the FEM, an alternate numerical approach that can accurately predict the explosive spalling of heated steel FRC is still desired.

2.3.3 Progressive gradual spalling

It is reported that when the cement paste weakens owing to chemical degradation (micro-level) and internal cracking (meso-level), a process known as sloughing off takes place. This spalling occurs when the concrete reaches a too high temperature (instead of heating rate). Due to its diminished strength at high temperatures, little pieces of concrete fall without producing a sound when they are heated to a high enough temperature. Gravity pulls the broken concrete particles from the cross-section of a slab that has been heated from below, increasing the likelihood of this kind of spalling occurring. When all four sides of the columns are heated, significant pore pressures develop on the hot sidewalls, pushing a portion of moisture further into the column's colder center [2]. The compression of the heated surfaces caused by the thermal gradient and external loading results in internal pressure, and the whole heated surface may go off with a boom. This phenomenon reduces the efficiency of the column's cross-section considerably and advances other failure modes, such as strength loss, shear, and buckling. Based on real-world testing conducted in the early 1990s [146] and the research into the 1999 Mont Blanc fire and other tunnel fires, tunnel fires can spread swiftly and burn for an extended amount of time [204]. An examination of the impacts of fire-induced concrete spalling is a standard part of traditional structural fire engineering design to reduce the danger of structural collapse during fires in tunnels [205].

Several studies revealed that the presence of macro and micro PPFs and the temperature of the surface when the first spalling event occurs have a negative impact on the time until the first spalling event [204]. Another research revealed that even though spalling was progressing, it came to a standstill between 9 and 18 minutes after the tests began. These circumstances demonstrate that the rate at which fire heats up significantly affects the occurrence, depth, and kind of spalling [79,206]. The higher the heating rate is, the more likely progressive spalling will occur, with shorter spalling times, shallower spalling depths, and less energy consumed. Slower-heating fires cause greater temperature disparities at the spalling depths. Temperatures at spalling depth were as high as 240 °C [79]. According to Liu [71], such temperatures coincide with the thermo-hygral spalling type. The sole specific spalling mechanism can never occur without the effect of other mechanisms. Due to the imposed mechanical loading, the thermo-mechanical mechanism had an evident influence on the results of this study [207]. However, because the loading was applied using a force-controlled hydraulic actuator, the thermal expansion of concrete did not contribute to the formation of stresses in the

vertical direction along the exposed sides of the samples. Therefore, the sample might expand without experiencing an increase in compressive stress [208]. As a result, it cannot be called a constrained structure. However, the findings of the study revealed that “faster” concrete specimen heating results in progressive spalling with less damage per single spalling event, but “slower” heating results in a longer spalling time but a single deeper one-time damage [204]. Aside from that, faster heating rates necessitate less total energy and a less steep temperature gradient to cause spalling [206].

Based on these data, researchers should focus on "slow" and "rapid" heating regimes to cover both identified types of spalling destruction [79]. The quick vaporization of free and chemically bonded water in the concrete matrix during heating causes increases internal pore pressure, which eventually leads to concrete degradation and collapse at the surface [209]. Thus, spalling occurs when porosity in the matrix is insufficient for vapor to escape, thereby causing small to large pieces of concrete to separate from the substrate. This phenomenon can happen in different ways. Spalling can be progressive (due to a slow rise in temperature) or explosive (when huge parts of the concrete are lost all at once, potentially exposing the reinforcement beneath the surface) during fire circumstances.

2.3.4 Corner spalling

As a result of a concrete corner fracturing, the term "corner spalling" is used to describe this kind of spalling. (i.e., beams or corners of columns fall off). When heated inhomogeneously, concrete deforms (ovalization) around an evenly heated reinforcement bar. Splitting stresses in concrete result from differences in deformation, causing the corner of a column or slab to come off due to splitting cracks. According to reports, an analytical spalling model has been proposed [210,211] and has verified the results in Bažant [212], who confirmed two forms of spalling: triangle and layer spalling. In actuality, corner spalling is usually detected in the laboratory or situ (Fig. 11).

By this point in time, three forms of spalling were defined: corner, layer, and triangle spalling [211]. Spalling of concrete prompted by corrosion of steel has been studied in the past. Through on-site research and analysis, it was recommended that the loss of the radius of rebar of up to 50 μm was required for cover of concrete encrusted spalling [213]. To cause concrete cover spalling, a corrosion-induced fracture width of 0.50–1.0 mm was predicted [214]. A corrosion-persuaded fracture width of 0.1 to 1.0 mm was needed [213]. A theoretical approach was suggested that utilized mechanics of fracture and the opening of cracks in concrete to detect when concrete cover spalling due to corrosion of steel reinforcement began [182]. When the critical

fracture width surpassed 0.5 mm, layered spalling was anticipated. Spalling occurs when the crack's width exceeds a 1.0 mm critical limit [214].

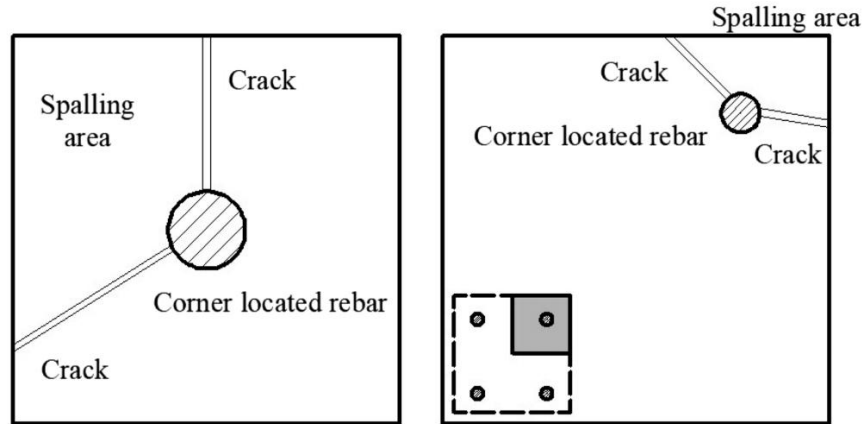


Fig. 11: Corner spalling: Courtesy to Zhao et al.’s test (Adapted from [211])

Another study found that concrete spalling happened most frequently at the corners of columns, where the spalling reached to the reinforcement bars through the exposed cross-section in some spots [77]. FIB refers to this sort of spalling as corner spalling [9] and thermal stresses in the element cause it. Because of the crushed sand utilized, the surface of the concrete was uniform in color and look, with little black dots randomly dispersed throughout [76]. As the size of the basalt aggregates increased, the surface appearance became smoother and darker, indicating a vitreous aspect. Most happened between 5 and 20 minutes after the exposure when the furnace temperature was between 500 and 750 and 100 °C was the temperature of the columns, i.e., during evaporating water present inside the concrete [77]. Overall, spalling occurred mainly at the corners of columns during the fire resistance tests and, in some instances, spread over the whole column's exposed cross-sections.

2.3.5 Explosive spalling

Increasing pore pressures and the thermal stress caused by cross-sectional temperature gradients results in explosive spalling. The explosive spalling of fire-damaged concrete occurs as an outcome of cracking that results from the decomposition of binder and aggregates, and accumulative stress resulting from pore pressure build-up [8]. As a result of the pressure gradient from the heated side to the cooler side, a “moisture blockage” (i.e., a region of high pore pressure) develops on the heat-exposed side, thereby pushing pressure deeper into the cooler area of the concrete. If the permeability of the concrete was low, the stress from the build-up of pore pressure would build up more on the hot side, thus causing the entire heated surface to explode and blow out

with a loud bang. Explosive spalling is particularly damaging because it lowers the insulating capability of the concrete cover by reducing the section (the face is protected from further damage by the evacuation of fragments) [8]. Fire spalling refers to the abrupt separation of concrete splinters from a hot surface caused by cracking and pore pressure buildup [157]. Under these occurrences, studies carried out to investigate the fracture behavior caused by fire on hot concrete subjected to sustained pore pressure support the notion that spalling is often instigated by a integration of mechanical stress and pore pressure [187,215]. Concrete spalling attributable to the system of pore pressure significantly increases the overall thermal damage to the fire-damaged structure, leads to higher repair costs, and, in some cases, compromises structural stability by reducing the mechanical performance of the structural member and removing reinforcing protection [8]. High-performance concrete is particularly susceptible to this spalling (high pore pressure) because of its essential material characteristics, such as unbalanced fracture behavior and limited permeability.

Multiple researchers investigated the strength properties of concrete contacted to elevated temperatures while also applying preload [44,49,104,171,216]. None of the pre-loaded specimens in their studies could withstand loads above 700 °C; approximately 1/3 of these specimens collapsed because of explosive spalling at temperatures that range from 320 - 360 °C while being fired under a constant preload [217,218]. All preloaded cubes that were heated at a rate of 32 °C per minute showed spalling [12]. Columns and beams, which receive heat from several directions, are more prone to spalling than any other structural component [86]. It is possible that large areas of the cross-section might explode if the moisture-clogged concrete is heated from both sides, resulting in a huge increase in pressure in the pore space. [105]. Furthermore, in the case of protecting the concrete surface with an insulating coating, this form of spalling can occur even after the fire has been extinguished for an extended period [167]. Excessive pore pressure within the concrete causes explosive spalling [78]. When concrete is exposed to fire, free and bond water within the concrete begin to evaporate. If the concrete has limited permeability, then pore pressure begins to build up, thereby causing stresses to be induced on the internal structure of the concrete [8].

Several researchers [78,168,219–221] investigated the use of PPF to prevent explosive spalling. Several studies [70–72,74,76,77,83,123] found that the increased temperatures and spalling are primarily produced by a temperature gradient and increased pore pressure in concrete. [143,175]. Also, high vapor pressure is produced by the interior moisture of concrete at high temperatures. In contrast, thermal stress arises in the concrete owing to the difference in coefficients of thermal evolution between the particles and the cement [176,222]. Compressive stresses are created on the surface due to the temperature gradient developed by one-sided heating, hence resulting in interior cracking (Fig. 12). In most circumstances, the combination of the two mechanisms

outlined above is required for explosive spalling [12,14,121,124,143,174]. The good dispersion of PPFs used to restrict spalling showed remarkable results preventing developing cracks [70,174]. They might connect several different types of pores, including air pores, gel and capillary [53]. When concrete containing PPFs is subjected to high temperatures, the PPF melts and forms wide and long tunnels in the concrete [223]. These channels link to other pores and provide a pathway for vapor to exit, which aids in the heating stages in decreasing vapor pressure inside the concrete element. Additionally, the channels reduce thermal stress due to the freeze-thaw cycles generate less damage when entrained air is present in concrete. [70,224,225].

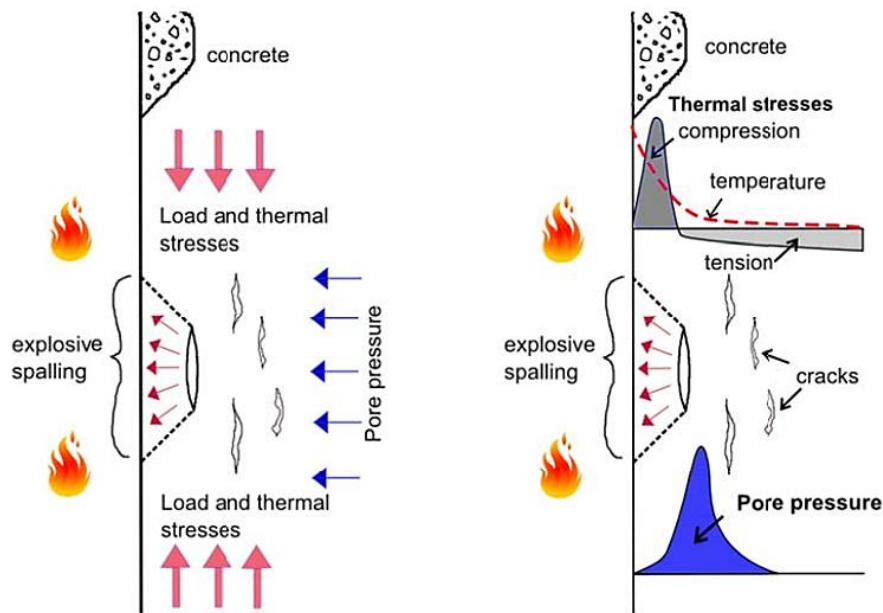


Fig. 12: Stresses close to the heated surface (Adapted from [226])

2.3.6 Post-cooling spalling

It is possible to have post-cooling spalling after a fire has been extinguished, during the extinguishing process, or even after the concrete has cooled [227]. This sort of spalling was seen in calcareous aggregate-containing concrete. Rehydration of CaO to Ca(OH)_2 after cooling, which expands more than 44%, is a possible explanation for this. [71,228]. This phenomenon happened when concrete cooled, and moisture returned to the surface. The expansion caused by rehydration induces significant internal cracking on the meso-level, thereby resulting in total concrete strength loss [157,229]. As long as the water is available to rehydrate the CaO in the dehydrated zone, pieces of concrete will continue to fall down because of the expansion that resulted from the formation of Ca(OH)_2 . If no spalling happens during cooling, substantial post-cooling spalling, including the full disintegration of concrete, may occur weeks after cooling at ambient temperatures and have a major impact on the performance of the building [230]. The second part of Khoury's description [9] should be expanded to

include exposure to high and quickly elevated temperatures, as seen in fire because delayed spalling can occur even after a long period of exposure to high temperatures. Spalling happened after the 300 mm HSC specimen had been detached from the furnace and permitted to release heat at ambient temperature. The sloughing-off thermal chemical spalling that occurs at extremely higher temperatures and the post-cooling spalling that occurs after being exposed to extremely higher temperatures have been described previously [84,85]. The breakdown of cement-aggregate bonds, for example, Ca(OH)_2 and calcium silicate hydroxide, is the most common cause of thermal-chemical spalling [161].

Thermal-chemical spalling occurs at a temperature of approximately 750 °C, which is a relatively high temperature. In the previously mentioned experiment, the 300 mm specimens were heated for approximately 3.5 hours. The temperature of the specimen core has been revealed to continue rising for a length of time even after the furnace was turned off [84]. As a result, the greatest observed core and gas temperatures were 713 and 1213 °C, respectively, indicating that most specimens had been heated to more than 700 °C (Fig. 13) [231]. Post-cooling spalling can therefore be regarded as reasonable [85]. In another investigation, the sloughing-off spalling type of thermal-chemical spalling was seen in all test specimens at exceptionally high temperatures (700 °C and 800 °C) [91]. Samples showed signs of post-cooling thermal-chemical spalling in the form of a web of microscopic cracks after cooling. Chemical-thermal-spalling occurred as a result of the breakdown of aggregate cement linkages; calcium silicate hydroxide and Ca(OH)_2 [84,85,232].

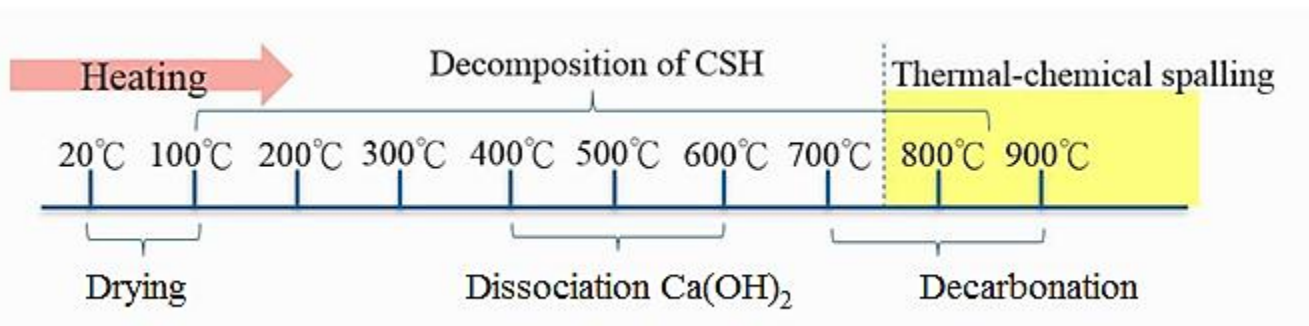


Fig. 13: Temperature range of thermal-chemical spalling (post-cooling spalling) (Adapted from [231])

According to their influence on concrete strength loss, high temperatures are classified into three groups, called 20 – 400, 400 – 800, and > 800 °C, according to their influence on concrete strength loss [232]. Unlike normal strength concrete (NSC), HSC largely retained its original strength during the temperature range of 20 – 400 °C. Most of the strength of HSC and NSC was lost between 400 and 800 °C, particularly at temperatures beyond 600 °C. Merely a tiny percentage of the required strength of concrete was preserved at temperatures over 800 °C. Heating exposure has a substantial effect on the tensile strength of steel when the temperature

approaches 700 °C. It has been shown in tests that heating exposure may significantly influence the tensile strength of steel [233]. Due to these findings, 700 and 800 °C heating temperatures were expected to severely diminish the load-carrying capability and toughness of fired samples at the uppermost temperatures [234,235]. After being heated to 700 and 900 °C for 180 minutes and subsequently released heats at a room condition, the residual flexural response of five simply supported RC T-beams was examined for the influence of 31.6 kN of service loading at extreme temperatures. All beams were put through a series of static four-point bending tests following the fire test until they failed. They reached the conclusion that a continuous 31.6 kN service loads had a detrimental influence on the post-heated flexural performance of the RC beams. Post-fire stiffness and ductility were more strongly influenced than strength [236].

A nonlinear analysis model for reinforced concrete beams that utilize the ABAQUS finite element program is also proposed [237]. The suggested model considered the properties of steel and concrete during and after a fire (e.g., during a heating phase in the steady and transient state and a cooling stage in the open air) [89]. Following a fire assault, considerable plastic deformations in reinforced concrete beams were found. Reinforced concrete beam performance is impacted by several elements, including the physical and mechanical deterioration of its component materials due to fire and heat dispersion through the member.

3 Fire-induced spalling behavior of HSC conform to ISO 834 standard fire test

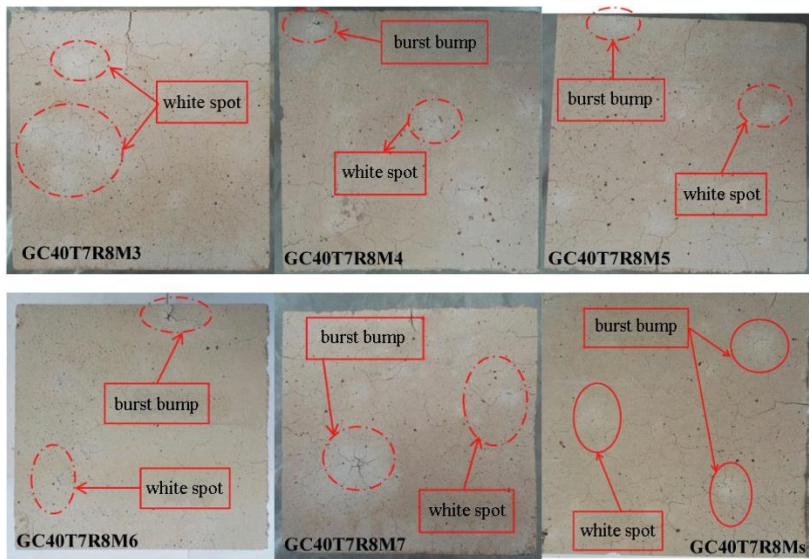
It is reported that alkali-activated high-strength concrete (AA-HSC) is considered more resistant to high temperatures than regular concrete [63,238]. The residual compressive strength of AA-HSCs is greater than that of OPC in recent experiments [81], during exposure to high temperatures results in better splitting strength retention [10]. The fire-induced spalling behavior of AA-HSC must be defined before it can be used in structural applications. Only a small amount of data on AA-HSC spalling behavior is currently available. Two types of simulated fire tests were effective on AA-HSC and OPC concretes with compressive strengths between 40 to and 100 MPa: the standard fire exposure test and rapid surface temperature exposure test [239]. AA-HSC specimens did not show any signs of spalling; nevertheless, the specimens made of Portland cement-based concrete did show signs of fire-induced spalling. A heating system rate comparable to the ISO 834 standard fire exposure is used. When using FA-based AA-HSC and OPC concretes, it is reported comparable findings in 39 to 58 MPa compressive strengths [81]. Acoustic emission measurements on two kinds of FA-based AA-HSCs, composed of expanded clay (low weight) aggregates or quartz aggregates, were employed to analyze the composites' spalling pattern and cracking [81]. There were no symptoms of spalling in these specimens after they were subjected to the ISO834 standard fire for 30 minutes. However, the aggregate size

significantly influences the spalling of concrete at fires [240]. It is found that when the maximum size of aggregates was smaller than 10 mm, explosive spalling happened in both standard strength of OPC, HSC and AA-HSC [124]. Concretes with a maximum of 14 mm aggregate size showed no signs of spalling. Table 6 displays the temperature information provided by various researchers at the time of spalling of unrestrained and unloaded specimens. If the spalling temperature can't be accurately measured, it should be somewhere between the reported surface and core temperatures (Table 6) [156]. In brief, the experimental results typically match the hypothesized thermo-hygral spalling temperature range.

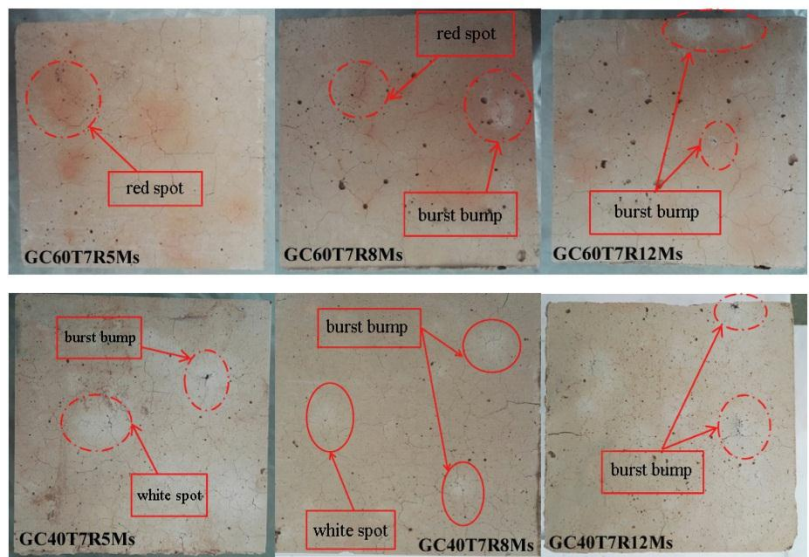
Table 6: Information on the temperature at the time of spalling of unconstrained and unloaded specimens

Spalling	Surface	Temperature		Heating rate, °C/min	Heating methods	Refs
		Gas	Core			
<400 °C	–	300, 400 °C	–	1 - 3	Radiant heater	[163]
250–300 °C	–	–	–	1	Heating–cooling cycles	[202]
240–450 °C	–	300, 450 °C	240–280 °C	5	Heating–cooling cycles	[241]
190–250 °C	–	–	–	6	Heating–cooling cycles	[114]
<315 °C	–	315 °C	–	1	Heating–cooling cycles	[242]
<355 °C	355 °C	–	–	0.1 and 1	Heating–cooling cycles	[243]
150–319 °C	245, 291, 319 °C	–	150, 223, 262 °C	3 - 6	Radiant heater	[143]
256–433 °C	297–433 °C	–	256–304 °C	-	Standard fire - ISO 834	[121]
<455 °C	–	425, 455 °C	–	2.5	The fire-heating test	[244]
<400 °C	–	400 °C	–	1 - 10	The fire-heating test	[4]

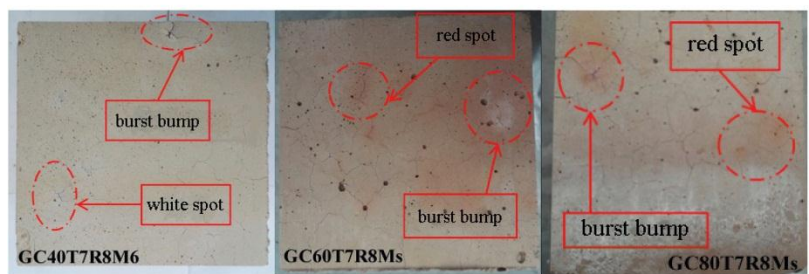
After being exposed to various increased temperature levels, specimens were visually evaluated, and observations of physical characteristics such as the amount of spall, color change, or cracking were noted (Fig. 14) [156]. One of the most important factors that impact the concrete explosive spalling is the concrete's moisture level. The probability of spalling is usually assumed to increase with moisture content [245,246]. As can be seen in Fig. 14a, the appearance of surface of six different series of samples after contacted to 700 °C. [156]. Evidently, none of these specimens were subjected to severe amounts of spallings. After being heated to greater than 700 °C, the minerals admixtures-based concrete became a light pink tint, and many cracks developed. No severe concrete spalls were seen in these samples, despite the presence of several burst bumps on the surface (Fig. 14b). The condition of these specimens after being exposed to 700 °C is shown in Fig. 14c [156]. Higher compressive strength samples showed greater heat cracking but no significant spalling in any of the samples [1,247]. Different concrete kinds have different densities and pore structures, but the temperature gradients created during heating are identical [2]. Significant studies have been conducted to generate more knowledge about the performance of several types of concrete, including the mechanism of spalling and behavior during fire [2,12,70,144,163,167,172].



(a) With different moisture contents



(b) With different heating rates



(c) With different strength levels

Fig. 14: Exposure to extreme temperatures on AA-HSC specimens (Adapted from [156])

In addition to considering AACs, a more environmentally friendly binder than OPC [124,133,248], numerous studies also revealed that AA-HSC was outperformed by normal concrete in terms of mechanicalness and durability [156,245,249]. Further studies revealed that AAC also performs better than OPC concrete at elevated temperatures [58,135,250]. Although understanding the strength and fracture properties of AA-HSC at higher temperatures during a fire is critical, the spalling mechanism and spalling behavior of AAC concrete during a fire are also considered a critical matter [240,250–252].

Spalling affects the load capacity of structural elements and the stiffness of approximately all types of concrete. It reduces their cross-sectional area and propagation of cracks through the entire cross-section [253]. Reinforcements have been exposed to fire due to the spalling of concrete covers on construction components, impacting the reinforcement steel's mechanical behavior and, as a result, its overall structural capability. Although AA-HSC demonstrated greater resistance to fire than its OPC concrete counterpart, only a few researchers have explicitly investigated AA-HSC's spalling behavior during a fire. The spalling of AA-HSC panels in the presence of hydrocarbons has been investigated [254]. The researchers subjected 200 mm thick FA-based AA-HSC panels to a hydrocarbon fire for two hours in line with EN 1991-1-2 [255], where they have not recorded any explosive spalling noises in this case. However, only two of the four panels tested showed any concrete spalling, with an average of 4.65 %. A study on the spalling behavior of FA/MK-based AA-HSC cubes treated to fire with degree about 700 °C in an electric kiln was recently published [156].

It is noticed less spalling in FA-MK AA-HSC than in OPC concrete, owing to the former's strongly linked pore structures and reduced strength degradation. Another study exposed FA-based AA-HSC to cyclic heating of up to 550 °C and found that the compressive strength remained steady even after heating cycles [256]. It is also reported the exposure of FA-based AA-HSC samples with a 125–175 mm thickness to gas fire in a incinerator for two 120 minutes [249]. Additionally, they reported no spalling of AA-HSC after two hours of exposure to a gas fire. The panels in the preceding experiments were not restrained in-plane from simulating the actual-state scenario of bi-axial stress accurately, and the vapor pressure within the networks of the samples was not measured because of the increase in concrete temperature [245]. These two variables are critical in comprehending the spalling behavior of AA-HSC during a fire. After being heated to 1000 °C, each AA-HSC sample exhibited cracking and a color change (from dark gray to light brown) on its surface (Fig. 15) [59]. Consequently, the oxidation of iron species inside FA particles during heating is to blame for the color change [28,257]. Table 7 shows the possibility of spalling in various HSCs subjected to high-temperature exposure, as reported by previous researchers.

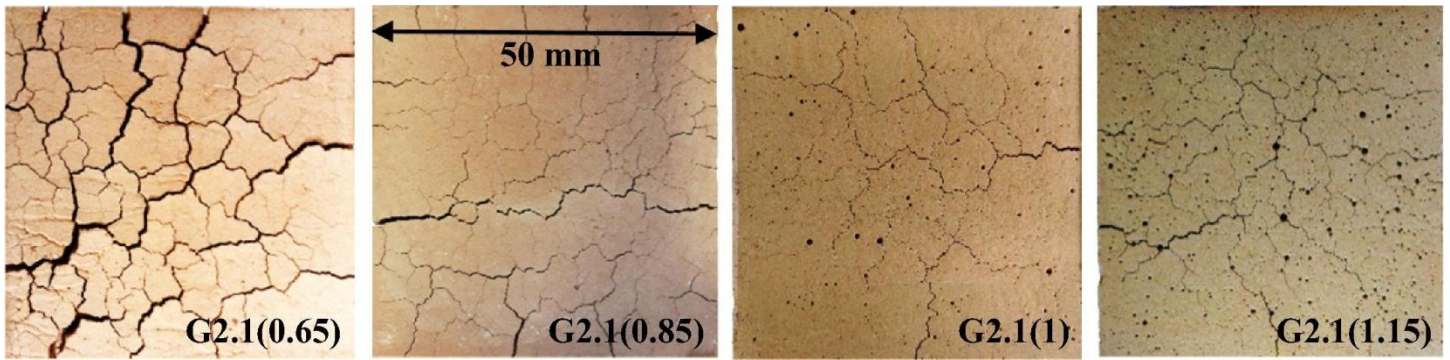


Fig. 15: Outer-face of AA-HSC specimens exposed to 1000 °C (Adapted from [59])

Table 7: Possibility of spalling in various HSCs subjected to high temperature exposure, as reported by previous researchers.

Possibility of spalling (%)	Specimen Size, mm)	Compressive Strength, MPa	Heating Rate, °C/min	Temperature of spalling, °C	No. of tested samples	Fibers. %	Type of concrete	Refs.
82.1	100 × 200	101.6	5	600	3	-	UHPC	[14]
100% spalled after one hour	100 × 200	80	In line with ISO-834 curve	-	-	0.05 and 0.1% PPF of 0.04 mm dia.	HSC	[179]
14.39	160 × 320	39- 72	1	450	264(38)	-	HSC	[243]
100	100 × 200	93-128	5	600	60	-	UHPC	[186]
No spalled after one hour	100 × 200	80	In line with ISO-834 curve	-	-	0.012, 0.025% PPF of 0.02 mm dia.	HSC	[179]
12.73	100 × 200	50-98	5	300	165(21)	-	HSC	[138]
100% spalled after one hour	100 × 200	80	In line with ISO-834 curve	-	-	0.2% PPF of 0.04 mm dia.	HSC	[179]
42.5	160 × 320	80 - 88	5	400	40(17)	-	HSC	[143]
12.0	160 × 320	73 - 81	1	600	25(3)	-	HSC	[85]
100% spalled after one hour	100 × 200	80	In line with ISO-834 curve	-	-	0.05% PPF of 0.02 mm dia.	HSC	[179]
18.18	160 × 320	110	7.5	-	33(6)	-	HSC	[258]

In regard to the relationship of spalling resistant steel fibers/PPFs dosage with compressive strength, steel and PPFs have both been widely employed to minimize the risk of HSC spalling [12,114]. Steel fibers, in particular, are an efficient approach to increase strengths, leading to reduce spalling and improve residual

strength properties in HSC [168]. The compressive strength, moisture content, and density of HSC are all important factors in explosive spalling [259]. As a result, HSC without fibers might operate worse even than identical concrete grades in terms of temperature resistance, thus, adding steel fibers to HSC (e. g. reactive powder concrete) can increase its durability to high temperatures [260]. One of the most serious issues with HSC is that it degrades when exposed to high temperatures, resulting in loss of strengths and elastic module, cracking, spalling and damages of concrete [261]. HSC has a thick microstructure compared to NSC, making it more susceptible to spalling by preventing water vapor from exiting and resulting in high pore pressure [195]. Previous research revealed that using fibers like PPFs, to increase HSC fire resistance [262]. In comparison steel fibers with PPFs and they have a low melting point, melting at around 160-170 °C in the HSC and producing selectively small holes across the HSC matrix. This pores enable for high levels of dispersion. meanwhile, steel fiber can improve strengths, resistance to tensile cracking, ductility, post-cracking strength, and energy absorption [195]. Steel fibers have a high thermal conductivity, which reduces temperature gradients and eliminates spalling [263]. It is revealed that the addition of 50 kg/m³ of steel fibers to SCC-HSC has been shown to lower pore pressure over one-dimensional spalling experiments [166]. Hybrid fibers (PPFs and steel fibers) can increase the compressive and tensile strengths and strengthened fracture resistance in HSC matrixes to reach excellent performance [264,265]. Fig. 16 presents the reported regression models to compute the correlations between the relative compressive strength and high temperature with different dosage of steel fibers and PPFs as well as with different proportion of SCM contents [264].

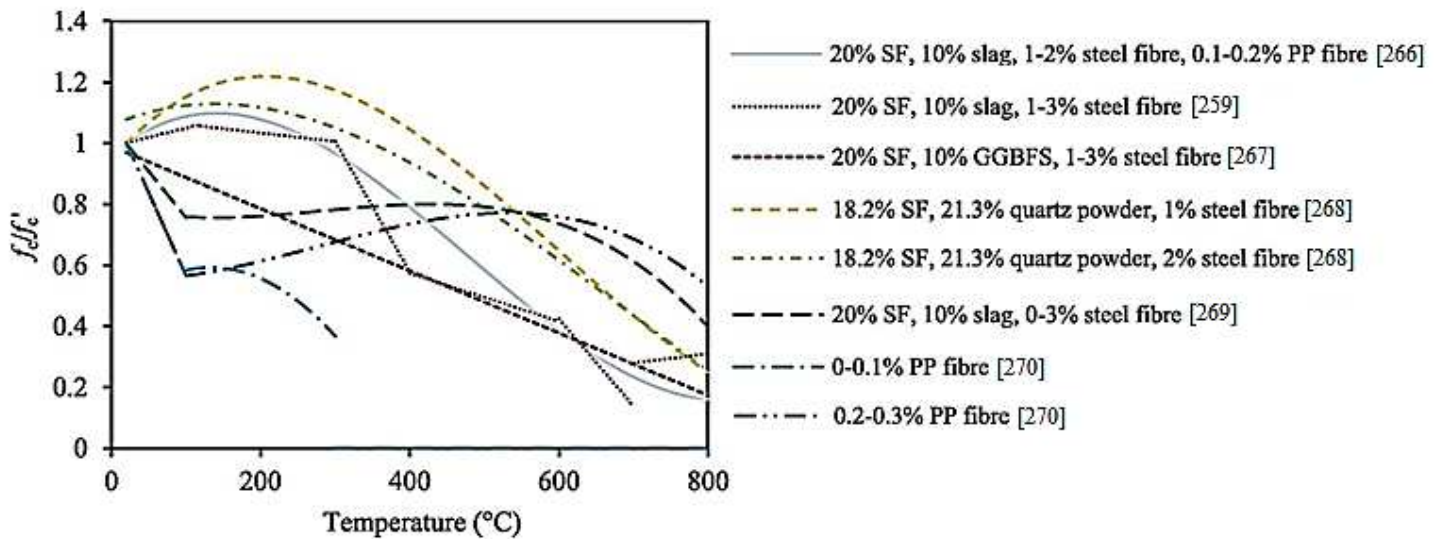


Fig. 16: The relationship between the relative compressive strength and high temperature with different dosage of steel fibers and PPFs (Raw data adapted from [259,264,266–270])

For example, it is studied the addition of 0.2 vol.% PPFs and/or steel fibers to improve the ductility of the HSC that leads to enhance the spalling resistance [271]. It is found that PPF enhanced the HSC spalling resistance whereas steel fiber reduces spalling time. However, the steel fiber does not appear to help with spalling. These findings are consistent with those of Sideris [272], who discovered that steel fiber had a similar influence on high-temperature spalling resistance in HSC. It is also discovered that a 0.15% 12-mm-long PPF dosage may prevent spalling in 68 MPa HSC [273], whereas another study revealed that a PPF dosage beyond 0.20% can prevent spalling in 147 MPa UHPC [274]. The result showed that a 0.20 vol.% PPF intake had a significant effect. These findings, when compared to prior study findings, reveal that the suppression of spalling damage by PPFs is connected to the high-temperature and concrete strength system. It is also exhibited that concrete strength with PPF lengths of 12 and 19 mm had outstanding spalling resistance at high temperatures, and the strength residual rate improved with PPF length [271]. These findings are consistent with those of Bentz [275], who found that the spalling resistance of a long fiber is superior to that of a short fiber in HSC. The addition of PPF with a length of 12 mm to concrete successfully prevents spalling damages to samples in the current testing range.

Moreover, the inclusion of PPFs or steel fibers to the concrete mix can improve the strengths, contributing to improve the fire-induced spalling in HSC members [71,276–278]. PPFs in concrete mix can create a random distribution of macropores and micropores within the concrete microstructure [220]. The high vapor pressure created within a concrete part is dissipated through these pores. Spalling in HSC members can also be reduced by increasing the concrete's compressive and tensile strengths by including steel fibers into the mix [279]. Only a few research have looked at using hybrid fibers (a mix of steel fibers and PPFs) to prevent fire-induced spalling in HSC members [102,280]. The inclusion of hybrid fibers results in greater compressive and tensile strengths and higher porosity, which reduces fire-induced spalling in an HSC component. Numerous research have been conducted to determine the impact of PPFs on the compressive strength and fire resistance of concrete [115,116,147,166,167,170]. The number of PPFs used to prevent spalling typically varies from 1 to 3.5 kg/m³, with few research employing quantities outside of this range [220]. For example, for the lightweight aggregate concrete, amounts ranging from 1.5 to 3.5 kg/m³ have been investigated, with the conclusion that 1.5 kg/m³ is the best value [281]. Previous research has employed PPFs weighing less than 1 kg/m³, such as 0.6 kg/m³, however few studies suggest that 1 kg/m³ of PPFs is best for preventing fire-induced spalling [203]. On the fire performance of HSC columns with hybrid fiber reinforcement (PPFs and steel fibers) only insufficient information is known [282]. In comparison to steel and/or PPFs-reinforced and plain HSC columns, results from numerical analyses and fire resistance testing suggested that hybrid-fiber-reinforced HSC columns

perform better in fire. In brief, the inclusion of hybrid fibers to reinforce HSC was revealed to improve the mechanical strengths and to better enrich the fire resistance and prevent the likelihood of growth spalling.

4 Roles and assessment techniques of HSC spalling

4.1 Spalling tendency

It is reported that the need to study the critical parameters that have the most impact on spalling becomes highly imperative so that fire designers, developers, and builders may assess the likelihood of spalling confidently [283]. However, the available knowledge about the mechanisms, behavior, and parameters that affect the fire spalling of HSC is still infrequent. The readers may find parallel works using a much wider range of variables in prior investigations [284,285]. Many studies have been conducted to model HPC's spalling tendency and provide various solutions, such as active spalling prevention, materials that provide passive or alternate mixture proportions [286]. Adding PPFs appears to be a successful option among the recommended alternatives [8,41,96,225]. PPF melts between 160 °C and 168 °C, whereas HSC begins to spall between 190 and 250 °C [287]. At higher temperatures, melting PPFs creates a new channel for releasing internal vapor stresses [286]. The inclusion of monofilament PPFs more than 2 kg/m³ in HSC is recommended by Eurocode 2. However, the size of the fibers is not defined [288]. According to several studies, concrete spalling can be avoided by using even lower amounts of fibers [3,178,286].

Also, the moisture ratio of 3.5% in concrete was slightly higher than the typically considered safe limits. The concrete with the highest filler tends to spall as it ages [289,290]. When limestone is used as a filler in SCC, the particles of limestone practically never dissolve until the temperature reaches 700 °C, and the loss in the weight of the SCC is significantly less than that of HSC before reaching to 700 °C [291]. Similarly, limestone is frequently used as a filler when creating self-compacting concrete. However, tests have revealed that when exposed to fire, this phenomenon results in increased spalling tendencies [290]. The research conducted on SCC concrete revealed that self-compacting concrete has a significant tendency to spall, but it may be overcoming this challenge by adding a small amount of PPFs to SCC.

Pan et al. [124] found that many AAC and OPC specimens failed explosively during temperature exposure. The sudden fracturing of concrete at elevated temperatures is known as explosive spalling. This phenomenon is followed by a loud bang, which instantly indicates the release of a significant quantity of energy, where the fragments are hurled in all directions because of the released energy. The spalled concrete particles were split into very small bits during this procedure. According to the findings of another study [223], PPF's cross-sectional area may impact the residual mechanical indexes and the probability of FRC spalling

when subjected to high temperatures. External loading, in particular, changed the concrete's mechanical properties and raised the danger of spalling and brittle failure. In concrete specimens that contain PPFs, a trend for reduced interior damage that resulted from internal stress developed by confined pore pressure is observed [289]. This can be seen by looking at the ultrasonic measurements results. The maximum heating rate, 5 °C/min, led to the rapid sound velocity for concrete that contains PPFs. However, this was not readily apparent when heating rates and accompanying thermal gradients were reduced to 1 and 2 °C per minute. Nonetheless, a heating rate of 5 °C per minute is more realistic than 1 or 2 °C per minute in a genuine fire scenario. Furthermore, specimens with a higher C30/37 concrete strength class had a greater propensity to spall independent of the SCC mixture type; however, when PPFs were added to the mixtures, no explosive behavior was observed, and a considerable decrease in the mechanical characteristics of concrete was observed [286]. Moreover, cover distance, longitudinal reinforcement ratio, and tie diameter have a link to the spalling occurrence (i.e., These components would decrease the chances of spall and raise the possibility of not spall if they were increased) [292].

4.2 Residual strength tests

High-temperature exposure has a negative impact on the mechanical performance of concrete [94,293–295]. High-strength concrete is more susceptible to increasing temperatures, with a quicker deterioration and loss of compressive strength throughout the whole temperature range [45,296]. It is reported that when heated to temperatures of 300 °C and 600 °C, normal strength concrete loses 10 to 20% and 60 to 75% of its initial compressive strength, respectively. At the same time, high-strength concrete loses up to 40% of its original strength at temperatures of up to 450 °C [46]. Normal strength concrete is outperformed at high temperatures, exhibiting higher residual strength at initial temperatures that range from 150 to 300 °C, including an inside autoclave producing additional concrete hydration by dry hardening and steam generation [297,298]. As the temperature rises, the dehydration of hydration products may cause a wide range of reactions in concrete. Normal strength concrete suffers fluctuation in strength from the ambient temperature of less than 300 °C, followed by a progressive reduction when the temperature exceeds 300 °C. The residual compressive strength diminishes dramatically between 400 and 600 °C. The majority of compressive strength loss occurs within this temperature range because of the decomposition of hydration products. As the exposed temperature reaches approximately 800 °C, compressive strength reduces by about 80% of its ambient temperature strength [133,299]. However, in the case of HSC, a dense microstructure of HSC prevents effective evaporation of moisture at high temperatures. This results in pore pressure buildup, the rapid development of microfractures, and a faster loss of strength in HSC at high temperatures than NSC [133,298,300].

As mentioned previously, unlike regular strength concrete, HSC exhibits explosive spalling, where even at very low temperatures of 350 – 400 °C, spalling occurs in HSC [301]. A high portion of calcium silicate hydrate (CSH) decomposes at a temperature of less than 400 °C, decomposing and coarsening the pore structure of the hardened cement paste, resulting in HSC. As a result, a high portion of its strength is lost even below 400 °C. Furthermore, at higher exposure temperatures of 600 °C, high-strength concrete loses more compressive strength than normal concrete [302]. Because the pore structure becomes more coarse and the pore diameter increases at higher temperatures in NSC than in HSC, HSC maintained a larger percentage value of residual compressive strength than NSC; hence, the NSC strength gradually decreased in rate more than that of HSC [303]. This result is consistent with recent findings, which found that concrete with greater original strength (93 MPa) and lower w/b ratio had higher residual compressive strength. Therefore, because of the reduced moisture content and decrease in pore width, they are more resistant to temperature rise than concrete, with lower initial strength (51 MPa) and larger w/b ratio [241]. Generally, most researchers agreed that the addition of supplemental cementitious material (SCM) or fibers to NSC and HSC increases their residual compressive strength at elevated temperatures [304–306].

The literature review also has three steady-state temperature experiments for measuring the mechanical characteristics of concrete at extreme temperatures, which are described as literature (Fig. 17). The first type of test is called a “stressed” test, where before being heated, the specimen is preloaded with a constant load, and the preload is kept up without change during the heating period. Preload was up to 40% of the concrete’s ultimate strength at room temperature. In this instance, the rate of heating is often maintained continuously until the required heat is attained to maintain quasi-steady thermal settings throughout the process of heating [307]. It is necessary to perform a break time at the anticipated heat to verify that the thermal pitch is as unchanging as possible before applying increasing loads until the specimen fails in compression (Fig. 17a). A preload is not used in the second kind of test (the unstressed), and the specimen is directly warmed to the desired temperature at a steady pace throughout the procedure [308]. The maximum temperature is also maintained for a defined time to attain the thermal steady-state condition in this test. Following that, the specimen is subjected to a high-stress level until it fails (Fig. 17b). There is no preload applied during the heating process in the third kind of test (unstressed), and The sample has been cooled to room temperature (perhaps under carefully monitored circumstances), i.e. at a fixed- rate of cooling) earlier loading into pressure until the sample is crushed (Fig. 17c) [308]. According to studies that explores the influences of fires contacted on concrete properties [241,309], the behavior of NSC at raised heat differs from that of HSC at the same temperature. There were two significant differences between HSC and NSC under high-temperature contacts, as reviewed in [42,73] in the evaluation of

HSC behavior. The review of HSC behavior in fire discovered two leading differences between HSC and NSC at higher levels of exposure to temperatures: (1) relative strength loss at level of heats between 100 and 400 °C, and (2) explosive spalling was observed in HSC test specimens at level of heats between 200 and 400 °C [47]. It is well-known that several models exist for estimating the remaining compressive strength of concrete after exposure to high temperatures [288,293,310]. Yet existing prototypes were advanced for NSC or extrapolated from incomplete HSC test results that did not capture all essential aspects [311].

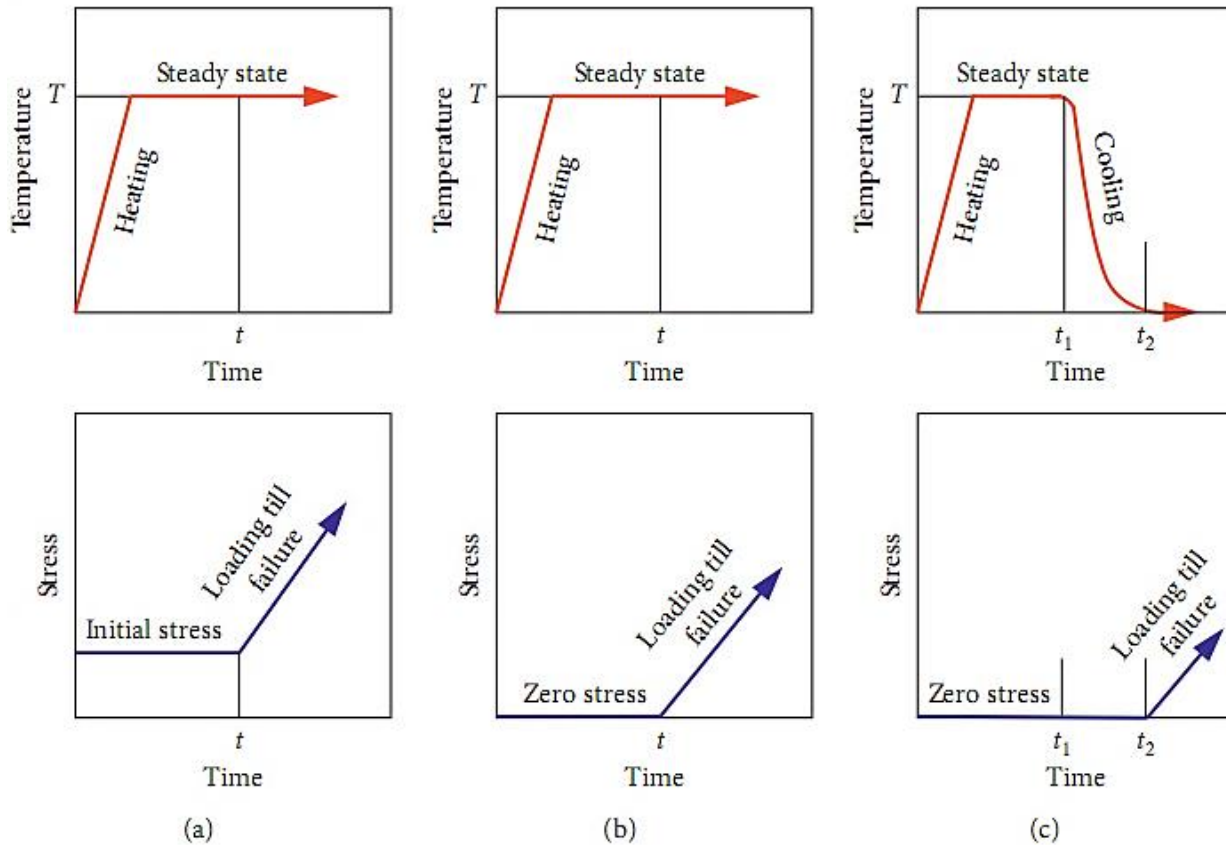


Fig. 17: Loading and temperature history diagrams for the different tests procedures: a) stressed, b) unstressed, and c) residual property (Adapted from [48])

4.3 Sorptivity test

Sorptivity is a measurement of a material's ability to absorb and transport water by capillary suction, and it is used to determine the microstructure and qualities that are critical for durability. Moisture movement in concrete is influenced by its permeability [217]. Lower permeability makes it difficult for moisture trapped in concrete to escape, causing pore pressure to build up [312]. Consequently, less permeable concrete is more prone to thermal spalling when heated, whereas concrete with a higher permeability is less vulnerable [71]. All microcracks, pore number, size, and connectivity are related to permeability, which affects the spalling behavior

when concrete exposes to temperature. Measuring the permeability of concrete directly at elevated temperature conditions is difficult. Concrete's sorptivity, measured in terms of water absorption, may be observed as a degree of the capillary forces that allow fluids to be haggard into and retained inside the concrete's pore structure [313].

However, limited information regarding the concrete's bulk properties can be obtained because the sorptivity test is performed on the concrete's surface. The surface condition of concrete influences its sorptivity. Additionally, the original moisture level of concrete affected the additional water absorption [314]. Several sorptivity experiments were performed on an OPC sample that included the addition of sand and the partial replacement of cement with mineral admixtures, such as SF, sandstone, limestone and FA. As the concrete's strength increased, sorptivity decreased but remained nearly persistent for water-immersed concretes [315]. Concrete containing 10% MK and 10% SF is studied for its initial surface absorption, sorptivity and water absorption. The finding revealed that when compared with OPC concrete, the presence of SF and MK condensed the concrete's sorptivity, water absorption and initial surface absorption significantly [316]. MK and SF substantially affected concrete shrinkage, permeability, and mechanical properties with water-to-binder ratios of 0.25 and 0.35 [317]. MK and SF concrete had higher 28-day compressive strength than control concretes, and their sorptivity coefficients dropped as MK and SF were introduced. Concrete with the lowest sorptivity, notably those with 15% MK or SF, had the highest compressive strengths [318]. When limestone particles were added to the cement paste, the strength of the concrete was greatly raised [319].

A novel kind of ECCs has been developed with higher ductility and medium fiber content while having lower brittleness than low-strength concrete [320]. Under a tensile load, ECC develops micro fractures, exhibiting a pseudo-strain-hardening behavior [321]. ECC has a 3 – 5% tensile strain capacity compared with 0.01% for standard concrete [322]. Engineered Cementitious Composites' strain-hardening behavior makes them attractive for structural applications [323,324]. The fiber amount fraction of ECC is restricted to 2% volume of the concrete to keep the composites' permeability at a minimum [322]. ECC's high strain capacity is attributed to the formation of numerous cracks rather than a incessant growth in the opening of cracks. ECC's damage acceptance and measured crack width increase infrastructure longevity and serviceableness. HSC features several distinct characteristics, comprising tensile characteristic greater to other FRCs. HSCs are suited for variety of concrete structures [325] and are frequently utilized in coupling beams and overlays of bridge deck. As a result of its tight fracture breadth and nearly spread out micro-structure, ECC has a high durability level [326]. Repetitive cracking and strain-hardening activity in ECCs persists after 200 days of exposure to the environment, with a ductility of more than 2% [323]. Because of its low permeability, ECC's long-term

durability attributes are more desirable than normal concrete. Previous studies on the durability properties of HSCs have employed either the polyvinyl alcohol fiber-reinforced (FR) ECC or the polyethylene FRECC as a reinforcement material [327,328].

With a w/b ratio of 0.36, it is possible to make SCCs incorporating FA by substituting 0 – 80 % of the cement replacement with FA. According to the findings of the tests, SCCs with cure times of 1, 28, and 56 days exhibit an efficient rise in absorption of water with increasing FA concentration. Nevertheless, higher FA concentration decreased compressive strength [329], meaning that an inverse connection between water absorption and strengths has been authorized. The same relationship was realized between compressive strength and sorptivity [330]. In another study, durability studies, including water absorption tests, were conducted on SCCs with FA percentages that range from 0 to 85% [331]. FA-SCCs had greater water absorption than conventional concretes of comparable strength. Similarly, SCC with a considerable amount of SF and FA is also examined for compressive strength and water absorption [332]. According to their findings, the FA-containing SCC absorbed more water than the control concrete; however, the water absorption decreases as the SF content increases [318]. In summary, HSC demonstrated decreasing strength properties and water absorption increment as FA content increased, even smaller than the reference concrete while adding SF into the mixtures of SCC resulted in increased strengths and decreased water absorption. In addition, Fig. 18 shows the strength of cubes at the 28-day and sorptivity coefficients [318].

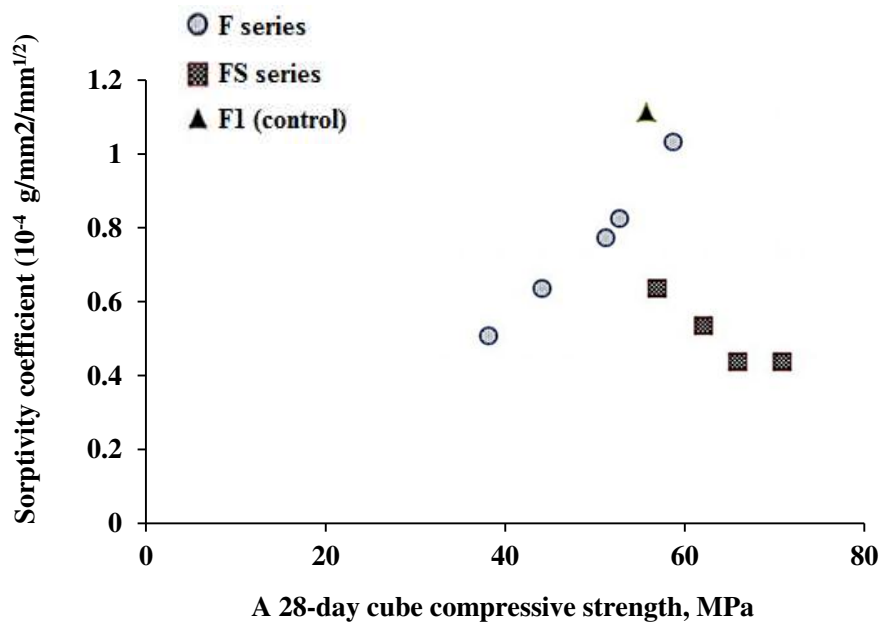


Fig. 18: Coefficient of sorptivity versus compressive strength at 28-day (Adapted from [318])

The F- and FS-series SCCs are clearly less sorptive than the control SCC. The 28-day cube strength of the F-series SCC is lower than that of the control, but the cube strength of the FS-series SCC is considerably higher. Several studies have also shown an increasing trend in compressive strength as a function of sorptivity for SCC with the inclusion of FA [315,329]. Nevertheless, the development is upturned when SF is included in present mixtures of the SCC. As a result, a definitive association between and strength sorptivity cannot be established. These major results contrast with those of other researchers [330]. Contingent on the amount of cementitious materials in the mixtures of SCC and other ecological conditions like the curing technique, dissimilar compressive strengths and sorptivity may be obtained [333]. As a sole display for determining sorptivity in the mixes of SCC, the strength may be incorrect [318].

4.4 X-ray diffraction/computed tomography

The direct approach for determining the crystalline phases present in concrete is X-ray diffraction (XRD) [334]. This method is used to evaluate each phase of hydration products to forecast HSC performance. XRD is a well-known method for studying mineral crystal structures that have been extensively utilized to discover biominerals at fungi-mineral interfaces [335,336]. For example, the full three-dimensional fracture pattern in spalled samples of HSC is practically obtained using X-ray computed tomography (X-ray CT) and XRD to determine the initial microstructure and post spalling test to analyze the damage pattern on fire spalling HSC samples so as to better understand the spalling and prevention processes of the employed fibres. The microstructure of the HSC samples has a role in the primary fracture characteristics. Thus, both the X-ray CT and XDR are considered as significant tools used to capture SEM images for microstructural changes of HSC. The non-destructive X-ray CT will be used to evaluate the effects of thermo-mechanical loads during fire experiments. The HSC spalled specimens' extracted damage pattern may indicate an additional fracture plane beyond those found by physical inspection of the exterior face. In-situ 3D recreation of concrete microstructure will be possible with X-ray CT, which will provide significantly more information than 2D microscopy. Likewise, XRD including SEM have been used to visualize the surface of calcite precipitates, and it has proven successful in characterizing the composition and morphology of hydrated precipitates [337,338]. The amount and distribution of the generated hydration products determine mechanical performance efficiency. Consequently, determining the overall quantity and distribution of hydrated precipitates throughout the specimen is essential for assessing the concrete's performance under all circumstances [339]. Microscopic observatory can characterize cracks and pores volume and obtain two-dimensional data, such as crack width and length [340].

Several previous studies harnessed the utilization of XRD techniques in concrete chemistry to characterize the amount and type of crystalline hydration products in approximately all types of concrete and mortar [341]. Due to the attenuation of X-rays when they enter materials of various densities, X-ray CT can be utilized to assess the interior structure of fractures [342]. In a high-resolution X-ray CT investigation, the attenuation of X-rays from various places of an object depends on the item's atomic number and density [343,344]. This type of test does not require any chemical treatment, only by simply preparing the samples, such as grinding them into powder. It offers essential data (picturing and quantification) regarding the intrinsic matrix structure [345]. X-ray CT has recently become a popular tool in material research [346]. To achieve high-quality photos, the obtained resolution is crucial. The most common X-ray beam shape in laboratories is conical, and it is possible to change the magnification by simply shifting your sample between the light source and detector. As a result, larger items will have a lower resolution, whereas smaller samples will have a higher resolution [339]. Using XRD, determining the concentration of the essential elements for the formation of important hydration products, such as the determination of calcium, silica and aluminum content, which are primarily responsible for the performance development of concrete samples, can be determined [347].

Further approaches are available to analyze the hydration products, including an environmental scanning electron microscope and FTIR equipped with an energy dispersive spectroscopy (EDS) [348,349]. Notably, determining the amount of hydration products added into the matrix exactly by employing FTIR or XRD is difficult due to the overlapping diffraction peaks of several materials as in XRD and the decomposition in more than one component at the same range of temperature in case of FTIR [350]. XRD and FTIR can generate value about the progress of the hydration process by comparing results from XRD or/and FTIR for the same sample for multiple test ages or comparing those data for different types of mixtures [348].

The XRD, SEM, and mercury intrusion porosimetry (MIP) are just a few of the microscopic inspection techniques used to examine HSC specimens at high temperatures for the presence of cracks and pores [351]. High-temperature heating alters the internal microstructure of concrete, resulting in changes to its macroscopic performance [352]. The SEM, polarized light microscopy (PLM), and XRD were used to evaluate the fracture initiation and crack spread of HSC in the range between 250 and 750 °C [49]. The results revealed that when the temperature rose, the mechanical performance of concrete systems decreased because of the deterioration of its material. After being contacted to elevated between 200 and 800 °C, SEM was used to examine the microstructural morphology of hybrid-FRCs [353]. The findings indicate that at 400 °C, the mechanical performance of concrete systems reached the maximum due to the high density of its microstructure and ITZs at that temperature degree.

However, as the temperature rises above 400 °C, most cement hydrate begins to decompose, and some micropores appear due to developed internal stress in the ITZs, thereby reducing the density of microstructure, thus the mechanical properties of the specimens decrease. MIP was used to measure the change in porosity and pore size distribution of HSC following high temperature of 800 °C, and the finding revealed that with the increase in temperature degree, the permeability of specimens increases due to the increment and expansion of cracks approximately at all levels of sizes of cracks [354]. In summary, image analysis and non-destructive X-ray CT techniques are typically used to investigate the interior microstructure of HSC to determine the impacts of re-curing and reheating on microstructure levels. These techniques revealed that the creation of cracks in the zones between binder and aggregates and the degradation of binder components induce an increase in cracks' connectivity, which increased in total pore volume.

5 Strategies to prevent spalling in HSC

Adapting several strategies to modify the cementitious materials could play a significant role in enhancing the mechanical performance and microstructural homogeneity of concrete systems, thereby overcoming the shortcomings of HSC in high-temperature conditions [2,220]. One more practical option involves creating permeability in concrete by incorporating PPFs in HSC. These fibers melt at temperatures that range from 160 °C –170 °C, thereby forming a regular network of cracks within the concrete matrix [355]. This regular network of cracks created by melting PPFs enables the dissipation of high vapor pressures that form inside concrete at elevated temperatures, assisting in spalling mitigation [2,42]. Table 8 presents the preventive measures for HSC spalling [75].

Table 8: Preventive measures of HSC spalling

Materials used	Degree of efficiency	Mechanism of spalling preventive measures	Footnotes	Refs.
GPC	High	When a geopolymer is exposed to high temperatures, the pore volume and average pore width expand, increasing spalling resistance.	Increase permeability, enhancing pore connection and reduction strength loss	[156]
PPF	Very high	Formulation of channels and pores using the melted synthetic fiber can lead to release vapor and reduce pore pressure build-up.	Dropping strength as a result of the pores insertion	[70,104,115,166,167]
Recycled tyer steel fibers	High	The major steel reinforcement is protected by keeping spalled concrete adhered to the heated surface.	Enhancing concrete bond	[147]
Air-entraining	Very high	Creating channels and pores to	Compressive strength	[355,356]

agent		release vapor and decrease pore pressure build-up.	can be reduced by 5% with a 1% increase in entrained air spaces.	
Polymer fibers (e.g. PPF)	Very high	The melting of PFs creates empty channels, which improves gas or water vapor permeability through concrete. After melting the PF, the temperature difference between inserted fibers and matrix allows for the formation of an interconnected network of fractures in the matrix.	Enhancing permeability and cracks connection	[96]
Thermal barrier	Very high	Plummeting concrete temperature	It required additional work that leads to upsurge the cost of labor	[357]
Steel fibers	High	Preventing cracking patterns and spalling Even before the fibers melt, the massive difference in thermal expansion coefficient between concrete and polymer fibers causes tiny fractures.	Higher material cost	[115,166–168]
Low-density polyethylene, PPF, and polyamide 66	High		Enhancing permeability and network cracks connection	[222]
Low expansion and small-size aggregates	High	Using cement paste to improve thermal compatibility	When moisture is trapped in porous aggregates, it causes extreme violent spalling.	[93,154,169]

However, the inclusion of PPFs needs precise technique to ensure that it is distributed uniformly within the concrete matrix and that it does not scatter during the mixing process, necessitating more efforts in placing compaction and finishing, particularly in RC components with crowded reinforcement [50]. Steel fiber has been successful in preventing fire-induced spalling because of its higher tensile strength and greater ductility at temperatures between 100 and 400°C [276]. However, similar to the difficulties in PPF, the inclusion of steel fibers reinforced onto concrete systems faces several challenges in terms of non-dispersion insurance during mixing, placing, and finishing, thereby making the practical application of these strategies in the field challenging [355].

HSC fire resistance applications may be addressed in a variety of ways, as has been established via research and development [355], including restricting the use to areas with a high risk of fire, modifying the mix design by adding various fibers, optimizing concrete elements dimensions, and providing insulation [2]. Additionally, knowing fire behavior becomes critical as concrete advances and evolves, thereby allowing for selecting a

specific concrete type based on the anticipated attributes for a project [73]. Material engineers' preferences for achieving project objectives influence how a concrete type is manufactured. HSC has been reasonably established for construction projects requiring high mechanical performance. The improving predictability of its fire behavior might make it more popular [219,239]. Moreover, understanding the properties of the microstructure and the properties of the binder materials can increase the possibility of predicting spalling for most types of concrete, including HSC and self-compacting concrete, and predicting the behavior of each type of concrete during and after exposing for fire [358].

HSC use in constructed infrastructure is increasing, though its vulnerabilities to fire require an intensive examination to prove the reliability of its behavior at elevated temperatures. The HSC's fire behavior data clearly demonstrates that it performs worse at elevated temperatures than NS [138,219,239]. The low mechanical performance of HSC at elevated temperatures is ascribed to the quick loss of binder components and the growth of cracks due to the quick development of thermal stress caused by high compacted microstructure, the latter of which is the primary defect of HSC [6,42].

Also, it is found that when used as an substitute to HSC in fire-resistant applications, air-entrained HSC may increase workability in the fresh stage owing to the ball bearing effect and provide much-required porosity in the toughened state attributable to the purposefully entrained air in concrete [51]. Although it is possible to achieve high strength in air-entrained concrete, doing so requires careful planning and execution since integrating air into HSC develops problematic to manage in the existence of superplasticizers [359]. In addition, variety of chemical compositions in superplasticizers and air entraining agents (AEAs) yield systems that are incompatible in their fresh condition and interrupt the air void networks after they have solidified [356].

In concrete, the network of air void is assessed by the exact surface area of spacing factor and air voids [360,361]. Concrete that has been hardened should have an elongation smaller than 200 μm to achieve maximum freeze–thaw durability [362], where several studies have largely referred to these values. The chemical incompatibilities cause disturbances in both (L and α) parameters, resulting in contradicting findings for distinct admixture combinations [363]. Furthermore, identifying an appropriate AEA can be difficult in a superplasticizer concrete mix [355]. Only a few extensive studies successfully address all aspects that characterize the air void network in either fresh or hardened concretes to incorporate air in the superplasticized mix [314]. In this study, synthetic detergent-based AEA and naphthalene-based superplasticizers were the best steady chemical consolidation amongst several mixtures with different levels of alkali in cement [364]. Although the spacing factor and particular surface are typically utilized to maximize freeze–thaw durability, they are not used to optimize fire endurance [355]. Aside from improving freeze–thaw durability, the specific

modification of air bubbles by adjusting the specific surface of the air void system and spacing factor might lead to improving HSC performance against spalling by fire. Furthermore, the performance of HSC and cement plain with different levels of reinforcing fibers was studied to determine their performance at elevated temperatures. [42].

Researchers use various methods for high-temperature testing on HSC or normal strength concrete due to the lack of well-established criteria, which is one of the main reasons for substantial variability in the results related to performance at the elevated temperatures of diverse types of concrete [355]. Typically, for fire tests on HSC, a rate of heating of 2 –5 °C per 60 seconds is adapted for samples with a 100 mm diameter and a 200 mm height [12,239]. However, while studying spalling behavior in HSC, a greater rate of heating of 10 °C per 60 seconds is commonly utilized [2,365]. The hardened strengths of concrete specimens at extreme heats may be evaluated using three basic test scenarios based on loading and heating scenarios. [138,276]. These conditions include residual test, unstressed and stress, where the mechanical test results rely highly on the methodologies used [355]. Therefore, the characterizations of material properties under unstressed test settings are regarded to be typical of material properties at elevated temperatures.

6 Modelling of heat-induced spalling

A variety of explosive and non-explosive types of spalling exist and may ultimately compromise the overall structure's integrity if structural components are reduced in cross-section or reinforcing steel is contacted straight to heat when the cover material is removed [366]. The processes and causes of spalling behavior have allegedly been studied extensively in experimental settings [2,159,171]. Accordingly, various numerical models have been proposed to simulate these difficult phenomena at varying degrees of interpretation [163,180,278,366,367]. Based on the finding of the previous studies, there is general agreement that the concrete structure's permeability, moisture content, heating rate, and section shape and size all play a role in spalling [70–72,74,76,77,83]. However, the primary mechanism that drives spalling is still under debate. According to some researchers, pore pressure is the most significant parameter [71,72,87,92], while others emphasize that the internal stresses developed thermally is the main reason for concrete spalling in fire, and yet others refer that these two factors combine to create spalling [2,6,12,13,70–72,74,76,77,83,123]

Many physical and chemical aspects of HSC are discussed at elevated temperatures to design models that can predict the behavior and performance [366], including mass and heat transfer between liquid, gaseous, and solid states; state alters between vapor and liquid water; chemically related drying of free thermal expansion and water;; convection-persuaded thermal stress; mechanical and thermal disintegration of material

characteristics; the coupled mechanical-thermo-hygro interface of transport characteristics [201]; and the coupled hygro-mechanica -thermo interaction of transport characteristics [155,368]. Notably, the more the model includes a larger set of parameters that have a relationship or influence on spalling behavior, the more reliable the model is to predict the occurrence of spalling. Therefore, the continuous development and updating of the concrete fragmentation model are necessary [366].

Spalling is predicted and described by a group of concrete models that consider all three stages in a completely connected way [368–370]; this has proved essential in adequately representing the behavior of concrete at increased temperatures [371]. Other studies [277,372] have also introduced several models in this area, but that models are whichever less advanced or incline to have formulations developed from other models [368,369]. Although similar, the three phases of these linked models vary in a amount of fundamental aspects, including the basic creations, constitutive laws, and state equations used [366]. Some models differs significantly from others in which mechanical failure of materials is considered [373]. In contrast to other models that rely on pore pressures or stress criteria to predict the occurrence of spalling [277,374], some models do not make any assumptions about the processes that cause spalling in advance. It has also been shown that the Modified von Mises damage creation used in the model reflects damage patterns more accurately than other formulations [374], which indicates that the model is well positioned to offer insight into the processes that occur throughout the spalling process [366].

A study reported mechanical pattern damage induced solely by means of vapor pressure in HSC with early moisture content of 90% (Fig. 19) [141], demonstrating the role of efficient vapor pressure and efficient leading primary stress in concrete damage at elevated temperatures. The surface damage appeared when the temperature at surface hits 555.5 °C, although no internal spalling during the entire heating sequence about 600 °C is observed [141]. The damage in the former occurs in the region of high vapor pressure, whereas the damage in the later groups and spreads toward the deepest central area as the thermal extension coefficient reduces. Various theoretical models were created to understand spalling better. The mechanisms of vapor pressure [6,138,140,375] and the mechanisms of gradient-induced thermal stress of temperature [15,139,376] are the two hypotheses that have been suggested so far to explain spalling. A notion of moisture–clog spalling had also postulated in the former. Vapor pressure may only play a minor part in the occurrence of fire-spalling, with thermal stress-induced possible energy playing the leading role [375]. A chemo-plastic model was introduced to evaluate the fire-spalling of the rings of concrete in the channel tunnel [15]. The researchers employed plastic strain to determine the concrete spalling depth and discovered that the compressive stress created by restricted thermal dilatation causes fire spalling.

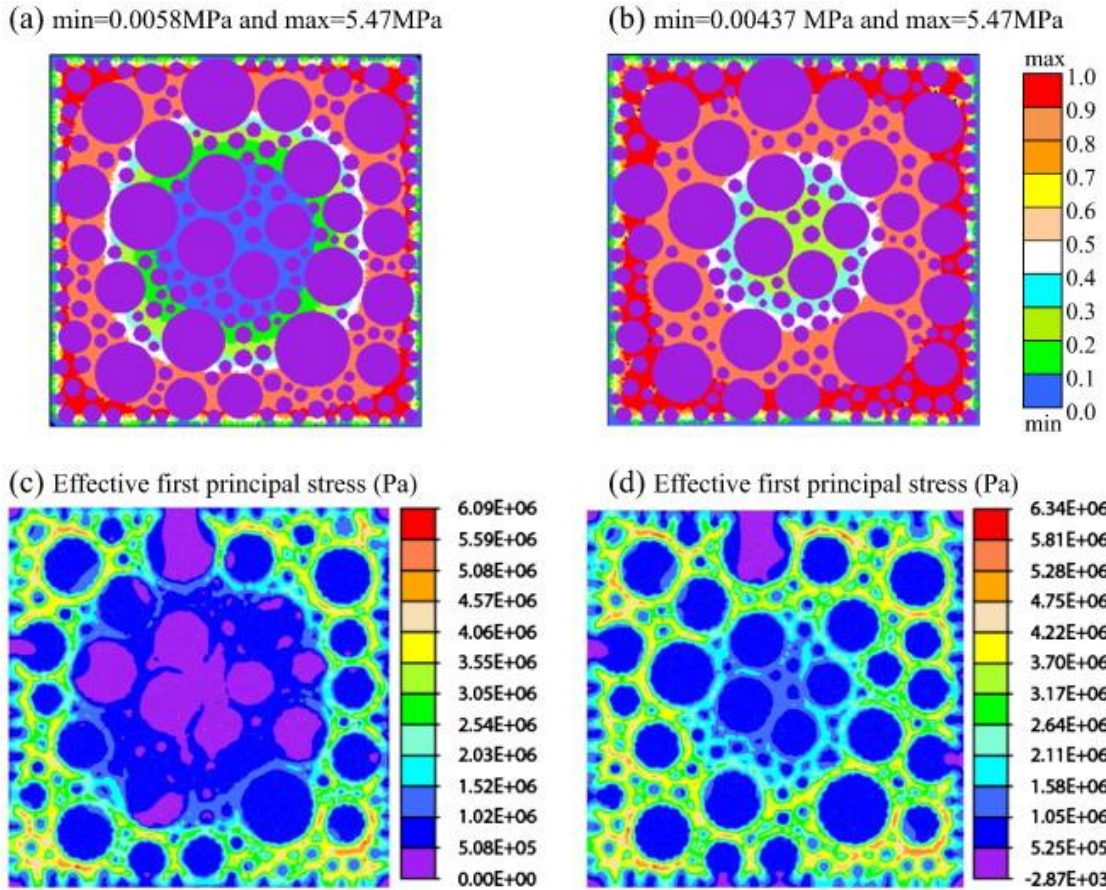


Fig. 19: Sample with early moisture content of 90%, operative vapor pressure at (a) 555 °C and (b) 600 °C, and operative early main stress instigated completely by vapor pressure at (c) 555 °C and (d) 600 °C (Adapted from [141])

The thermo-mechanical behavior of concrete was studied using a fully coupled model, and four indices were utilized to predict spalling [374]. To mimic the spalling of concrete elements, one-dimensional models [277] were designed based on the fire damages to concrete elements are used [366]. Furthermore, the effect of changing mechanical parameters on the destruction to fired concrete has been examined numerically [201]. Several scholars [377–379] have also undertaken several investigations on small specimens’ macro-level to describe the elevated temperature of concrete microstructures. Furthermore, spalling is studied on an arithmetic parallel-averaged meso-level [370]. It was found that the plane of spalling tracks parallel to the practical compressive force since the model assumed equal stresses and different stressors. A mesoscopic elastic-thermal damage models and fracture-based zero-thickness interface components are used to investigate fractures in heated concrete persuaded by heat gradients and thermal capacity mismatches between cement paste and the aggregates matrix [141,177,380,381]. Further, Table 9 outlines some of the most often used analytical models for pore pressure-induced spalling [93].

Table 9: Analytical models focused of HSC spalling attributable to high pore pressure

Type of model [93]	Details of the developed models	Refs.
Moisture clog	<ul style="list-style-type: none"> – A number of temperature-dependent concrete factors have already been considered. – The T = 100 °C isotherm governs moisture migration. – Spalling as a result of moisture clogging. 	[382,383]
Moisture clog	<ul style="list-style-type: none"> – The spalling liability curve is used to determine the possibility of spalling based on pore saturation and permeability. – The moisture clog model has been upgraded. – The T = 100 °C is the starting point for moisture migration as vapor movement. 	[246]
Moisture and vapor movement	<ul style="list-style-type: none"> – Vapor drag is caused by friction in the concrete, which affects moisture transport. – The pressure differential between the colder interior parts and the heated surface causes the moisture blockage to migrate. – Starting at T = 100 °C, vapor movement is relative to the heating rate. 	[384]
Vapor movement, moisture clog, and pore pressure	<ul style="list-style-type: none"> – To produce spalling, the sum of thermal stresses, load, pore pressure must be higher than the tensile strength. – When the vaporization front reaches its maximum, peak pressure is reached. – The model's accuracy is highly dependent on the input parameters. 	[93]
Heat and moisture migration	<ul style="list-style-type: none"> – For an in-depth study of the danger of spalling, includes nonlinear terms of moisture migration and heat flow. – Numerically solved thermo-hygro mechanical model – As a result of the temperature-dependent permeability, pressure is released in the form of vapor. 	[369]
Vapor movement and mobility of water	<ul style="list-style-type: none"> – Engineering approach for determining the risk of explosive spalling. – Failure as a result of the concrete's tensile strength surpassing EN 1992-1-2. – The development of pressure inside the pores of concrete as a temperature's function is addressed. – The mobility of water in a liquid form is not taken into account. 	[277]

7 Conclusion

According to a critical review, high-strength concrete (HSC) is a suitable structural concrete material for ensuring long-term durability and guaranteeing the safety and security of human life and property. It is reported that the need to a complete literature research on up-to-date state-of-the-art advancements associated to the fire spalling behavior of HSC applied to elevated temperatures and during a fire is highly imperative to identify the current behavior of HSC during a fire. However, it is found that this material has surpassed cement-based HSCs in the infrastructure, building and construction sectors because of its greater hardened and durability properties at elevated temperatures during fires. Over the last few decades, HSC has attracted a great deal of interest and a strong desire to participate as a consequence of its high early strength, low energy cost, sustainability, less

brittleness, excellent durability, and its exceptional fireproof concrete structures material due to its intrinsic inorganic structure and ceramic-like properties, as well as its low brittleness.

The issue of spalling in buildings has been known for decades, but it has lately been brought to light in many locations throughout the globe due to the fire resistance of recently developed concrete kinds has been brought into doubt resulting severe damage caused by spalling and the non-operational duration of tunnels following a fire. For example, it is reported that surface spalling may also be considered a subset of explosive spalling, exhibiting the utmost extreme sort of spalling. As the fire continues to pose a significant threat to human community. In order to fully understand these scientific facts, there has been a wide variety of observations of concrete spalling during fire experiments, including spalling with slow (1 °C/min.) or fast (250 °C/min.) heating, preventing after some time or making progress, spalling at the start of the fire or after some time, cracking along or through aggregate grains, from gradual to explosive spalling, limited to the level of reinforcing or extending far beyond it.

Based on previous extensive experimental and numerical models, it has been generally agreed that spalling in HSC at high temperatures and during fires is influenced by a combination of countless factors of materials for instance " saturation level, permeability, aggregate type and size, presence of reinforcement and cracking," factors of geometric for example " size and shape of section," and environmental factors such as " heating profile, load level, and heating rate." Besides, the influences of fiber length, dosage, and type on the resistance of HSC spalling with the ultimate compressive strength under various heating environments exhibited that the system of the spalling resistance of HSC mixed with steel fibers can delay the spalling time but does not clearly ease the spalling concept, but when recently confirmed with PPFs can improve the spalling resistance of concrete. In conclusion, it is also observed that the addition of cementitious materials and fibers are part of the strategies to prevent spalling in HSC.

This article examines the methods, influencing variables, and forms of fire spalling in detail. This literature also provides in-depth evaluations of the behaviors, modeling, and prevention of fire spalling in HSC applications. Based on this thorough examination, the subsequent hotspot research focuses were identified and suggested for further investigations and inquiries by academics globally.

- Heat-induced explosive spalling in a fire is a genuine threat to structural concrete and has gained significant study interest in past few decades.
- The process of HSC's explosive spalling residues a critical issue that must be addressed.
- Innovations in construction materials, such as enhanced grain size distributions and the use of extra-fine particles, have resulted in concrete kinds that are more durable, strong, and workable. However, these

high-performance concrete kinds have been demonstrated to be more prone to spalling during a fire than typical concrete types.

- A consensus has yet to be reached among researchers and practitioners as to which factors contribute most to concrete spalling in the presence of fire. The influence of steel fiber length and diameter on violent spalling has not been thoroughly investigated.
- Fibers and aggregates are still being studied to see whether they might help minimize HSC explosive spalling.
- It is a critical to better understand the underlying mechanisms causing concrete spalling, create an accurate prediction models, and improve (in terms of efficacy and cost) the strategies for preventing spalling in practice.
- Given to the intricacy of concrete spalling when exposed to fire, the reasons behind HSC's worse thermal performance are not entirely undiscovered.
- Even while fiber and aggregates have been shown to minimize the explosive spalling of HSC, their design processes remain a mystery but the process of fire spalling for HSC during a fire, on the other hand, remains fully unknown.
- Establishing suitable fire-safety measures is a key necessity in building design to ensure its occupants' safety.
- Moreover, there is no verified guideline to allow the design of HSC mixtures to eliminate spalling, nor are there any standardized, widely recognized, reproducible test procedures to accurately measure or verify spalling resistance for a specific mix in a given application. As a result, no models that can forecast spalling with adequate accuracy to be employed in design exist.

8 Acknowledgments

The authors gratefully acknowledge the financial support given by Deanship of Scientific Research at Prince Sattam bin Abdulaziz University, Alkharj, Saudi Arabia and the cooperation of the Department of Civil Engineering, Faculty of Engineering and IT, Amran University, Yemen, for this research.

Conflicts of Interest: The authors declare no conflicts of interest.

References

- [1] Y. Fu, L. Li, Study on mechanism of thermal spalling in concrete exposed to elevated temperatures, *Mater. Struct. Constr.* 44 (2011) 361–376. <https://doi.org/10.1617/s11527-010-9632-6>.

- [2] P. Kalifa, F.D. Menneteau, D. Quenard, Spalling and pore pressure in HPC at high temperatures, *Cem. Concr. Res.* 30 (2000) 1915–1927. [https://doi.org/10.1016/S0008-8846\(00\)00384-7](https://doi.org/10.1016/S0008-8846(00)00384-7).
- [3] J. Li, Z. Wu, C. Shi, Q. Yuan, Z. Zhang, Durability of ultra-high performance concrete – A review, *Constr. Build. Mater.* 255 (2020). <https://doi.org/10.1016/j.conbuildmat.2020.119296>.
- [4] J.C. Liu, K.H. Tan, Fire resistance of ultra-high performance strain hardening cementitious composite: Residual mechanical properties and spalling resistance, *Cem. Concr. Compos.* 89 (2018) 62–75. <https://doi.org/10.1016/j.cemconcomp.2018.02.014>.
- [5] S. Wang, V.C. Li, Engineered cementitious composites with high-volume fly ash, *ACI Mater. J.* (2007). <https://doi.org/10.14359/18668>.
- [6] G. Sanjayan, L.J. Stocks, Spalling of high-strength silica fume concrete in fire, *ACI Mater. J.* 90 (1993) 170–173. <https://doi.org/10.14359/4015>.
- [7] R.K. Chaudhary, T. Roy, V. Matsagar, Member and structural fragility of reinforced concrete structure under fire, *J. Struct. Fire Eng.* 11 (2020) 409–435. <https://doi.org/10.1108/JSFE-02-2019-0015>.
- [8] F. Lo Monte, R. Felicetti, C. Rossino, Fire spalling sensitivity of high-performance concrete in heated slabs under biaxial compressive loading, *Mater. Struct. Constr.* 52 (2019). <https://doi.org/10.1617/s11527-019-1318-0>.
- [9] F. Fingerloos, Buchbesprechung: fib Bulletin 38: Fire design of concrete structures – materials, structures and modelling, *Beton- Und Stahlbetonbau.* 102 (2007) 662–662. <https://doi.org/10.1002/best.200790131>.
- [10] H.H. Bache, Densified Cement / Ultra-Fine Particle-Based Materials, Second Int. Conf. Superplast. Concr. (1981) 1–34.
- [11] K. Hertz, Explosion of silica-fume concrete, *Fire Saf. J.* 8 (1984) 77. [https://doi.org/10.1016/0379-7112\(84\)90057-2](https://doi.org/10.1016/0379-7112(84)90057-2).
- [12] P. Zhang, L. Kang, J. Wang, J. Guo, S. Hu, Y. Ling, Mechanical properties and explosive spalling behavior of steel-fiber-reinforced concrete exposed to high temperature-A review, *Appl. Sci.* 10 (2020). <https://doi.org/10.3390/app10072324>.
- [13] M. Yoon, G. Kim, Y. Kim, T. Lee, G. Choe, E. Hwang, J. Nam, Creep behavior of high-strength concrete subjected to elevated temperatures, *Materials (Basel).* 10 (2017). <https://doi.org/10.3390/ma10070781>.
- [14] J.C. Liu, Z. Zhang, A machine learning approach to predict explosive spalling of heated concrete, *Arch. Civ. Mech. Eng.* 20 (2020). <https://doi.org/10.1007/s43452-020-00135-w>.
- [15] F.-J. Ulm, P. Acker, M. Lévy, The “Chunnel” Fire. II: Analysis of Concrete Damage, *J. Eng. Mech.* 125 (1999) 283–289. [https://doi.org/10.1061/\(asce\)0733-9399\(1999\)125:3\(283\)](https://doi.org/10.1061/(asce)0733-9399(1999)125:3(283)).
- [16] K.E. Petersen, Assessment of Accident Frequencies and Consequences for a New Danish Tunnel, in: *Reliab. Data Collect. Use Risk Availab. Assess.*, 1986: pp. 357–363. https://doi.org/10.1007/978-3-642-82773-0_36.
- [17] W. Matthes, A. Vollpracht, Y. Villagrán, S. Kamali-Bernard, D. Hooton, E. Gruyaert, M. Soutsos, N. De Belie, Ground granulated blast-furnace slag, in: *RILEM State-of-the-Art Reports*, 2018. https://doi.org/10.1007/978-3-319-70606-1_1.
- [18] M. Amran, G. Murali, N.H.A. Khalid, R. Fediuk, T. Ozbakkaloglu, Y.H. Lee, S. Haruna, Y.Y. Lee, Slag uses in making an ecofriendly and sustainable concrete: A review, *Constr. Build. Mater.* 272 (2021). <https://doi.org/10.1016/j.conbuildmat.2020.121942>.
- [19] V. Arularasi, P. Thamilselvi, S. Avudaiappan, E.I.S. Flores, M. Amran, R. Fediuk, N. Vatin, M. Karelina, Rheological behavior and strength characteristics of cement paste and mortar with fly ash and GGBS admixtures, *Sustain.* 13 (2021). <https://doi.org/10.3390/su13179600>.
- [20] V.G. Karayannis, K.G. Moustakas, A.N. Baklavariadis, A.E. Domopoulou, Sustainable ash-based geopolymers, *Chem. Eng. Trans.* (2018). <https://doi.org/10.3303/CET1863085>.
- [21] S. Kumar, P. Sangwan, D.R.M. V, S. Bidra, Utilization of Rice Husk and Their Ash : A Review, *J.*

- Chem. Environ. Sci. (2013).
- [22] A. Siddika, M.R. Amin, M.A. Rayhan, M.S. Islam, M.A. Al Mamun, R. Alyousef, Y.H. Mugahed Amran, Performance of sustainable green concrete incorporated with fly ash, rice husk ash, and stone dust, *Acta Polytech.* 61 (2021) 279–291. <https://doi.org/10.14311/AP.2021.61.0279>.
- [23] M. Amran, R. Fediuk, G. Murali, N. Vatin, M. Karelina, T. Ozbakkaloglu, R.S. Krishna, A.S. Kumar, D.S. Kumar, J. Mishra, Rice husk ash-based concrete composites: A critical review of their properties and applications, *Crystals.* 11 (2021) 1–33. <https://doi.org/10.3390/cryst11020168>.
- [24] S.G.S. Dharmendra S. Ravat, S. V Dave, Utilization of Red Mud in Geopolymer Concrete-A Review, *Int. J. Adv. Eng. Res.* 4 (2017).
- [25] Y.H.M. Amran, R. Alyousef, H. Alabduljabbar, M. El-Zeadani, Clean production and properties of geopolymer concrete; A review, *J. Clean. Prod.* 251 (2020) 119679. <https://doi.org/10.1016/j.jclepro.2019.119679>.
- [26] J. Payá, F. Agrela, J. Rosales, M.M. Morales, M.V. Borrachero, Application of alkali-activated industrial waste, in: *New Trends Eco-Efficient Recycl. Concr.*, 2019. <https://doi.org/10.1016/b978-0-08-102480-5.00013-0>.
- [27] P. Duxson, G.C. Lukey, J.S.J. van Deventer, Thermal evolution of metakaolin geopolymers: Part 1 - Physical evolution, *J. Non. Cryst. Solids.* 352 (2006) 5541–5555. <https://doi.org/10.1016/j.jnoncrysol.2006.09.019>.
- [28] W.D.A. Rickard, C.S. Kealley, A. Van Riessen, Thermally induced microstructural changes in fly ash geopolymers: Experimental results and proposed model, *J. Am. Ceram. Soc.* 98 (2015) 929–939. <https://doi.org/10.1111/jace.13370>.
- [29] T. Bakharev, Thermal behaviour of geopolymers prepared using class F fly ash and elevated temperature curing, *Cem. Concr. Res.* 36 (2006) 1134–1147. <https://doi.org/10.1016/j.cemconres.2006.03.022>.
- [30] O.G. Rivera, W.R. Long, C.A. Weiss, R.D. Moser, B.A. Williams, K. Torres-Cancel, E.R. Gore, P.G. Allison, Effect of elevated temperature on alkali-activated geopolymeric binders compared to portland cement-based binders, *Cem. Concr. Res.* 90 (2016) 43–51. <https://doi.org/10.1016/j.cemconres.2016.09.013>.
- [31] V.F.F. Barbosa, K.J.D. MacKenzie, Synthesis and thermal behaviour of potassium sialate geopolymers, *Mater. Lett.* 57 (2003) 1477–1482. [https://doi.org/10.1016/S0167-577X\(02\)01009-1](https://doi.org/10.1016/S0167-577X(02)01009-1).
- [32] J.L. Provis, S.A. Bernal, Geopolymers and related alkali-activated materials, *Annu. Rev. Mater. Res.* 44 (2014) 299–327. <https://doi.org/10.1146/annurev-matsci-070813-113515>.
- [33] J. Temuujin, A. van Riessen, R. Williams, Influence of calcium compounds on the mechanical properties of fly ash geopolymer pastes, *J. Hazard. Mater.* 167 (2009) 82–88. <https://doi.org/10.1016/j.jhazmat.2008.12.121>.
- [34] S.A. Bernal, J.L. Provis, B. Walkley, R. San Nicolas, J.D. Gehman, D.G. Brice, A.R. Kilcullen, P. Duxson, J.S.J. Van Deventer, Gel nanostructure in alkali-activated binders based on slag and fly ash, and effects of accelerated carbonation, *Cem. Concr. Res.* 53 (2013) 127–144. <https://doi.org/10.1016/j.cemconres.2013.06.007>.
- [35] S.A. Bernal, E.D. Rodríguez, R. Mejía De Gutiérrez, M. Gordillo, J.L. Provis, Mechanical and thermal characterisation of geopolymers based on silicate-activated metakaolin/slag blends, *J. Mater. Sci.* 46 (2011) 5477–5486. <https://doi.org/10.1007/s10853-011-5490-z>.
- [36] Y. Li, K.H. Tan, E.H. Yang, Influence of aggregate size and inclusion of polypropylene and steel fibers on the hot permeability of ultra-high performance concrete (UHPC) at elevated temperature, *Constr. Build. Mater.* 169 (2018) 629–637. <https://doi.org/10.1016/j.conbuildmat.2018.01.105>.
- [37] Y. Li, P. Pimienta, N. Pinoteau, K.H. Tan, Effect of aggregate size and inclusion of polypropylene and steel fibers on explosive spalling and pore pressure in ultra-high-performance concrete (UHPC) at

- elevated temperature, *Cem. Concr. Compos.* 99 (2019) 62–71.
<https://doi.org/10.1016/j.cemconcomp.2019.02.016>.
- [38] J. Du, W. Meng, K.H. Khayat, Y. Bao, P. Guo, Z. Lyu, A. Abu-obeidah, H. Nassif, H. Wang, New development of ultra-high-performance concrete (UHPC), *Compos. Part B Eng.* 224 (2021).
<https://doi.org/10.1016/j.compositesb.2021.109220>.
- [39] S. Ahmad, M. Rasul, S.K. Adekunle, S.U. Al-Dulaijan, M. Maslehuddin, S.I. Ali, Mechanical properties of steel fiber-reinforced UHPC mixtures exposed to elevated temperature: Effects of exposure duration and fiber content, *Compos. Part B Eng.* 168 (2019) 291–301.
<https://doi.org/10.1016/j.compositesb.2018.12.083>.
- [40] C.P. Gu, G. Ye, W. Sun, Ultrahigh performance concrete-properties, applications and perspectives, *Sci. China Technol. Sci.* 58 (2015) 587–599. <https://doi.org/10.1007/s11431-015-5769-4>.
- [41] G. Lee, D. Han, M.C. Han, C.G. Han, H.J. Son, Combining polypropylene and nylon fibers to optimize fiber addition for spalling protection of high-strength concrete, *Constr. Build. Mater.* 34 (2012) 313–320.
<https://doi.org/10.1016/j.conbuildmat.2012.02.015>.
- [42] L. Phan, Fire Performance of High-Strength Concrete: A Report of the State-of-the-Art, *Fire Res.* (1996) 118. <http://scholar.google.com/scholar?hl=en&btnG=Search&q=intitle:Fire+Performance+of+High-Strength+Concrete+:+A+Report+of+the+State-of-the-Art#0>.
- [43] A. Agrawal, V. Kodur, Residual response of fire-damaged high-strength concrete beams, *Fire Mater.* 43 (2019) 310–322. <https://doi.org/10.1002/fam.2702>.
- [44] V.I. Korsun, K. Khon, V.Q. Ha, A.O. Baranov, Strength and deformations of high-strength concrete under short-term heating conditions up to + 90°C, in: *IOP Conf. Ser. Mater. Sci. Eng.*, 2020.
<https://doi.org/10.1088/1757-899X/896/1/012035>.
- [45] Y.N. Chan, G.F. Peng, M. Anson, Residual strength and pore structure of high-strength concrete and normal strength concrete after exposure to high temperatures, *Cem. Concr. Compos.* 21 (1999) 23–27.
[https://doi.org/10.1016/S0958-9465\(98\)00034-1](https://doi.org/10.1016/S0958-9465(98)00034-1).
- [46] F. Aslani, M. Bastami, Constitutive relationships for normal-and high-strength concrete at elevated temperatures, *ACI Mater. J.* 108 (2011) 355–364. <https://doi.org/10.14359/51683106>.
- [47] H.M. Elsanadedy, Residual Compressive Strength of High-Strength Concrete Exposed to Elevated Temperatures, *Adv. Mater. Sci. Eng.* 2019 (2019). <https://doi.org/10.1155/2019/6039571>.
- [48] L.T. Phan, N.J. Carino, Fire performance of high strength concrete: Research needs, in: *Struct. Congr. 2000 Adv. Technol. Struct. Eng.*, 2004. [https://doi.org/10.1061/40492\(2000\)181](https://doi.org/10.1061/40492(2000)181).
- [49] O.A. Abdulkareem, A.M. Mustafa Al Bakri, H. Kamarudin, I. Khairul Nizar, A.A. Saif, Effects of elevated temperatures on the thermal behavior and mechanical performance of fly ash geopolymer paste, mortar and lightweight concrete, *Constr. Build. Mater.* (2014).
<https://doi.org/10.1016/j.conbuildmat.2013.09.047>.
- [50] H. Mazaheripour, S. Ghanbarpour, S.H. Mirmoradi, I. Hosseinpour, The effect of polypropylene fibers on the properties of fresh and hardened lightweight self-compacting concrete, *Constr. Build. Mater.* 25 (2011) 351–358. <https://doi.org/10.1016/j.conbuildmat.2010.06.018>.
- [51] K.S. Chia, M.H. Zhang, Workability of air-entrained lightweight concrete from rheology perspective, *Mag. Concr. Res.* 59 (2007) 367–375. <https://doi.org/10.1680/macr.2007.59.5.367>.
- [52] A. Scanlon, Fundamentals of High Performance Concrete, *J. Struct. Eng.* 127 (2001) 976–976.
[https://doi.org/10.1061/\(asce\)0733-9445\(2001\)127:8\(976\)](https://doi.org/10.1061/(asce)0733-9445(2001)127:8(976)).
- [53] R. Jansson, L. Boström, The influence of pressure in the pore system on fire spalling of concrete, *Fire Technol.* 46 (2010) 217–230. <https://doi.org/10.1007/s10694-009-0093-9>.
- [54] R. Zhao, J.G. Sanjayan, Geopolymer and Portland cement concretes in simulated fire, *Mag. Concr. Res.* 63 (2011) 163–173. <https://doi.org/10.1680/macr.9.00110>.

- [55] L. Vickers, A. van Riessen, W. Rickard, *Fire-resistant Geopolymers: Role of Fibres and Fillers to Enhance Thermal Properties*, 2015.
- [56] V.F.F. Barbosa, K.J.D. MacKenzie, Thermal behaviour of inorganic geopolymers and composites derived from sodium polysialate, *Mater. Res. Bull.* 38 (2003) 319–331. [https://doi.org/10.1016/S0025-5408\(02\)01022-X](https://doi.org/10.1016/S0025-5408(02)01022-X).
- [57] D.L.Y. Kong, J.G. Sanjayan, Damage behavior of geopolymer composites exposed to elevated temperatures, *Cem. Concr. Compos.* 30 (2008) 986–991. <https://doi.org/10.1016/j.cemconcomp.2008.08.001>.
- [58] D.L.Y. Kong, J.G. Sanjayan, Effect of elevated temperatures on geopolymer paste, mortar and concrete, *Cem. Concr. Res.* 40 (2010) 334–339. <https://doi.org/10.1016/j.cemconres.2009.10.017>.
- [59] A. Kashani, T.D. Ngo, B. Walkley, P. Mendis, Thermal performance of calcium-rich alkali-activated materials: A microstructural and mechanical study, *Constr. Build. Mater.* 153 (2017) 225–237. <https://doi.org/10.1016/j.conbuildmat.2017.07.119>.
- [60] R.S. Amran, M., Huang, S. S., Debbarma, S., & Rashid, Fire resistance of geopolymer concrete: A critical review, *Constr. Build. Mater.* 324 (2022) 126722.
- [61] M. Amran, R. Fediuk, H.S. Abdelgader, G. Murali, T. Ozbakkaloglu, Y.H. Lee, Y.Y. Lee, Fiber-reinforced alkali-activated concrete: A review, *J. Build. Eng.* 45 (2022). <https://doi.org/10.1016/j.job.2021.103638>.
- [62] W.D.A. Rickard, L. Vickers, A. van Riessen, Performance of fibre reinforced, low density metakaolin geopolymers under simulated fire conditions, *Appl. Clay Sci.* 73 (2013) 71–77. <https://doi.org/10.1016/j.clay.2012.10.006>.
- [63] W.D.A. Rickard, A. Van Riessen, Performance of solid and cellular structured fly ash geopolymers exposed to a simulated fire, *Cem. Concr. Compos.* 48 (2014) 75–82. <https://doi.org/10.1016/j.cemconcomp.2013.09.002>.
- [64] Y.H.M. Amran, M.G. Soto, R. Alyousef, M. El-Zeadani, H. Alabduljabbar, V. Aune, Performance investigation of high-proportion Saudi-fly-ash-based concrete, *Results Eng.* (2020). <https://doi.org/10.1016/j.rineng.2020.100118>.
- [65] M. Amran, R. Fediuk, G. Murali, S. Avudaiappan, T. Ozbakkaloglu, N. Vatin, M. Karelina, S. Klyuev, A. Gholampour, Fly ash-based eco-efficient concretes: A comprehensive review of the short-term properties, *Materials (Basel)*. 14 (2021). <https://doi.org/10.3390/ma14154264>.
- [66] C.E. White, J.L. Provis, T. Proffen, J.S.J. Van Deventer, The effects of temperature on the local structure of metakaolin-based geopolymer binder: A neutron pair distribution function investigation, *J. Am. Ceram. Soc.* 93 (2010) 3486–3492. <https://doi.org/10.1111/j.1551-2916.2010.03906.x>.
- [67] R.S.M. Rashid, S.M. Salem, N.M. Azreen, Y.L. Voo, M. Haniza, A.A. Shukri, M.S. Yahya, Effect of elevated temperature to radiation shielding of ultra-high performance concrete with silica sand or magnetite, *Constr. Build. Mater.* 262 (2020) 120567. <https://doi.org/10.1016/j.conbuildmat.2020.120567>.
- [68] N.M. Azreen, R.S.M. Rashid, Y.H. Mugahed Amran, Y.L. Voo, M. Haniza, M. Hairie, R. Alyousef, H. Alabduljabbar, Simulation of ultra-high-performance concrete mixed with hematite and barite aggregates using Monte Carlo for dry cask storage, *Constr. Build. Mater.* 263 (2020). <https://doi.org/10.1016/j.conbuildmat.2020.120161>.
- [69] N.M. Azreen, R.S.M. Rashid, M. Haniza, Y.L. Voo, Y.H. Mugahed Amran, Radiation shielding of ultra-high-performance concrete with silica sand, amang and lead glass, *Constr. Build. Mater.* 172 (2018) 370–377. <https://doi.org/10.1016/j.conbuildmat.2018.03.243>.
- [70] X. Liu, G. Ye, G. De Schutter, Y. Yuan, L. Taerwe, On the mechanism of polypropylene fibres in preventing fire spalling in self-compacting and high-performance cement paste, *Cem. Concr. Res.* 38 (2008) 487–499. <https://doi.org/10.1016/j.cemconres.2007.11.010>.

- [71] J.C. Liu, K.H. Tan, Y. Yao, A new perspective on nature of fire-induced spalling in concrete, *Constr. Build. Mater.* 184 (2018) 581–590. <https://doi.org/10.1016/j.conbuildmat.2018.06.204>.
- [72] L.T. Phan, Pore pressure and explosive spalling in concrete, *Mater. Struct. Constr.* 41 (2008) 1623–1632. <https://doi.org/10.1617/s11527-008-9353-2>.
- [73] L.T. Phan, N.J. Carino, Review of Mechanical Properties of HSC at Elevated Temperature, *J. Mater. Civ. Eng.* 10 (1998) 58–65. [https://doi.org/10.1061/\(asce\)0899-1561\(1998\)10:1\(58\)](https://doi.org/10.1061/(asce)0899-1561(1998)10:1(58)).
- [74] P. Rattanachu, W. Tangchirapat, C. Jaturapitakkul, Water Permeability and Sulfate Resistance of Eco-Friendly High-Strength Concrete Composed of Ground Bagasse Ash and Recycled Concrete Aggregate, *J. Mater. Civ. Eng.* (2019). [https://doi.org/10.1061/\(ASCE\)MT.1943-5533.0002740](https://doi.org/10.1061/(ASCE)MT.1943-5533.0002740).
- [75] H.-S. So, Spalling Prevention of High Performance Concrete at High Temperatures, in: *High Perform. Concr. Technol. Appl.*, 2016. <https://doi.org/10.5772/64551>.
- [76] Y. Anderberg, Spalling phenomena of HPC and OC, in: *Int. Work. Fire Perform. High-Strength Concr.* NIST, 1997: pp. 69–73.
- [77] A.M. GIL, B. FERNANDES, F.L. BOLINA, B.F. TUTIKIAN, Experimental analysis of the spalling phenomenon in precast reinforced concrete columns exposed to high temperatures, *Rev. IBRACON Estruturas E Mater.* 11 (2018) 856–875. <https://doi.org/10.1590/s1983-41952018000400011>.
- [78] M.R. Bangi, T. Horiguchi, Pore pressure development in hybrid fibre-reinforced high strength concrete at elevated temperatures, *Cem. Concr. Res.* 41 (2011) 1150–1156. <https://doi.org/10.1016/j.cemconres.2011.07.001>.
- [79] S.H. Chang, S.W. Choi, J. Lee, Determination of the combined heat transfer coefficient to simulate the fire-induced damage of a concrete tunnel lining under a severe fire condition, *Tunn. Undergr. Sp. Technol.* 54 (2016) 1–12. <https://doi.org/10.1016/j.tust.2016.01.022>.
- [80] S. Jacobsen, E.J. Sellevold, Self healing of high strength concrete after deterioration by freeze/thaw, *Cem. Concr. Res.* 26 (1996) 55–62. [https://doi.org/10.1016/0008-8846\(95\)00179-4](https://doi.org/10.1016/0008-8846(95)00179-4).
- [81] P.K. Sarker, S. Kelly, Z. Yao, Effect of fire exposure on cracking, spalling and residual strength of fly ash geopolymer concrete, *Mater. Des.* 63 (2014) 584–592. <https://doi.org/10.1016/j.matdes.2014.06.059>.
- [82] Y. Zhang, M. Zeiml, M. Maier, Y. Yuan, R. Lackner, Fast assessing spalling risk of tunnel linings under RABT fire: From a coupled thermo-hydro-chemo-mechanical model towards an estimation method, *Eng. Struct.* 142 (2017) 1–19. <https://doi.org/10.1016/j.engstruct.2017.03.068>.
- [83] M. Shamalta, A. Breunese, W. Peelen, J. Fellingner, Numerical modelling and experimental assessment of concrete spalling in fire, *Heron.* 50 (2005) 303–319.
- [84] E. Annerel, L. Taerwe, Revealing the temperature history in concrete after fire exposure by microscopic analysis, *Cem. Concr. Res.* 39 (2009) 1239–1249. <https://doi.org/10.1016/j.cemconres.2009.08.017>.
- [85] Z. Xing, A.L. Beaucour, R. Hebert, A. Noumowe, B. Ledesert, Influence of the nature of aggregates on the behaviour of concrete subjected to elevated temperature, *Cem. Concr. Res.* 41 (2011) 392–402. <https://doi.org/10.1016/j.cemconres.2011.01.005>.
- [86] F. Lo Monte, P.G. Gambarova, Corner spalling and tension stiffening in heat-damaged R/C members: a preliminary investigation, *Mater. Struct. Constr.* 48 (2015) 3657–3673. <https://doi.org/10.1617/s11527-014-0429-x>.
- [87] J.C. Liu, K.H. Tan, Mechanism of PVA fibers in mitigating explosive spalling of engineered cementitious composite at elevated temperature, *Cem. Concr. Compos.* 93 (2018) 235–245. <https://doi.org/10.1016/j.cemconcomp.2018.07.015>.
- [88] Z.P. Bažant, Analysis of pore pressure, thermal stress and fracture in rapidly heated concrete, *Nist.* (1997) 155–164.
- [89] V.K.R. Kodur, A. Agrawal, An approach for evaluating residual capacity of reinforced concrete beams exposed to fire, *Eng. Struct.* 110 (2016) 293–306. <https://doi.org/10.1016/j.engstruct.2015.11.047>.

- [90] V. Francioso, C. Moro, A. Castillo, M. Velay-Lizancos, Effect of elevated temperature on flexural behavior and fibers-matrix bonding of recycled PP fiber-reinforced cementitious composite, *Constr. Build. Mater.* 269 (2021). <https://doi.org/10.1016/j.conbuildmat.2020.121243>.
- [91] A.F. Izzet, N. Oukaili, N.A. Harbi, Post-fire serviceability and residual strength of composite post-tensioned concrete T-beams, *SN Appl. Sci.* 3 (2021). <https://doi.org/10.1007/s42452-020-04116-9>.
- [92] G.A. Khoury, Polypropylene fibres in heated concrete. Part 2: Pressure relief mechanisms and modelling criteria, *Mag. Concr. Res.* 60 (2008) 189–204. <https://doi.org/10.1680/mac.2007.00042>.
- [93] E.W.H. Klingsch, Explosive spalling of concrete in fire, *ETH Union.* (2014) 252.
- [94] T. Gupta, S. Siddique, R.K. Sharma, S. Chaudhary, Effect of elevated temperature and cooling regimes on mechanical and durability properties of concrete containing waste rubber fiber, *Constr. Build. Mater.* 137 (2017) 35–45. <https://doi.org/10.1016/j.conbuildmat.2017.01.065>.
- [95] V.K.R. Kodur, Performance of high strength concrete-filled steel columns exposed to fire, *Can. J. Civ. Eng.* 25 (1998) 975–981. <https://doi.org/10.1139/198-023>.
- [96] D. Zhang, A. Dasari, K.H. Tan, On the mechanism of prevention of explosive spalling in ultra-high performance concrete with polymer fibers, *Cem. Concr. Res.* 113 (2018) 169–177. <https://doi.org/10.1016/j.cemconres.2018.08.012>.
- [97] M. Saravanja, S. Anders, W. Klingsch, Wirkung unterschiedlicher Fasern und Fasergehalte auf das Verhalten ultrahochfester Betone (UHPC) bei hohen Temperaturen, in: *Baust. Und Konstr.*, 2012: pp. 469–475. https://doi.org/10.1007/978-3-642-29573-7_45.
- [98] M. Ozawa, S. Uchida, T. Kamada, H. Morimoto, Study of mechanisms of explosive spalling in high-strength concrete at high temperatures using acoustic emission, *Constr. Build. Mater.* 37 (2012) 621–628. <https://doi.org/10.1016/j.conbuildmat.2012.06.070>.
- [99] J.Y. Lee, T. Yuan, H.O. Shin, Y.S. Yoon, Strategic use of steel fibers and stirrups on enhancing impact resistance of ultra-high-performance fiber-reinforced concrete beams, *Cem. Concr. Compos.* 107 (2020). <https://doi.org/10.1016/j.cemconcomp.2019.103499>.
- [100] G.S.E. Bikakis, C.D. Kalfountzos, E.E. Theotokoglou, Elastic buckling response of rectangular GLARE fiber-metal laminates subjected to shearing stresses, *Aerosp. Sci. Technol.* 87 (2019) 110–118. <https://doi.org/10.1016/j.ast.2019.02.020>.
- [101] P. Folino, M. Ripani, H. Xargay, N. Rocca, Comprehensive analysis of Fiber Reinforced Concrete beams with conventional reinforcement, *Eng. Struct.* 202 (2020). <https://doi.org/10.1016/j.engstruct.2019.109862>.
- [102] T.T. Tran, T.M. Pham, H. Hao, Effect of hybrid fibers on shear behaviour of geopolymer concrete beams reinforced by basalt fiber reinforced polymer (BFRP) bars without stirrups, *Compos. Struct.* 243 (2020). <https://doi.org/10.1016/j.compstruct.2020.112236>.
- [103] T.T. Tran, T.M. Pham, Z. Huang, W. Chen, H. Hao, M. Elchalakani, Impact response of fibre reinforced geopolymer concrete beams with BFRP bars and stirrups, *Eng. Struct.* 231 (2021). <https://doi.org/10.1016/j.engstruct.2020.111785>.
- [104] P.N. Hiremath, S.C. Yaragal, Performance evaluation of reactive powder concrete with polypropylene fibers at elevated temperatures, *Constr. Build. Mater.* 169 (2018) 499–512. <https://doi.org/10.1016/j.conbuildmat.2018.03.020>.
- [105] Y. Li, P. Pimienta, N. Pinoteau, K.H. Tan, Effect of aggregate size and inclusion of polypropylene and steel fibers on explosive spalling and pore pressure in ultra-high-performance concrete (UHPC) at elevated temperature, *Cem. Concr. Compos.* 99 (2019) 62–71. <https://doi.org/10.1016/j.cemconcomp.2019.02.016>.
- [106] J.C. Mindeguia, P. Pimienta, A. Noumowé, M. Kanema, Temperature, pore pressure and mass variation of concrete subjected to high temperature - Experimental and numerical discussion on spalling risk, *Cem.*

- Concr. Res. 40 (2010) 477–487. <https://doi.org/10.1016/j.cemconres.2009.10.011>.
- [107] P. Ren, X. Hou, V.K.R. Kodur, C. Ge, Y. Zhao, W. Zhou, Modeling the fire response of reactive powder concrete beams with due consideration to explosive spalling, *Constr. Build. Mater.* 301 (2021). <https://doi.org/10.1016/j.conbuildmat.2021.124094>.
- [108] ISO 834-1, Fire-resistance tests - Elements of building construction - Part 1: General requirements, ISO Stand. (1999) 1–21. <https://www.sis.se/api/document/preview/615580/>.
- [109] X. Hou, P. Ren, Q. Rong, W. Zheng, Y. Zhan, Comparative fire behavior of reinforced RPC and NSC simply supported beams, *Eng. Struct.* 185 (2019) 122–140. <https://doi.org/10.1016/j.engstruct.2019.01.097>.
- [110] P. Ren, X. Hou, Q. Rong, W. Zheng, Quantifying Fire Insulation Effects on the Fire Response of Hybrid-Fiber Reinforced Reactive Powder Concrete Beams, *Fire Technol.* 56 (2020) 1487–1525. <https://doi.org/10.1007/s10694-019-00937-2>.
- [111] C. Kahanji, F. Ali, A. Nadjai, Explosive spalling of ultra-high performance fibre reinforced concrete beams under fire, *J. Struct. Fire Eng.* 7 (2016) 328–348. <https://doi.org/10.1108/JSFE-12-2016-023>.
- [112] S. Mubarak, M., Muhammad Rashid, R. S., Amran, M., Fediuk, R., Vatin, N., & Klyuev, Mechanical Properties of High-Performance Hybrid Fibre-Reinforced Concrete at Elevated Temperatures, *Sustainability.* 13 (2021) 13392.
- [113] Y. Ju, L. Wang, H. Liu, K. Tian, An experimental investigation of the thermal spalling of polypropylene-fibered reactive powder concrete exposed to elevated temperatures, *Sci. Bull.* 60 (2015) 2022–2040. <https://doi.org/10.1007/s11434-015-0939-0>.
- [114] P. Kalifa, G. Chéné, C. Gallé, High-temperature behaviour of HPC with polypropylene fibres - From spalling to microstructure, *Cem. Concr. Res.* 31 (2001) 1487–1499. [https://doi.org/10.1016/S0008-8846\(01\)00596-8](https://doi.org/10.1016/S0008-8846(01)00596-8).
- [115] M.R. Bangi, T. Horiguchi, Effect of fibre type and geometry on maximum pore pressures in fibre-reinforced high strength concrete at elevated temperatures, *Cem. Concr. Res.* 42 (2012) 459–466. <https://doi.org/10.1016/j.cemconres.2011.11.014>.
- [116] J. Eidan, I. Rasoolan, A. Rezaeian, D. Poorveis, Residual mechanical properties of polypropylene fiber-reinforced concrete after heating, *Constr. Build. Mater.* 198 (2019) 195–206. <https://doi.org/10.1016/j.conbuildmat.2018.11.209>.
- [117] H.Y. Zhang, V. Kodur, S.L. Qi, L. Cao, B. Wu, Development of metakaolin-fly ash based geopolymers for fire resistance applications, *Constr. Build. Mater.* 55 (2014) 38–45. <https://doi.org/10.1016/j.conbuildmat.2014.01.040>.
- [118] Cheng, T. W., & Chiu, J. P. (2003). Fire-resistant geopolymer produced by granulated blast furnace slag. *Minerals engineering*, 16(3), 205-210., (n.d.).
- [119] P. Duan, C. Yan, W. Zhou, W. Luo, Thermal Behavior of Portland Cement and Fly Ash–Metakaolin-Based Geopolymer Cement Pastes, *Arab. J. Sci. Eng.* 40 (2015) 2261–2269. <https://doi.org/10.1007/s13369-015-1748-0>.
- [120] W. Hu, H. Cai, M. Yang, X. Tong, C. Zhou, W. Chen, Fe-C-coated fibre Bragg grating sensor for steel corrosion monitoring, *Corros. Sci.* 53 (2011) 1933–1938. <https://doi.org/10.1016/j.corsci.2011.02.012>.
- [121] B.B.G. Lottman, E.A.B. Koenders, C.B.M. Blom, J.C. Walraven, Spalling of fire exposed concrete, *Heron.* 62 (2017) 129–166.
- [122] P. Shuttleworth, Fire Protection of Concrete Tunnel Linings, *Third Int. Conf. Tunn. Fires.* (2001) 157–165.
- [123] H.R. Thomas, *The Finite Element Method in the Static and Dynamic Deformation and Consolidation of Porous Media. Second Edition*, by R. W. Lewis and B. A. Schrefler, Wiley, New York, 1998. ISBN: 0-471-92809-7. GB 75.00, *Int. J. Numer. Methods Eng.* 48 (2000) 787–787.

- [https://doi.org/10.1002/\(sici\)1097-0207\(20000620\)48:5<787::aid-nme941>3.0.co;2-9](https://doi.org/10.1002/(sici)1097-0207(20000620)48:5<787::aid-nme941>3.0.co;2-9).
- [124] Z. Pan, J.G. Sanjayan, D.L.Y. Kong, Effect of aggregate size on spalling of geopolymer and Portland cement concretes subjected to elevated temperatures, *Constr. Build. Mater.* 36 (2012) 365–372. <https://doi.org/10.1016/j.conbuildmat.2012.04.120>.
- [125] L.A. ASHTON, S.C.C. BATE, A.W. HILL, A.J. HARRIS, D.J.G. SHENNAN, F. WALLEY, O.J. MASTERMAN, J. BORROWSKI, R.J.M. SUTHERLAND, A.B. HARMAN, G.W. SHORTER, T.Z. HARMATHY, D.C. GATENBY, DISCUSSION. THE FIRE-RESISTANCE OF PRESTRESSED CONCRETE BEAMS., *Proc. Inst. Civ. Eng.* 20 (1961) 305–320. <https://doi.org/10.1680/iicep.1961.11228>.
- [126] L. Phan, N.J. Carino, D. Duthinh, E. Garboczi, International Workshop on Fire Performance of High-Strength Concrete, *NIST Spec. Publ.* 919. (1997) 1–179. <http://www.fire.nist.gov/bfrlpubs/fire97/art221.html>.
- [127] V. Babrauskas, Fire safety design and concrete, *Fire Saf. J.* 23 (1994) 439–442. [https://doi.org/10.1016/0379-7112\(94\)90007-8](https://doi.org/10.1016/0379-7112(94)90007-8).
- [128] Z. Abdollahnejad, M. Mastali, M. Falah, T. Luukkonen, M. Mazari, M. Illikainen, Construction and demolition waste as recycled aggregates in alkali-activated concretes, *Materials (Basel)*. 12 (2019). <https://doi.org/10.3390/ma12234016>.
- [129] D.. D.L.Y. Kong, J.G.J.G. Sanjayan, K. Sagoe-Crentsil., K. Sagoe-Crentsil, Comparative performance of geopolymers made with metakaolin and fly ash after exposure to elevated temperatures, *Cem. Concr. Res.* 37 (2007) 1583–1589. <https://doi.org/10.1016/j.cemconres.2007.08.021>.
- [130] A.M. Rashad, S.R. Zeedan, The effect of activator concentration on the residual strength of alkali-activated fly ash pastes subjected to thermal load, *Constr. Build. Mater.* 25 (2011) 3098–3107. <https://doi.org/10.1016/j.conbuildmat.2010.12.044>.
- [131] T.J. Brown, K.K. Sagoe-Crentsil, A.H. Taylor, Comparative assessment of medium-term properties and performance of fly ash and metakaolin geopolymer systems, *J. Aust. Ceram. Soc.* 43 (2007) 131–137.
- [132] N.A. Farhan, M.N. Sheikh, M.N.S. Hadi, Experimental Investigation on the Effect of Corrosion on the Bond Between Reinforcing Steel Bars and Fibre Reinforced Geopolymer Concrete, *Structures*. (2018). <https://doi.org/10.1016/j.istruc.2018.03.013>.
- [133] C.S. Poon, S. Azhar, M. Anson, Y.L. Wong, Performance of metakaolin concrete at elevated temperatures, *Cem. Concr. Compos.* 25 (2003) 83–89. [https://doi.org/10.1016/S0958-9465\(01\)00061-0](https://doi.org/10.1016/S0958-9465(01)00061-0).
- [134] I. Papayianni, T. Valliasis, Heat deformations of fly ash concrete, *Cem. Concr. Compos.* 27 (2005) 249–254. <https://doi.org/10.1016/j.cemconcomp.2004.02.014>.
- [135] F. Qu, W. Li, Z. Tao, A. Castel, K. Wang, High temperature resistance of fly ash/GGBFS-based geopolymer mortar with load-induced damage, *Mater. Struct. Constr.* 53 (2020). <https://doi.org/10.1617/s11527-020-01544-2>.
- [136] Z. Zhang, J.L. Provis, A. Reid, H. Wang, Mechanical, thermal insulation, thermal resistance and acoustic absorption properties of geopolymer foam concrete, *Cem. Concr. Compos.* (2015). <https://doi.org/10.1016/j.cemconcomp.2015.03.013>.
- [137] K.D. Hertz, Danish investigations on silica fume concretes at elevated temperatures, *ACI Mater. J.* 89 (1992) 345–347. <https://doi.org/10.14359/9750>.
- [138] L.T. Phan, N.J. Carino, Effects of test conditions and mixture proportions on behavior of high-strength concrete exposed to high temperatures, *ACI Mater. J.* 99 (2002) 54–66. <https://doi.org/10.14359/11317>.
- [139] R. Jansson, Material properties related to fire spalling of concrete, 2008.
- [140] G.-F. Peng, Evaluation of Fire Damage to High Performance Concrete, *Proquest Diss. Publ.* 6 (2000).
- [141] J. Zhao, J.J. Zheng, G.F. Peng, K. Van Breugel, A meso-level investigation into the explosive spalling mechanism of high-performance concrete under fire exposure, *Cem. Concr. Res.* 65 (2014) 64–75.

- <https://doi.org/10.1016/j.cemconres.2014.07.010>.
- [142] M. Guerrieri, S. Fragomeni, An experimental investigation into the influence of specimen size, in-situ pore pressures and temperatures on the spalling of difference size concrete panels when exposed to a hydrocarbon fire, in: MATEC Web Conf., 2013. <https://doi.org/10.1051/mateconf/20130601002>.
- [143] G. Debicki, R. Haniche, F. Delhomme, An experimental method for assessing the spalling sensitivity of concrete mixture submitted to high temperature, *Cem. Concr. Compos.* 34 (2012) 958–963. <https://doi.org/10.1016/j.cemconcomp.2012.04.002>.
- [144] A. Rahim, U.K. Sharma, K. Murugesan, P. Arora, Effect of load on thermal spalling of reinforced concrete containing various mineral admixtures, in: MATEC Web Conf., 2013. <https://doi.org/10.1051/mateconf/20130601006>.
- [145] E. Chakrawarthi, V., Avudaiappan, S., Amran, M., Dharmar, B., Raj Jesuarulraj, L., Fediuk, R., Aepuru, R., Vatin, N. and Saavedra Flores, Impact Resistance of Polypropylene Fibre-Reinforced Alkali-Activated Copper Slag Concrete, *Materials (Basel)*. 14 (2021) 7735.
- [146] C. Maraveas, A.A. Vrakas, Design of concrete tunnel linings for fire safety, *Struct. Eng. Int. J. Int. Assoc. Bridg. Struct. Eng.* 24 (2014) 319–329. <https://doi.org/10.2749/101686614X13830790993041>.
- [147] F.P. Figueiredo, S.S. Huang, H. Angelakopoulos, K. Pilakoutas, I. Burgess, Effects of Recycled Steel and Polymer Fibres on Explosive Fire Spalling of Concrete, *Fire Technol.* 55 (2019) 1495–1516. <https://doi.org/10.1007/s10694-019-00817-9>.
- [148] T. Lucio-Martin, J. Puentes, M.C. Alonso, Effect of geometry in concrete spalling risk subjected to high temperatures for thermal inertia studies, *Proc. from 6th Int. Work. Concr. Spalling.* 1 (2019) 71–80.
- [149] Z.O. Pehlivanli, I. Uzun, I. Demir, Mechanical and microstructural features of autoclaved aerated concrete reinforced with autoclaved polypropylene, carbon, basalt and glass fiber, *Constr. Build. Mater.* 96 (2015) 428–433. <https://doi.org/10.1016/j.conbuildmat.2015.08.104>.
- [150] Hammer TA, High-strength concrete phase 3, compressive strength and e- modulus at elevated temperatures., 1995.
- [151] S.Y.N. Chan, G.F. Peng, M. Anson, Fire behavior of high-performance concrete made with silica fume at various moisture contents, *ACI Mater. J.* 96 (1999) 405–409. <https://doi.org/10.14359/640>.
- [152] T. Tho-In, V. Sata, P. Chindaprasirt, C. Jaturapitakkul, Pervious high-calcium fly ash geopolymer concrete, *Constr. Build. Mater.* (2012). <https://doi.org/10.1016/j.conbuildmat.2011.12.028>.
- [153] J.C. Liu, Y. Zhang, A simplified model to predict thermo-hygral behaviour and explosive spalling of concrete, *J. Adv. Concr. Technol.* 17 (2019) 419–433. <https://doi.org/10.3151/jact.17.419>.
- [154] V.K.R. Kodur, L. Phan, Critical factors governing the fire performance of high strength concrete systems, *Fire Saf. J.* 42 (2007) 482–488. <https://doi.org/10.1016/j.firesaf.2006.10.006>.
- [155] C.T. Davie, C.J. Pearce, N. Bićanić, Coupled heat and moisture transport in concrete at elevated temperatures - Effects of capillary pressure and adsorbed water, *Numer. Heat Transf. Part A Appl.* 49 (2006) 733–763. <https://doi.org/10.1080/10407780500503854>.
- [156] H.Y. Zhang, G.H. Qiu, V. Kodur, Z.S. Yuan, Spalling behavior of metakaolin-fly ash based geopolymer concrete under elevated temperature exposure, *Cem. Concr. Compos.* 106 (2020). <https://doi.org/10.1016/j.cemconcomp.2019.103483>.
- [157] G.A. Houry, Concrete Spalling Review, *Design.* (2000) 60.
- [158] V.K.R. Kodur, R. McGrath, Effect of silica fume and lateral confinement on fire endurance of high strength concrete columns, *Can. J. Civ. Eng.* 33 (2006) 93–102. <https://doi.org/10.1139/105-089>.
- [159] K.D. Hertz, Limits of spalling of fire-exposed concrete, *Fire Saf. J.* 38 (2003) 103–116. [https://doi.org/10.1016/S0379-7112\(02\)00051-6](https://doi.org/10.1016/S0379-7112(02)00051-6).
- [160] V. Huon, B. Cousin, B. Wattrisse, O. Maisonneuve, Investigating the thermo-mechanical behaviour of cementitious materials using image processing techniques, *Cem. Concr. Res.* 39 (2009) 529–536.

- <https://doi.org/https://doi.org/10.1016/j.cemconres.2009.03.008>.
- [161] U. Schneider, Concrete at high temperatures - A general review, *Fire Saf. J.* 13 (1988) 55–68. [https://doi.org/10.1016/0379-7112\(88\)90033-1](https://doi.org/10.1016/0379-7112(88)90033-1).
- [162] P. Sukontasukkul, S. Jamnam, M. Sappakittipakorn, K. Fujikake, P. Chindaprasirt, Residual flexural behavior of fiber reinforced concrete after heating, *Mater. Struct. Constr.* 51 (2018). <https://doi.org/10.1617/s11527-018-1210-3>.
- [163] G.A. Khoury, C.E. Majorana, F. Pesavento, B.A. Schrefler, Modelling of heated concrete, *Mag. Concr. Res.* 54 (2002) 77–101. <https://doi.org/10.1680/macr.2002.54.2.77>.
- [164] A. Behnood, H. Ziari, Effects of silica fume addition and water to cement ratio on the properties of high-strength concrete after exposure to high temperatures, *Cem. Concr. Compos.* 30 (2008) 106–112. <https://doi.org/10.1016/j.cemconcomp.2007.06.003>.
- [165] S. Deeny, T. Stratford, R.P. Dhakal, P.J. Moss, A.H. Buchanan, Spalling of concrete: Implications for structural performance in fire, in: *Futur. Mech. Struct. Mater. - Proc. 20th Australas. Conf. Mech. Struct. Mater. ACMSM20, 2008*: pp. 231–235.
- [166] Y. Ding, C. Zhang, M. Cao, Y. Zhang, C. Azevedo, Influence of different fibers on the change of pore pressure of self-consolidating concrete exposed to fire, *Constr. Build. Mater.* 113 (2016) 456–469. <https://doi.org/10.1016/j.conbuildmat.2016.03.070>.
- [167] G.F. Peng, W.W. Yang, J. Zhao, Y.F. Liu, S.H. Bian, L.H. Zhao, Explosive spalling and residual mechanical properties of fiber-toughened high-performance concrete subjected to high temperatures, *Cem. Concr. Res.* 36 (2006) 723–727. <https://doi.org/10.1016/j.cemconres.2005.12.014>.
- [168] V.K.R. Kodur, F.-P. Cheng, T.-C. Wang, M.A. Sultan, Effect of Strength and Fiber Reinforcement on Fire Resistance of High-Strength Concrete Columns, *J. Struct. Eng.* 129 (2003) 253–259. [https://doi.org/10.1061/\(asce\)0733-9445\(2003\)129:2\(253\)](https://doi.org/10.1061/(asce)0733-9445(2003)129:2(253)).
- [169] J.C. Mindeguia, P. Pimienta, H. Carré, C. La Borderie, Experimental analysis of concrete spalling due to fire exposure, *Eur. J. Environ. Civ. Eng.* 17 (2013) 453–466. <https://doi.org/10.1080/19648189.2013.786245>.
- [170] G.F. Peng, Z.S. Huang, Change in microstructure of hardened cement paste subjected to elevated temperatures, *Constr. Build. Mater.* 22 (2008) 593–599. <https://doi.org/10.1016/j.conbuildmat.2006.11.002>.
- [171] L.A. Bockeria, V. Arakelyan, Effect of fire on concrete and concrete structures, *Prog. Struct. Eng. Mater.* 2 (2010) 429–447. <https://academic.oup.com/icvts/article-lookup/doi/10.1510/icvts.2006.149260A>.
- [172] D.P. Bentz, Fibers, percolation, and spelling of high-performance concrete, *ACI Struct. J.* 97 (2000) 351–359. <https://doi.org/10.14359/9878>.
- [173] X.H. Wang, S. Jacobsen, J.Y. He, Z.L. Zhang, S.F. Lee, H.L. Lein, Application of nanoindentation testing to study of the interfacial transition zone in steel fiber reinforced mortar, *Cem. Concr. Res.* 39 (2009) 701–715. <https://doi.org/10.1016/j.cemconres.2009.05.002>.
- [174] Y. Li, Y. Zhang, E.H. Yang, K.H. Tan, Effects of geometry and fraction of polypropylene fibers on permeability of ultra-high performance concrete after heat exposure, *Cem. Concr. Res.* 116 (2019) 168–178. <https://doi.org/10.1016/j.cemconres.2018.11.009>.
- [175] F. Zunino, J. Castro, M. Lopez, Thermo-mechanical assessment of concrete microcracking damage due to early-age temperature rise, *Constr. Build. Mater.* 81 (2015) 140–153. <https://doi.org/10.1016/j.conbuildmat.2014.12.126>.
- [176] Z.H. Shui, R. Zhang, W. Chen, D.X. Xuan, Effects of mineral admixtures on the thermal expansion properties of hardened cement paste, *Constr. Build. Mater.* 24 (2010) 1761–1767. <https://doi.org/10.1016/j.conbuildmat.2010.02.012>.
- [177] Y.F. Fu, Y.L. Wong, C.A. Tang, C.S. Poon, Thermal induced stress and associated cracking in cement-

- based composite at elevated temperatures - Part I: Thermal cracking around single inclusion, *Cem. Concr. Compos.* 26 (2004) 99–111. [https://doi.org/10.1016/S0958-9465\(03\)00086-6](https://doi.org/10.1016/S0958-9465(03)00086-6).
- [178] Y.S. Heo, J.G. Sanjayan, C.G. Han, M.C. Han, Relationship between inter-aggregate spacing and the optimum fiber length for spalling protection of concrete in fire, *Cem. Concr. Res.* 42 (2012) 549–557. <https://doi.org/10.1016/j.cemconres.2011.12.002>.
- [179] Y.S. Heo, J.G. Sanjayan, C.G. Han, M.C. Han, Limited effect of diameter of fibres on spalling protection of concrete in fire, *Mater. Struct. Constr.* 45 (2012) 325–335. <https://doi.org/10.1617/s11527-011-9768-z>.
- [180] G. Mazzucco, C.E. Majorana, V.A. Salomoni, Numerical simulation of polypropylene fibres in concrete materials under fire conditions, *Comput. Struct.* 154 (2015) 17–28. <https://doi.org/10.1016/j.compstruc.2015.03.012>.
- [181] D. Wang, C. Shi, Z. Wu, J. Xiao, Z. Huang, Z. Fang, A review on ultra high performance concrete: Part II. Hydration, microstructure and properties, *Constr. Build. Mater.* 96 (2015) 368–377. <https://doi.org/10.1016/j.conbuildmat.2015.08.095>.
- [182] C. Wang, C. Yang, F. Liu, C. Wan, X. Pu, Preparation of Ultra-High Performance Concrete with common technology and materials, *Cem. Concr. Compos.* 34 (2012) 538–544. <https://doi.org/10.1016/j.cemconcomp.2011.11.005>.
- [183] A. Korpa, T. Kowald, R. Trettin, Phase development in normal and ultra high performance cementitious systems by quantitative X-ray analysis and thermoanalytical methods, *Cem. Concr. Res.* 39 (2009) 69–76. <https://doi.org/10.1016/j.cemconres.2008.11.003>.
- [184] S.D. Abyaneh, H.S. Wong, N.R. Buenfeld, Simulating the effect of microcracks on the diffusivity and permeability of concrete using a three-dimensional model, *Comput. Mater. Sci.* 119 (2016) 130–143. <https://doi.org/10.1016/j.commatsci.2016.03.047>.
- [185] J.C. Liu, K.H. Tan, Mechanism of PVA fibers in mitigating explosive spalling of engineered cementitious composite at elevated temperature, *Cem. Concr. Compos.* 93 (2018) 235–245. <https://doi.org/10.1016/j.cemconcomp.2018.07.015>.
- [186] J.C. Liu, Z. Zhang, Prediction of explosive spalling of heated steel fiber reinforced concrete using artificial neural networks, *J. Adv. Concr. Technol.* 18 (2020) 227–240. <https://doi.org/10.3151/jact.18.227>.
- [187] R. Felicetti, F. Lo Monte, P. Pimienta, A new test method to study the influence of pore pressure on fracture behaviour of concrete during heating, *Cem. Concr. Res.* 94 (2017) 13–23. <https://doi.org/10.1016/j.cemconres.2017.01.002>.
- [188] Y.Y. Amran, M., Fediuk, R., Abdelgader, H. S., Murali, G., Ozbakkaloglu, T., Lee, Y. H., & Lee, Fiber-reinforced alkali-activated concrete: A review, *J. Build. Eng.* 45 (2021) 103638. <https://doi.org/10.1016/j.jobbe.2021.103638>.
- [189] M. Amran, R. Fediuk, N. Vatin, Y.H. Lee, G. Murali, T. Ozbakkaloglu, S. Klyuev, H. Alabduljabber, Fibre-reinforced foamed concretes: A review, *Materials (Basel)*. (2020). <https://doi.org/10.3390/ma13194323>.
- [190] J. Kim, G.P. Lee, D.Y. Moon, Evaluation of mechanical properties of steel-fibre-reinforced concrete exposed to high temperatures by double-punch test, *Constr. Build. Mater.* 79 (2015) 182–191. <https://doi.org/10.1016/j.conbuildmat.2015.01.042>.
- [191] X. Hou, M. Abid, W. Zheng, G.Q. Waqar, Evaluation of residual mechanical properties of steel fiber-reinforced reactive powder concrete after exposure to high temperature using nondestructive testing, in: *Procedia Eng.*, 2017: pp. 588–596. <https://doi.org/10.1016/j.proeng.2017.11.118>.
- [192] S. Sanchayan, S.J. Foster, High temperature behaviour of hybrid steel–PVA fibre reinforced reactive powder concrete, *Mater. Struct. Constr.* 49 (2016) 769–782. <https://doi.org/10.1617/s11527-015-0537-2>.
- [193] X. Hou, P. Ren, Q. Rong, W. Zheng, Y. Zhan, Effect of fire insulation on fire resistance of hybrid-fiber

- reinforced reactive powder concrete beams, *Compos. Struct.* 209 (2019) 219–232.
<https://doi.org/10.1016/j.compstruct.2018.10.073>.
- [194] M. Abid, X. Hou, W. Zheng, R.R. Hussain, Effect of fibers on high-temperature mechanical behavior and microstructure of reactive powder concrete, *Materials (Basel)*. 12 (2019).
<https://doi.org/10.3390/ma12020329>.
- [195] M. Abid, X. Hou, W. Zheng, R.R. Hussain, High temperature and residual properties of reactive powder concrete – A review, *Constr. Build. Mater.* 147 (2017) 339–351.
<https://doi.org/10.1016/j.conbuildmat.2017.04.083>.
- [196] M. Abid, X. Hou, W. Zheng, R.R. Hussain, S. Cao, Z. Lv, Creep behavior of steel fiber reinforced reactive powder concrete at high temperature, *Constr. Build. Mater.* 205 (2019) 321–331.
<https://doi.org/10.1016/j.conbuildmat.2019.02.019>.
- [197] X. Hou, M. Abid, W. Zheng, R.R. Hussain, Effects of Temperature and Stress on Creep Behavior of PP and Hybrid Fiber Reinforced Reactive Powder Concrete, *Int. J. Concr. Struct. Mater.* 13 (2019).
<https://doi.org/10.1186/s40069-019-0357-9>.
- [198] R. Serrano, A. Cobo, M.I. Prieto, M. de las N. González, Analysis of fire resistance of concrete with polypropylene or steel fibers, *Constr. Build. Mater.* 122 (2016) 302–309.
<https://doi.org/10.1016/j.conbuildmat.2016.06.055>.
- [199] O. Czoboly, É. Lubl6y, V. Hlavicka, G.L. Balázs, O. Kéri, I.M. Szilágyi, Fibers and fiber cocktails to improve fire resistance of concrete, *J. Therm. Anal. Calorim.* 128 (2017) 1453–1461.
<https://doi.org/10.1007/s10973-016-6038-x>.
- [200] N. Yermak, P. Pliya, A.L. Beaucour, A. Simon, A. Noumowé, Influence of steel and/or polypropylene fibres on the behaviour of concrete at high temperature: Spalling, transfer and mechanical properties, *Constr. Build. Mater.* 132 (2017) 240–250. <https://doi.org/10.1016/j.conbuildmat.2016.11.120>.
- [201] C.T. Davie, H.L. Zhang, A. Gibson, Investigation of a continuum damage model as an indicator for the prediction of spalling in fire exposed concrete, *Comput. Struct.* 94–95 (2012) 54–69.
<https://doi.org/10.1016/j.compstruc.2011.12.002>.
- [202] A.N. Noumowe, R. Siddique, G. Debicki, Permeability of high-performance concrete subjected to elevated temperature (600 °C), *Constr. Build. Mater.* 23 (2009) 1855–1861.
<https://doi.org/10.1016/j.conbuildmat.2008.09.023>.
- [203] J. Bošnjak, J. Ožbolt, R. Hahn, Permeability measurement on high strength concrete without and with polypropylene fibers at elevated temperatures using a new test setup, *Cem. Concr. Res.* 53 (2013) 104–111. <https://doi.org/10.1016/j.cemconres.2013.06.005>.
- [204] C. Maluk, J. Tignard, A. Ridout, T. Clarke, R. Winterberg, Experimental study on the fire behaviour of fibre reinforced concrete used in tunnel applications, *Fire Saf. J.* 120 (2021).
<https://doi.org/10.1016/j.firesaf.2020.103173>.
- [205] C. Maluk, G. Pietro Terrasi, L. Bisby, A. Stutz, E. Hugi, Fire resistance tests on thin CFRP prestressed concrete slabs, *Constr. Build. Mater.* 101 (2015) 558–571.
<https://doi.org/10.1016/j.conbuildmat.2015.10.031>.
- [206] J. Holan, J. Novák, P. Müller, R. Štefan, Experimental investigation of the compressive strength of normal-strength air-entrained concrete at high temperatures, *Constr. Build. Mater.* 248 (2020).
<https://doi.org/10.1016/j.conbuildmat.2020.118662>.
- [207] I. Rickard, N. Gerasimov, L. Bisby, S. Deeny, Predictive testing for heat induced spalling of concrete tunnel linings - The potential influence of sustained mechanical loading, in: *Proc. from 5th Int. Work. Concr. Spalling, 2017*: pp. 337–344. <http://3-files.conferencemanager.dk/medialibrary/95B20059-9A60-444D-8AB2-6F7B3F8C58E9/images/Web-version.pdf>.
- [208] I. Rickard, L. Bisby, S. Deeny, C. Maluk, Predictive Testing for Heat Induced Spalling of Concrete

- Tunnels – The Influence of Mechanical Loading, in: *Struct. Fire Proc. 9th Conf.*, 2016: pp. 217–224.
- [209] W.K. Chow, Fire Safety Concern for Supertall Buildings, *ASHRAE Winter Conf. 7* (2014) 1–12.
- [210] I. Lau, C.-Q. Li, G. Fu, Prediction of Time to Corrosion-Induced Concrete Cracking Based on Fracture Mechanics Criteria, *J. Struct. Eng.* 145 (2019) 4019069. [https://doi.org/10.1061/\(asce\)st.1943-541x.0002352](https://doi.org/10.1061/(asce)st.1943-541x.0002352).
- [211] Y. Zhao, A.R. Karimi, H.S. Wong, B. Hu, N.R. Buenfeld, W. Jin, Comparison of uniform and non-uniform corrosion induced damage in reinforced concrete based on a Gaussian description of the corrosion layer, *Corros. Sci.* 53 (2011) 2803–2814. <https://doi.org/10.1016/j.corsci.2011.05.017>.
- [212] Z.P. Bazant, PHYSICAL MODEL FOR STEEL CORROSION IN CONCRETE SEA STRUCTURES - APPLICATION, *ASCE J Struct Div.* 105 (1979) 1155–1166. <https://doi.org/10.1061/jsdeag.0005169>.
- [213] A.A. Torres-Acosta, M. Martnez-Madrid, Residual Life of Corroding Reinforced Concrete Structures in Marine Environment, *J. Mater. Civ. Eng.* 15 (2003) 344–353. [https://doi.org/10.1061/\(asce\)0899-1561\(2003\)15:4\(344\)](https://doi.org/10.1061/(asce)0899-1561(2003)15:4(344)).
- [214] DuraCrete, General Guidelines for Durability Design and Redesign, Eur. Union-Brite Euram III, Proj. No. BE95-1347, Probabilistic Perform. -Based Durab. Des. *Concr. Struct.* (2000) 1–138.
- [215] F. Lo Monte, R. Felicetti, M.J. Miah, The influence of pore pressure on fracture behaviour of Normal-Strength and High-Performance Concretes at high temperature, *Cem. Concr. Compos.* 104 (2019). <https://doi.org/10.1016/j.cemconcomp.2019.103388>.
- [216] J.P. Firmo, J.R. Correia, L.A. Bisby, Fire behaviour of FRP-strengthened reinforced concrete structural elements: A state-of-the-art review, *Compos. Part B Eng.* 80 (2015) 198–216. <https://doi.org/10.1016/j.compositesb.2015.05.045>.
- [217] T.E.T. Buttignol, J.L.A.O. Sousa, T.N. Bittencourt, Ultra High-Performance Fiber-Reinforced Concrete (UHPRFC): a review of material properties and design procedures, *Rev. IBRACON Estruturas E Mater.* (2017). <https://doi.org/10.1590/s1983-41952017000400011>.
- [218] G.A. Khoury, Effect of fire on concrete and concrete structures, *Prog. Struct. Eng. Mater.* 2 (2000) 429–447. <https://doi.org/10.1002/pse.51>.
- [219] A. Behnood, M. Ghandehari, Comparison of compressive and splitting tensile strength of high-strength concrete with and without polypropylene fibers heated to high temperatures, *Fire Saf. J.* 44 (2009) 1015–1022. <https://doi.org/10.1016/j.firesaf.2009.07.001>.
- [220] W. Khaliq, V. Kodur, Effectiveness of Polypropylene and Steel Fibers in Enhancing Fire Resistance of High-Strength Concrete Columns, *J. Struct. Eng.* 144 (2018) 4017224. [https://doi.org/10.1061/\(asce\)st.1943-541x.0001981](https://doi.org/10.1061/(asce)st.1943-541x.0001981).
- [221] V. Afroughsabet, T. Ozbakkaloglu, Mechanical and durability properties of high-strength concrete containing steel and polypropylene fibers, *Constr. Build. Mater.* (2015). <https://doi.org/10.1016/j.conbuildmat.2015.06.051>.
- [222] D. Zhang, K.H. Tan, Effect of various polymer fibers on spalling mitigation of ultra-high performance concrete at high temperature, *Cem. Concr. Compos.* 114 (2020) 1–9. <https://doi.org/10.1016/j.cemconcomp.2020.103815>.
- [223] Y.S. Kim, T.G. Lee, G.Y. Kim, An experimental study on the residual mechanical properties of fiber reinforced concrete with high temperature and load, *Mater. Struct. Constr.* 46 (2013) 607–620. <https://doi.org/10.1617/s11527-012-9918-y>.
- [224] X. Liang, C. Wu, Y. Su, Z. Chen, Z. Li, Development of ultra-high performance concrete with high fire resistance, *Constr. Build. Mater.* 179 (2018) 400–412. <https://doi.org/10.1016/j.conbuildmat.2018.05.241>.
- [225] J. Bošnjak, A. Sharma, K. Grauf, Mechanical properties of concrete with steel and polypropylene fibres at elevated temperatures, *Fibers.* 7 (2019). <https://doi.org/10.3390/FIB7020009>.

- [226] V. Zhukov, Explosive failure of concrete during a fire, *Transl. No. DT.* (1970) 2124.
- [227] G.A. Houry, Passive fire protection of concrete structures, *Proc. Inst. Civ. Eng. Struct. Build.* 161 (2008) 135–145. <https://doi.org/10.1680/stbu.2008.161.3.135>.
- [228] G.A. Houry, Compressive strength of concrete at high temperatures: a reassessment, *Mag. Concr. Res.* (2009). <https://doi.org/10.1680/mac.1992.44.161.291>.
- [229] G.A. Houry, Compressive strength of concrete at high temperatures: A reassessment, *Mag. Concr. Res.* 44 (1992) 291–309. <https://doi.org/10.1680/mac.1992.44.161.291>.
- [230] E. Klingsch, A. Frangi, M. Fontana, Experimental Analysis of Concrete Strength at High Temperatures and after Cooling, *Acta Polytech.* 49 (2009). <https://doi.org/10.14311/1087>.
- [231] Z. Wu, S. Huen Lo, K. Hai Tan, K. Leung Su, High Strength Concrete Tests under Elevated Temperature, *Athens J. Technology Eng.* 6 (2019) 141–162. <https://doi.org/10.30958/ajte.6-3-1>.
- [232] B. Demirel, O. Keleştemur, Effect of elevated temperature on the mechanical properties of concrete produced with finely ground pumice and silica fume, *Fire Saf. J.* 45 (2010) 385–391. <https://doi.org/10.1016/j.firesaf.2010.08.002>.
- [233] F. Kigha, J. Sadeeq, O. Abejide, Effects of Temperature Levels and Concrete Cover Thickness on Residual Strength Characteristics of Fire Exposed Reinforced Concrete Beams, *Niger. J. Technol.* 34 (2015) 429. <https://doi.org/10.4314/njt.v34i3.1>.
- [234] A. Jadooe, R. Al-Mahaidi, K. Abdouka, Performance of heat-damaged partially-insulated RC beams strengthened with NSM CFRP strips and epoxy adhesive, *Constr. Build. Mater.* 159 (2018) 617–634. <https://doi.org/10.1016/j.conbuildmat.2017.11.020>.
- [235] A. Jadooe, R. Al-Mahaidi, K. Abdouka, Behaviour of heat-damaged partially-insulated RC beams using NSM systems, *Constr. Build. Mater.* 180 (2018) 211–228. <https://doi.org/10.1016/j.conbuildmat.2018.05.279>.
- [236] C. Thongchom, A. Lenwari, R.S. Aboutaha, Effect of sustained service loading on post-fire flexural response of reinforced concrete T-beams, *ACI Struct. J.* 116 (2019) 243–254. <https://doi.org/10.14359/51714477>.
- [237] V.K. Kodur, A. Agrawal, Critical Factors Governing the Residual Response of Reinforced Concrete Beams Exposed to Fire, *Fire Technol.* 52 (2016) 967–993. <https://doi.org/10.1007/s10694-015-0527-5>.
- [238] H.Y. Zhang, V. Kodur, B. Wu, L. Cao, F. Wang, Thermal behavior and mechanical properties of geopolymer mortar after exposure to elevated temperatures, *Constr. Build. Mater.* 109 (2016) 17–24. <https://doi.org/10.1016/j.conbuildmat.2016.01.043>.
- [239] M.T. Junaid, A. Khennane, O. Kayali, Performance of fly ash based geopolymer concrete made using non-pelletized fly ash aggregates after exposure to high temperatures, *Mater. Struct. Constr.* 48 (2015) 3357–3365. <https://doi.org/10.1617/s11527-014-0404-6>.
- [240] G.J.G. Gluth, W.D.A. Rickard, S. Werner, S. Pirskawetz, Acoustic emission and microstructural changes in fly ash geopolymer concretes exposed to simulated fire, *Mater. Struct. Constr.* 49 (2016) 5243–5254. <https://doi.org/10.1617/s11527-016-0857-x>.
- [241] L.T. Phan, J.R. Lawson, F.L. Davis, Effects of elevated temperature exposure on heating characteristics, spalling, and residual properties of high performance concrete, *Mater. Struct. Constr.* 34 (2001) 83–91. <https://doi.org/10.1007/bf02481556>.
- [242] H. Fares, A. Noumowe, S. Remond, Self-consolidating concrete subjected to high temperature. Mechanical and physicochemical properties, *Cem. Concr. Res.* 39 (2009) 1230–1238. <https://doi.org/10.1016/j.cemconres.2009.08.001>.
- [243] M. Kanéma, P. Pliya, A. Noumowé, J.-L. Gallias, Spalling, Thermal, and Hydrous Behavior of Ordinary and High-Strength Concrete Subjected to Elevated Temperature, *J. Mater. Civ. Eng.* 23 (2011) 921–930. [https://doi.org/10.1061/\(asce\)mt.1943-5533.0000272](https://doi.org/10.1061/(asce)mt.1943-5533.0000272).

- [244] B. Akturk, N. Yuzer, N. Kabay, Usability of Raw Rice Husk Instead of Polypropylene Fibers in High-Strength Concrete under High Temperature, *J. Mater. Civ. Eng.* 28 (2016) 4015072. [https://doi.org/10.1061/\(asce\)mt.1943-5533.0001341](https://doi.org/10.1061/(asce)mt.1943-5533.0001341).
- [245] M. Ozawa, F.U.A. Shaikh, A study on spalling behaviour of geopolymer mortars using ring restraint test, *Constr. Build. Mater.* 279 (2021). <https://doi.org/10.1016/j.conbuildmat.2021.122494>.
- [246] D. Han, Influential factors on the level of spalling in fire exposed concrete, *J. Ceram. Process. Res.* 17 (2016) 550–554. <https://doi.org/10.36410/JCPR.2016.17.6.550>.
- [247] M. García de Lomas, M.I. Sánchez de Rojas, M. Frías, Pozzolanic reaction of a spent fluid catalytic cracking catalyst in FCC-cement mortars, *J. Therm. Anal. Calorim.* 90 (2007) 443–447. <https://doi.org/10.1007/s10973-006-7921-7>.
- [248] M. Lahoti, K.H. Tan, E.H. Yang, A critical review of geopolymer properties for structural fire-resistance applications, *Constr. Build. Mater.* 221 (2019) 514–526. <https://doi.org/10.1016/j.conbuildmat.2019.06.076>.
- [249] P.K. Sarker, S. McBeath, Fire endurance of steel reinforced fly ash geopolymer concrete elements, *Constr. Build. Mater.* 90 (2015) 91–98. <https://doi.org/10.1016/j.conbuildmat.2015.04.054>.
- [250] F. Shaikh, S. Haque, Behaviour of Carbon and Basalt Fibres Reinforced Fly Ash Geopolymer at Elevated Temperatures, *Int. J. Concr. Struct. Mater.* 12 (2018). <https://doi.org/10.1186/s40069-018-0267-2>.
- [251] F.U.A. Shaikh, A. Hosan, Mechanical properties of steel fibre reinforced geopolymer concretes at elevated temperatures, *Constr. Build. Mater.* (2016). <https://doi.org/10.1016/j.conbuildmat.2016.03.158>.
- [252] S. Luhar, D. Nicolaidis, I. Luhar, Fire resistance behaviour of geopolymer concrete: An overview, *Buildings.* 11 (2021) 1–30. <https://doi.org/10.3390/buildings11030082>.
- [253] D.A. Crozier, J.G. Sanjayan, Tests of load-bearing slender reinforced concrete walls in fire, *ACI Struct. J.* 97 (2000) 243–251. <https://doi.org/10.14359/853>.
- [254] A.Z. Mohd Ali, J. Sanjayan, The spalling of geopolymer high strength concrete wall panels and cylinders under hydrocarbon fire, in: *MATEC Web Conf.*, 2016. <https://doi.org/10.1051/mateconf/20164702005>.
- [255] *Designers' Guide to EN 1991-1-4 Eurocode 1: Actions on structures, general actions part 1-4.* Wind actions, 2007. <https://doi.org/10.1680/dgte1.31524>.
- [256] F. Colangelo, R. Cioffi, G. Roviello, I. Capasso, D. Caputo, P. Aprea, B. Liguori, C. Ferone, Thermal cycling stability of fly ash based geopolymer mortars, *Compos. Part B Eng.* 129 (2017) 11–17. <https://doi.org/10.1016/j.compositesb.2017.06.029>.
- [257] A.M. Onaizi, N.H.A.S. Lim, G.F. Huseien, M. Amran, C.K. Ma, Effect of the addition of nano glass powder on the compressive strength of high volume fly ash modified concrete, *Mater. Today Proc.* (2021). <https://doi.org/10.1016/j.matpr.2021.08.347>.
- [258] G. Peng, J. Yang, Residual Mechanical Properties and Explosive Spalling Behavior of Ultra-High-Strength Concrete Exposed to High Temperature, *J. Harbin Inst. Technol. (New Ser.)* 24 (2017) 62–70. <https://doi.org/10.11916/j.issn.1005-9113.16096>.
- [259] W. Zheng, H. Li, Y. Wang, Compressive stress-strain relationship of steel fiber-reinforced reactive powder concrete after exposure to elevated temperatures, *Constr. Build. Mater.* 35 (2012) 931–940. <https://doi.org/10.1016/j.conbuildmat.2012.05.031>.
- [260] R.J. Hussein, N.A.A. Alwash, J.J. Alwash, Combining polypropylene and steel fiber to reduce spalling of reactive powder concrete subjected to fire flame, in: *AIP Conf. Proc.*, 2020. <https://doi.org/10.1063/5.0000101>.
- [261] C.T. Liu, J.S. Huang, Fire performance of highly flowable reactive powder concrete, *Constr. Build. Mater.* 23 (2009) 2072–2079. <https://doi.org/10.1016/j.conbuildmat.2008.08.022>.
- [262] V. Patel, B. Singh, P.N. Ojha, S. Adhikari, Mechanical Properties of Polypropylene Fiber Reinforced Concrete under Elevated Temperature, *J. Archit. Environ. Struct. Eng. Res.* 4 (2021).

- <https://doi.org/10.30564/jaeser.v4i2.3296>.
- [263] M. Abid, X. Hou, W. Zheng, G.Q. Waqar, Mechanical properties of steel fiber-reinforced reactive powder concrete at high temperature and after cooling, *Procedia Eng.* 210 (2017) 597–604. <https://doi.org/10.1016/j.proeng.2017.11.119>.
- [264] H. Wu, X. Lin, A. Zhou, A review of mechanical properties of fibre reinforced concrete at elevated temperatures, *Cem. Concr. Res.* 135 (2020). <https://doi.org/10.1016/j.cemconres.2020.106117>.
- [265] and M.E. Lesovik, Valery, Roman Fediuk, Mugahed Amran, Arbi Alaskhanov, Aleksandr Volodchenko, Gunasekaran Murali, Valery Uvarov, 3D-Printed Mortars with Combined Steel and Polypropylene Fibers, *Fibers.* 9 (2021) 79.
- [266] W. Zheng, H. Li, Y. Wang, Compressive behaviour of hybrid fiber-reinforced reactive powder concrete after high temperature, *Mater. Des.* 41 (2012) 403–409. <https://doi.org/10.1016/j.matdes.2012.05.026>.
- [267] W. Zheng, B. Luo, Y. Wang, Stress–strain relationship of steel-fibre reinforced reactive powder concrete at elevated temperatures, *Mater. Struct. Constr.* 48 (2015) 2299–2314. <https://doi.org/10.1617/s11527-014-0312-9>.
- [268] Y.-N.K. Y.-S. Tai, H.-H. Pan, Mechanical properties of steel fiber reinforced reactive powder concrete following exposure to high temperature reaching 800 C, *Nucl. Eng. Des.* 241 (2011) 2416–2424.
- [269] W. Zheng, B. Luo, Y. Wang, Compressive and tensile properties of reactive powder concrete with steel fibres at elevated temperatures, *Constr. Build. Mater.* 41 (2013) 844–851. <https://doi.org/10.1016/j.conbuildmat.2012.12.066>.
- [270] W. Zheng, B. Luo, Y. Wang, Microstructure and mechanical properties of RPC containing PP fibres at elevated temperatures, *Mag. Concr. Res.* 66 (2014) 397–408. <https://doi.org/10.1680/macr.13.00232>.
- [271] S. Bei, L. Zhixiang, Investigation on spalling resistance of ultra-high-strength concrete under rapid heating and rapid cooling, *Case Stud. Constr. Mater.* 4 (2016) 146–153. <https://doi.org/10.1016/j.cscm.2016.04.001>.
- [272] K.K. Sideris, P. Manita, A. Papageorgiou, E. Chaniotakis, Mechanical Characteristics of High Performance Fibre Reinforced Concretes at Elevated Temperatures, in: *Am. Concr. Institute, ACI Spec. Publ.*, 2003: pp. 973–988.
- [273] M. Ozawa, H. Morimoto, High-strength concrete reinforced jute fiber and water-soluble PVA fiber under high temperature, in: *Struct. Fire - Proc. Sixth Int. Conf. SiF'10, 2010*: pp. 864–871.
- [274] K.S. U. Munehiro, Study on Fire Resistance of Reinforced Concrete Columns with Ultra High Strength, *Mater. Tech. Res. Institute, Toda Corp.* 32 (2006) 1–13.
- [275] D.P. Bentz, Fibers, Percolation and spalling of HPC.pdf, *ACI Mater. J.* 97 (2001) 351–359. https://tsapps.nist.gov/publication/get_pdf.cfm?pub_id=860181.
- [276] W. Khaliq, V. Kodur, Thermal and mechanical properties of fiber reinforced high performance self-consolidating concrete at elevated temperatures, *Cem. Concr. Res.* 41 (2011) 1112–1122. <https://doi.org/10.1016/j.cemconres.2011.06.012>.
- [277] M.B. Dwaikat, V.K.R. Kodur, Hydrothermal model for predicting fire-induced spalling in concrete structural systems, *Fire Saf. J.* 44 (2009) 425–434. <https://doi.org/10.1016/j.firesaf.2008.09.001>.
- [278] M.Z. Naser, Heuristic machine cognition to predict fire-induced spalling and fire resistance of concrete structures, *Autom. Constr.* 106 (2019). <https://doi.org/10.1016/j.autcon.2019.102916>.
- [279] W. Khaliq, V.K.R. Kodur, Effect of high temperature on tensile strength of different types of high-strength concrete, *ACI Mater. J.* 108 (2011) 394–402. <https://doi.org/10.14359/51683112>.
- [280] G.L. Balázs, É. Lubl6y, Post-heating strength of fiber-reinforced concretes, *Fire Saf. J.* 49 (2012) 100–106. <https://doi.org/10.1016/j.firesaf.2012.01.002>.
- [281] A. Bilodeau, V.K.R. Kodur, G.C. Hoff, Optimization of the type and amount of polypropylene fibres for preventing the spalling of lightweight concrete subjected to hydrocarbon fire, *Cem. Concr. Compos.* 26

- (2004) 163–174. [https://doi.org/10.1016/S0958-9465\(03\)00085-4](https://doi.org/10.1016/S0958-9465(03)00085-4).
- [282] S. Yehia, G. Kashwani, Performance of Structures Exposed to Extreme High Temperature—An Overview, *Open J. Civ. Eng.* 3 (2013) 154–161. <https://doi.org/10.4236/ojce.2013.33018>.
- [283] M.Z. Naser, Autonomous Fire Resistance Evaluation, *J. Struct. Eng.* 146 (2020) 4020103. [https://doi.org/10.1061/\(asce\)st.1943-541x.0002641](https://doi.org/10.1061/(asce)st.1943-541x.0002641).
- [284] M.Z. Naser, A. Seitllari, Concrete under fire: an assessment through intelligent pattern recognition, *Eng. Comput.* 36 (2020) 1915–1928. <https://doi.org/10.1007/s00366-019-00805-1>.
- [285] J. McKinney, F. Ali, Artificial neural networks for the spalling classification & failure prediction times of high strength concrete columns, *J. Struct. Fire Eng.* 5 (2014) 203–214. <https://doi.org/10.1260/2040-2317.5.3.203>.
- [286] K.K. Sideris, P. Manita, Residual mechanical characteristics and spalling resistance of fiber reinforced self-compacting concretes exposed to elevated temperatures, *Constr. Build. Mater.* 41 (2013) 296–302. <https://doi.org/10.1016/j.conbuildmat.2012.11.093>.
- [287] H. Scaperklaus, Woven and nonwoven fabrics made from polypropylene, H. Scaperklaus. (1979) 6.
- [288] BS EN 1992-1-2 NA, BS EN 1992-1-2: Eurocode 2: Design of concrete structures - Part 1-2: General rules. Structural fire design, Part 1-1 Gen. Rules Rules Build. 3 (2008) 259.
- [289] R. Jansson, L. Boström, Factors influencing fire spalling of self compacting concrete, *Mater. Struct. Constr.* 46 (2013) 1683–1694. <https://doi.org/10.1617/s11527-012-0007-z>.
- [290] L. Boström, R. Jansson, Fire spalling of self-compacting concrete, in: 5th Int. RILEM Symp. Self-Compacting Concr., 2007: pp. 741–745. http://www.rilem.org/gene/main.php?base=500218&id_publication=59&id_papier=3052.
- [291] G. Ye, X. Liu, G. De Schutter, L. Taerwe, P. Vandeveldel, Phase distribution and microstructural changes of self-compacting cement paste at elevated temperature, *Cem. Concr. Res.* 37 (2007) 978–987. <https://doi.org/10.1016/j.cemconres.2007.02.011>.
- [292] M.Z. Naser, Observational Analysis of Fire-Induced Spalling of Concrete through Ensemble Machine Learning and Surrogate Modeling, *J. Mater. Civ. Eng.* 33 (2021) 4020428. [https://doi.org/10.1061/\(asce\)mt.1943-5533.0003525](https://doi.org/10.1061/(asce)mt.1943-5533.0003525).
- [293] T.T. Lie, E.L. Schaffer, Synopsis of a manual on structural fire protection, in: *Struct. Congr. XII*, 1994: pp. 1002–1005.
- [294] C. Zhai, L. Chen, Q. Fang, W. Chen, X. Jiang, Experimental study of strain rate effects on normal weight concrete after exposure to elevated temperature, *Mater. Struct. Constr.* 50 (2017). <https://doi.org/10.1617/s11527-016-0879-4>.
- [295] H. Elsanadedy, T. Almusallam, Y. Al-Salloum, R. Iqbal, Effect of high temperature on structural response of reinforced concrete circular columns strengthened with fiber reinforced polymer composites, *J. Compos. Mater.* 51 (2017) 333–355. <https://doi.org/10.1177/0021998316645171>.
- [296] M. Heikal, H. El-Didamony, T.M. Sokkary, I.A. Ahmed, Behavior of composite cement pastes containing microsilica and fly ash at elevated temperature, *Constr. Build. Mater.* 38 (2013) 1180–1190. <https://doi.org/10.1016/j.conbuildmat.2012.09.069>.
- [297] Antonius, A. Widhianto, D. Darmayadi, G.D. Asfari, Fire resistance of normal and high-strength concrete with contains of steel fibre, *Asian J. Civ. Eng.* 15 (2014) 655–669.
- [298] V. Kodur, Properties of concrete at elevated temperatures, *ISRN Civ. Eng.* 2014 (2014). <https://doi.org/10.1155/2014/468510>.
- [299] F.B. Varona, F.J. Baeza, D. Bru, S. Ivorra, Influence of high temperature on the mechanical properties of hybrid fibre reinforced normal and high strength concrete, *Constr. Build. Mater.* 159 (2018) 73–82. <https://doi.org/10.1016/j.conbuildmat.2017.10.129>.
- [300] H. Dilbas, M. Şimşek, Ö. Çakir, An investigation on mechanical and physical properties of recycled

- aggregate concrete (RAC) with and without silica fume, *Constr. Build. Mater.* 61 (2014) 50–59. <https://doi.org/10.1016/j.conbuildmat.2014.02.057>.
- [301] S.L. Suhaendi, T. Horiguchi, Effect of short fibers on residual permeability and mechanical properties of hybrid fibre reinforced high strength concrete after heat exposition, *Cem. Concr. Res.* 36 (2006) 1672–1678. <https://doi.org/10.1016/j.cemconres.2006.05.006>.
- [302] RILEM 129-MHT, Test Methods for Mechanical Properties of Concrete at High Temperatures, Part 4—Tensile Strength for Service and Accident Conditions, *Mater. Struct.* 33 (2000) 219–223. <http://scholar.google.com/scholar?hl=en&btnG=Search&q=intitle:Test+methods+for+mechanical+properties+of+concrete+at+high+temperatures+-+Part+4:+Tensile+strength+for+service+and+accident+conditions#1>.
- [303] C.S. Poon, S. Azhar, M. Anson, Y.L. Wong, Comparison of the strength and durability performance of normal- and high-strength pozzolanic concretes at elevated temperatures, *Cem. Concr. Res.* 31 (2001) 1291–1300. [https://doi.org/10.1016/S0008-8846\(01\)00580-4](https://doi.org/10.1016/S0008-8846(01)00580-4).
- [304] O.E. Babalola, P.O. Awoyera, D.H. Le, L.M. Bendezú Romero, A review of residual strength properties of normal and high strength concrete exposed to elevated temperatures: Impact of materials modification on behaviour of concrete composite, *Constr. Build. Mater.* 296 (2021). <https://doi.org/10.1016/j.conbuildmat.2021.123448>.
- [305] M. Amran, G. Murali, R. Fediuk, N. Vatin, Y. Vasilev, H. Abdelgader, Palm oil fuel ash-based eco-efficient concrete: A critical review of the short-term properties, *Materials (Basel)*. 14 (2021) 1–33. <https://doi.org/10.3390/ma14020332>.
- [306] M. Amran, A. Al-Fakih, S.H. Chu, R. Fediuk, S. Haruna, A. Azevedo, N. Vatin, Long-term durability properties of geopolymer concrete: An in-depth review, *Case Stud. Constr. Mater.* 15 (2021). <https://doi.org/10.1016/j.cscm.2021.e00661>.
- [307] P. Bamonte, P.G. Gambarova, High-Temperature Behavior of SCC in Compression: Comparative Study on Recent Experimental Campaigns, *J. Mater. Civ. Eng.* 28 (2016) 4015141. [https://doi.org/10.1061/\(asce\)mt.1943-5533.0001378](https://doi.org/10.1061/(asce)mt.1943-5533.0001378).
- [308] J. Huo, B. Jin, Q. Yu, Y. He, Y. Liu, Effect of microstructure variation on damage evolution of concrete at high temperatures, *ACI Mater. J.* 113 (2016) 547–558. <https://doi.org/10.14359/51689102>.
- [309] P.J.E. Sullivan, R. Sharshar, The performance of concrete at elevated temperatures (as measured by the reduction in compressive strength), *Fire Technol.* 28 (1992) 240–250. <https://doi.org/10.1007/BF01857693>.
- [310] V.K.R. Kodur, T.C. Wang, F.P. Cheng, Predicting the fire resistance behaviour of high strength concrete columns, *Cem. Concr. Compos.* 26 (2004) 141–153. [https://doi.org/10.1016/S0958-9465\(03\)00089-1](https://doi.org/10.1016/S0958-9465(03)00089-1).
- [311] C. V. Nielsen, C.J. Pearce, N. Bicanic, Improved phenomenological modelling of transient thermal strains for concrete at high temperatures, *Comput. Concr.* 1 (2004) 189–209. <https://doi.org/10.12989/cac.2004.1.2.189>.
- [312] M.H. Zhang, H. Li, Pore structure and chloride permeability of concrete containing nano-particles for pavement, *Constr. Build. Mater.* 25 (2011) 608–616. <https://doi.org/10.1016/j.conbuildmat.2010.07.032>.
- [313] C. Hall, C. Hall, Water sorptivity of mortars and concretes: A review, *Mag. Concr. Res.* 41 (1989) 51–61. <https://doi.org/10.1680/mac.1989.41.147.51>.
- [314] N.S. Martys, C.F. Ferraris, Capillary transport in mortars and concrete, *Cem. Concr. Res.* 27 (1997) 747–760. [https://doi.org/10.1016/S0008-8846\(97\)00052-5](https://doi.org/10.1016/S0008-8846(97)00052-5).
- [315] C. Tasdemir, Combined effects of mineral admixtures and curing conditions on the sorptivity coefficient of concrete, *Cem. Concr. Res.* 33 (2003) 1637–1642. [https://doi.org/10.1016/S0008-8846\(03\)00112-1](https://doi.org/10.1016/S0008-8846(03)00112-1).
- [316] H.A. Razak, H.K. Chai, H.S. Wong, Near surface characteristics of concrete containing supplementary cementing materials, *Cem. Concr. Compos.* 26 (2004) 883–889.

- <https://doi.org/10.1016/j.cemconcomp.2003.10.001>.
- [317] E. Güneyisi, M. Gesoğlu, S. Karaoğlu, K. Mermerdaş, Strength, permeability and shrinkage cracking of silica fume and metakaolin concretes, *Constr. Build. Mater.* 34 (2012) 120–130. <https://doi.org/10.1016/j.conbuildmat.2012.02.017>.
- [318] H.Y. Leung, J. Kim, A. Nadeem, J. Jaganathan, M.P. Anwar, Sorptivity of self-compacting concrete containing fly ash and silica fume, *Constr. Build. Mater.* 113 (2016) 369–375. <https://doi.org/10.1016/j.conbuildmat.2016.03.071>.
- [319] J.J. Chen, A.K.H. Kwan, Y. Jiang, Adding limestone fines as cement paste replacement to reduce water permeability and sorptivity of concrete, *Constr. Build. Mater.* 56 (2014) 87–93. <https://doi.org/10.1016/j.conbuildmat.2014.01.066>.
- [320] S. Wang, V.C. Li, High-early-strength engineered cementitious composites, *ACI Mater. J.* 103 (2006) 97–105. <https://doi.org/10.14359/15260>.
- [321] Z. Zhang, S. Qian, H. Ma, Investigating mechanical properties and self-healing behavior of micro-cracked ECC with different volume of fly ash, *Constr. Build. Mater.* 52 (2014) 17–23. <https://doi.org/10.1016/j.conbuildmat.2013.11.001>.
- [322] S. Wang, V.C. Li, Engineered cementitious composites with high-volume fly ash, *ACI Mater. J.* 104 (2007) 233–241. <https://doi.org/10.14359/18668>.
- [323] A.W. Dhawale, V.P. Joshi, Engineered Cementitious Composites for Structural Applications, *Int. J. Appl. or Innov. Eng. Manag.* 2 (2013) 198–205.
- [324] H. Liu, Q. Zhang, V. Li, H. Su, C. Gu, Durability study on engineered cementitious composites (ECC) under sulfate and chloride environment, *Constr. Build. Mater.* 133 (2017) 171–181. <https://doi.org/10.1016/j.conbuildmat.2016.12.074>.
- [325] M.D. Lepech, V.C. Li, Large-scale processing of engineered cementitious composites, *ACI Mater. J.* 105 (2008) 358–366. <https://doi.org/10.14359/19897>.
- [326] M.D. Lepech, V.C. Li, Water permeability of engineered cementitious composites, *Cem. Concr. Compos.* 31 (2009) 744–753. <https://doi.org/10.1016/j.cemconcomp.2009.07.002>.
- [327] S.F.U. Ahmed, H. Mihashi, A review on durability properties of strain hardening fibre reinforced cementitious composites (SHFRCC), *Cem. Concr. Compos.* 29 (2007) 365–376. <https://doi.org/10.1016/j.cemconcomp.2006.12.014>.
- [328] S. Muzenski, I. Flores-Vivian, K. Sobolev, Durability of superhydrophobic engineered cementitious composites, *Constr. Build. Mater.* 81 (2015) 291–297. <https://doi.org/10.1016/j.conbuildmat.2015.02.014>.
- [329] J.M. Khatib, Performance of self-compacting concrete containing fly ash, *Constr. Build. Mater.* 22 (2008) 1963–1971. <https://doi.org/10.1016/j.conbuildmat.2007.07.011>.
- [330] A. Kanellopoulos, M.F. Petrou, I. Ioannou, Durability performance of self-compacting concrete, *Constr. Build. Mater.* 37 (2012) 320–325. <https://doi.org/10.1016/j.conbuildmat.2012.07.049>.
- [331] P. Dinakar, K.G. Babu, M. Santhanam, Durability properties of high volume fly ash self compacting concretes, *Cem. Concr. Compos.* 30 (2008) 880–886. <https://doi.org/10.1016/j.cemconcomp.2008.06.011>.
- [332] W. Wongkeo, P. Thongsanitgarn, A. Ngamjarurojana, A. Chaipanich, Compressive strength and chloride resistance of self-compacting concrete containing high level fly ash and silica fume, *Mater. Des.* 64 (2014) 261–269. <https://doi.org/10.1016/j.matdes.2014.07.042>.
- [333] H.A. Mohamed, Effect of fly ash and silica fume on compressive strength of self-compacting concrete under different curing conditions, *Ain Shams Eng. J.* 2 (2011) 79–86. <https://doi.org/10.1016/j.asej.2011.06.001>.
- [334] P.Q. Zhao, P.M. Wang, X.P. Liu, Accuracy in quantitative phase analysis of Portland cement clinkers by

- Rietveld method, *Gongneng Cailiao/Journal Funct. Mater.* 46 (2015) 05095–05100. <https://doi.org/10.3969/j.issn.1001-9731.2015.05.019>.
- [335] P. Adamo, P. Violante, Weathering of rocks and neogenesis of minerals associated with lichen activity, *Appl. Clay Sci.* 16 (2000) 229–256. [https://doi.org/10.1016/S0169-1317\(99\)00056-3](https://doi.org/10.1016/S0169-1317(99)00056-3).
- [336] M.M.S. Tuason, J.M. Arocena, Calcium oxalate biomineralization by *Piloderma fallax* in response to various levels of calcium and phosphorus, *Appl. Environ. Microbiol.* 75 (2009) 7079–7085. <https://doi.org/10.1128/AEM.00325-09>.
- [337] A. Rosling, K.B. Suttle, E. Johansson, P.A.W. Van Hees, J.F. Banfield, Phosphorous availability influences the dissolution of apatite by soil fungi, *Geobiology.* 5 (2007) 265–280. <https://doi.org/10.1111/j.1472-4669.2007.00107.x>.
- [338] D.B. Gleeson, N. Clipson, K. Melville, G.M. Gadd, F.P. McDermott, Characterization of fungal community structure on a weathered pegmatitic granite., *Microb. Ecol.* 50 (2005) 360–368. <https://doi.org/10.1007/s00248-005-0198-8>.
- [339] J. Wang, J. Dewanckele, V. Cnudde, S. Van Vlierberghe, W. Verstraete, N. De Belie, X-ray computed tomography proof of bacterial-based self-healing in concrete, *Cem. Concr. Compos.* 53 (2014) 289–304. <https://doi.org/10.1016/j.cemconcomp.2014.07.014>.
- [340] J. Xu, X. Wang, Self-healing of concrete cracks by use of bacteria-containing low alkali cementitious material, *Constr. Build. Mater.* 167 (2018) 1–14. <https://doi.org/10.1016/j.conbuildmat.2018.02.020>.
- [341] H. Huang, G. Ye, D. Damidot, Characterization and quantification of self-healing behaviors of microcracks due to further hydration in cement paste, *Cem. Concr. Res.* 52 (2013) 71–81. <https://doi.org/10.1016/j.cemconres.2013.05.003>.
- [342] Q. Chen, Y. Su, M. Li, C. Qian, Calcium carbonate labeling for the characterization of self-healing cracks in cement-based materials, *Mater. Lett.* 292 (2021). <https://doi.org/10.1016/j.matlet.2021.129507>.
- [343] V. Cnudde, P.J.S. Jacobs, Monitoring of weathering and conservation of building materials through non-destructive X-ray computed microtomography, in: *Environ. Geol.*, 2004: pp. 477–485. <https://doi.org/10.1007/s00254-004-1049-5>.
- [344] V. Cnudde, M. Boone, J. Dewanckele, M. Dierick, L. Van Hoorebeke, P. Jacobs, 3D characterization of sandstone by means of X-ray computed tomography, *Geosphere.* 7 (2011) 54–61. <https://doi.org/10.1130/GES00563.1>.
- [345] J. Dewanckele, T. De Kock, M.A. Boone, V. Cnudde, L. Brabant, M.N. Boone, G. Fronteau, L. Van Hoorebeke, P. Jacobs, 4D imaging and quantification of pore structure modifications inside natural building stones by means of high resolution X-ray CT, *Sci. Total Environ.* 416 (2012) 436–448. <https://doi.org/10.1016/j.scitotenv.2011.11.018>.
- [346] V. Cnudde, M.N. Boone, High-resolution X-ray computed tomography in geosciences: A review of the current technology and applications, *Earth-Science Rev.* 123 (2013) 1–17. <https://doi.org/10.1016/j.earscirev.2013.04.003>.
- [347] Chemical Analysis of Silica Fume Infused Self Healing Concrete, *Int. J. Recent Technol. Eng.* 8 (2020) 1430–1432. <https://doi.org/10.35940/ijrte.f7720.038620>.
- [348] L.L. Kan, H.S. Shi, A.R. Sakulich, V.C. Li, Self-healing characterization of engineered cementitious composite materials, *ACI Mater. J.* 107 (2010) 617–624. <https://doi.org/10.14359/51664049>.
- [349] T.H. Ahn, T. Kishi, Crack self-healing behavior of cementitious composites incorporating various mineral admixtures, *J. Adv. Concr. Technol.* 8 (2010) 171–186. <https://doi.org/10.3151/jact.8.171>.
- [350] L.P. Esteves, On the hydration of water-entrained cement-silica systems: Combined SEM, XRD and thermal analysis in cement pastes, *Thermochim. Acta.* 518 (2011) 27–35. <https://doi.org/10.1016/j.tca.2011.02.003>.
- [351] F. Ren, C.H. Mattus, J.J.A. Wang, B.P. DiPaolo, Effect of projectile impact and penetration on the phase

- composition and microstructure of high performance concretes, *Cem. Concr. Compos.* 41 (2013) 1–8. <https://doi.org/10.1016/j.cemconcomp.2013.04.007>.
- [352] L. Yan, Y.M. Xing, J.J. Li, High-temperature mechanical properties and microscopic analysis of hybrid-fibrereinforced high-performance concrete, *Mag. Concr. Res.* 65 (2013) 139–147. <https://doi.org/10.1680/mac.12.00034>.
- [353] D. Zhao, R. Zhao, P. Jia, H. Liu, Microstructure and fatigue performance of high strength concrete under compression after exposure to elevated temperatures, *Eur. J. Environ. Civ. Eng.* (2019). <https://doi.org/10.1080/19648189.2019.1677507>.
- [354] S.A. Salih, M.R. Aldikheeli, F.M. Al-Zwainy, Microstructure analysis and residual strength of fiber reinforced eco-friendly self-consolidating concrete subjected to elevated temperature, *Int. J. Civ. Eng. Technol.* 9 (2018) 15–31.
- [355] W. Khaliq, F. Waheed, Mechanical response and spalling sensitivity of air entrained high-strength concrete at elevated temperatures, *Constr. Build. Mater.* 150 (2017) 747–757. <https://doi.org/10.1016/j.conbuildmat.2017.06.039>.
- [356] K.S. Al-Jabri, M. Hisada, A.H. Al-Saidy, S.K. Al-Oraimi, Performance of high strength concrete made with copper slag as a fine aggregate, *Constr. Build. Mater.* 23 (2009) 2132–2140. <https://doi.org/10.1016/j.conbuildmat.2008.12.013>.
- [357] W.D.A. Rickard, J. Temuujin, A. Van Riessen, Thermal analysis of geopolymer pastes synthesised from five fly ashes of variable composition, *J. Non. Cryst. Solids.* 358 (2012) 1830–1839. <https://doi.org/10.1016/j.jnoncrysol.2012.05.032>.
- [358] P. Bamonte, P.G. Gambarova, A study on the mechanical properties of self-compacting concrete at high temperature and after cooling, *Mater. Struct. Constr.* 45 (2012) 1375–1387. <https://doi.org/10.1617/s11527-012-9839-9>.
- [359] Z. Giergiczny, M.A. Glinicki, M. Sokołowski, M. Zielinski, Air void system and frost-salt scaling of concrete containing slag-blended cement, *Constr. Build. Mater.* 23 (2009) 2451–2456. <https://doi.org/10.1016/j.conbuildmat.2008.10.001>.
- [360] ASTM C 457/C 457M-12, Standard Test Method for Microscopical Determination of Parameters of the Air-Void System in Hardened Concrete 1, *ASTM Int.* 5 (2013) 1–15. <https://doi.org/10.1520/C0457>.
- [361] A.M. Onaizi, G.F. Huseien, N.H.A.S. Lim, M. Amran, M. Samadi, Effect of nanomaterials inclusion on sustainability of cement-based concretes: A comprehensive review, *Constr. Build. Mater.* 306 (2021). <https://doi.org/10.1016/j.conbuildmat.2021.124850>.
- [362] T.C. Powers, Willis, T. F., *The air requirement of frost-resistant concrete*, [Portland Cement Association], [Chicago], 1949.
- [363] A.A. Hilal, N.H. Thom, A.R. Dawson, On void structure and strength of foamed concrete made without/with additives, *Constr. Build. Mater.* 85 (2015) 157–164. <https://doi.org/10.1016/j.conbuildmat.2015.03.093>.
- [364] E.T. Dawood, M. Ramli, High strength characteristics of cement mortar reinforced with hybrid fibres, *Constr. Build. Mater.* 25 (2011) 2240–2247. <https://doi.org/10.1016/j.conbuildmat.2010.11.008>.
- [365] K.A. Mujedu, M.A. Ab-Kadir, N.N. Sarbini, M. Ismail, Microstructure and compressive strength of self-compacting concrete incorporating palm oil fuel ash exposed to elevated temperatures, *Constr. Build. Mater.* (2021). <https://doi.org/10.1016/j.conbuildmat.2020.122025>.
- [366] H.L. Zhang, C.T. Davie, A numerical investigation of the influence of pore pressures and thermally induced stresses for spalling of concrete exposed to elevated temperatures, *Fire Saf. J.* 59 (2013) 102–110. <https://doi.org/10.1016/j.firesaf.2013.03.019>.
- [367] C.M. Lee, K.J. Lee, C.H. Cho, Spalling effect on gamma-ray shielding performance in MACSTOR-400 (Korean CANDU spent fuel storage module), *Prog. Nucl. Energy.* 51 (2009) 163–169.

- <https://doi.org/10.1016/j.pnucene.2008.02.007>.
- [368] C.T. Davie, C.J. Pearce, N. Bićanić, A fully generalised, coupled, multi-phase, hygro-thermo-mechanical model for concrete, *Mater. Struct. Constr.* 43 (2010) 13–33. <https://doi.org/10.1617/s11527-010-9591-y>.
- [369] D. Gawin, C.E. Majorana, B.A. Schrefler, Numerical analysis of hygro-thermal behaviour and damage of concrete at high temperature, *Mech. Cohesive-Frictional Mater.* 4 (1999) 37–74. [https://doi.org/10.1002/\(SICI\)1099-1484\(199901\)4:1<37::AID-CFM58>3.0.CO;2-S](https://doi.org/10.1002/(SICI)1099-1484(199901)4:1<37::AID-CFM58>3.0.CO;2-S).
- [370] R. Tenchev, P. Purnell, An application of a damage constitutive model to concrete at high temperature and prediction of spalling, *Int. J. Solids Struct.* 42 (2005) 6550–6565. <https://doi.org/10.1016/j.ijsolstr.2005.06.016>.
- [371] D. Gawin, F. Pesavento, B.A. Schrefler, What physical phenomena can be neglected when modelling concrete at high temperature? A comparative study. Part 1: Physical phenomena and mathematical model, *Int. J. Solids Struct.* 48 (2011) 1927–1944. <https://doi.org/10.1016/j.ijsolstr.2011.03.004>.
- [372] R.K.K. Yuen, W.K. Kwok, S.M. Lo, J. Liang, Heat and mass transfer in concrete at elevated temperature, *Numer. Heat Transf. Part A Appl.* 51 (2007) 469–494. <https://doi.org/10.1080/10407780600829712>.
- [373] J.H. Chung, G.R. Consolazio, M.C. McVay, Finite element stress analysis of a reinforced high-strength concrete column in severe fires, *Comput. Struct.* 84 (2006) 1338–1352. <https://doi.org/10.1016/j.compstruc.2006.03.007>.
- [374] D. Gawin, F. Pesavento, B.A. Schrefler, Towards prediction of the thermal spalling risk through a multi-phase porous media model of concrete, *Comput. Methods Appl. Mech. Eng.* 195 (2006) 5707–5729. <https://doi.org/10.1016/j.cma.2005.10.021>.
- [375] Z.P. Bažant, Analysis of pore pressure, thermal stress and fracture in rapidly heated concrete, *Nist.* (1997) 155–164. <https://www.nist.gov/publications/analysis-pore-pressure-thermal-stress-and-fracture-rapidly-heated-concrete>.
- [376] J. Ye, W. Chen, L. Yin, Full-scale fire resistance tests on load-bearing C-shape cold-formed steel wall systems, *Tumu Gongcheng Xuebao/China Civ. Eng. J.* 46 (2013) 1–10.
- [377] S. Dal Pont, B.A. Schrefler, A. Ehrlacher, Experimental and finite element analysis of a hollow cylinder submitted to high temperatures, *Mater. Struct. Constr.* 38 (2005) 681–690. <https://doi.org/10.1617/14167>.
- [378] X. Li, R. Li, B.A. Schrefler, A coupled chemo-thermo-hygro-mechanical model of concrete at high temperature and failure analysis, *Int. J. Numer. Anal. Methods Geomech.* 30 (2006) 635–681. <https://doi.org/10.1002/nag.495>.
- [379] M.V.G. De Moraes, P. Pliya, A. Noumowé, A.L. Beaucour, S. Ortola, Contribution to the explanation of the spalling of small specimen without any mechanical restraint exposed to high temperature, in: *Nucl. Eng. Des.*, 2010: pp. 2655–2663. <https://doi.org/10.1016/j.nucengdes.2010.04.041>.
- [380] Y.F. Fu, Y.L. Wong, C.S. Poon, C.A. Tang, Numerical tests of thermal cracking induced by temperature gradient in cement-based composites under thermal loads, *Cem. Concr. Compos.* 29 (2007) 103–116. <https://doi.org/10.1016/j.cemconcomp.2006.09.002>.
- [381] Q. Ma, R. Guo, Z. Zhao, Z. Lin, K. He, Mechanical properties of concrete at high temperature—A review, *Constr. Build. Mater.* 93 (2015) 371–383. <https://doi.org/10.1016/j.conbuildmat.2015.05.131>.
- [382] T.Z. Harmathy, Effect of Moisture on the Fire Endurance of Building Elements, in: *Moisture Mater. Relat. to Fire Tests*, 2009: pp. 74–74–22. <https://doi.org/10.1520/stp48429s>.
- [383] T.Z. Harmathy, M.A. Sultan, J.W. MacLaurin, COMPARISON OF SEVERITY OF EXPOSURE IN ASTM E 119 AND ISO 834 FIRE RESISTANCE TESTS., *J. Test. Eval.* 15 (1987) 371–375. <https://doi.org/10.1520/jte11036j>.
- [384] C. Meyer-Ottens, Zur frage der abplatzungen an bauteilen aus beton bei brandbeanspruchungen., *Dtsch Ausschuss Stahlbet.* (1975).